About the Internal Structure of Neutron Star Merger Products

Biannual Physics Day of the HIC for FAIR (expert group 1) University Frankfurt Feb. 15, 2016

Matthias Hanauske, Kentaro Takami, Luciano Rezzolla, Filippo Galeazzi, Bruno Mundim, Luke Bovard and Jens Papenfort
Andreas Zacchi, Jürgen Schaffner-Bielich, Bruno Franzon, Stefan Schramm and Horst Stöcker

Frankfurt Institute for Advanced Studies
Johann Wolfgang Goethe-University
Institute for Theoretical Physics
Department of Relativistic Astrophysics
Frankfurt am Main, Germany

PRL 116, 061102 (2016) Selected for a Viewpoint in *Physics*
PHYSICAL REVIEW LETTERS
week ending
12 FEBRUARY 2016

Observation of Gravitational Waves from a Binary Black Hole Merger

Advanced LIGO (Laser Interferometer Gravitational Wave Observatory) has detected the gravitational waves produced in a merger of two black holes.

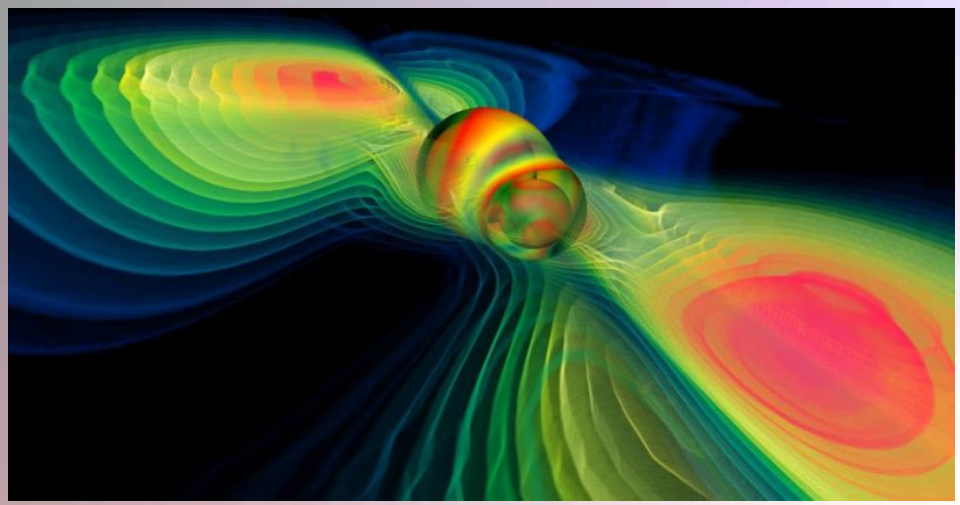

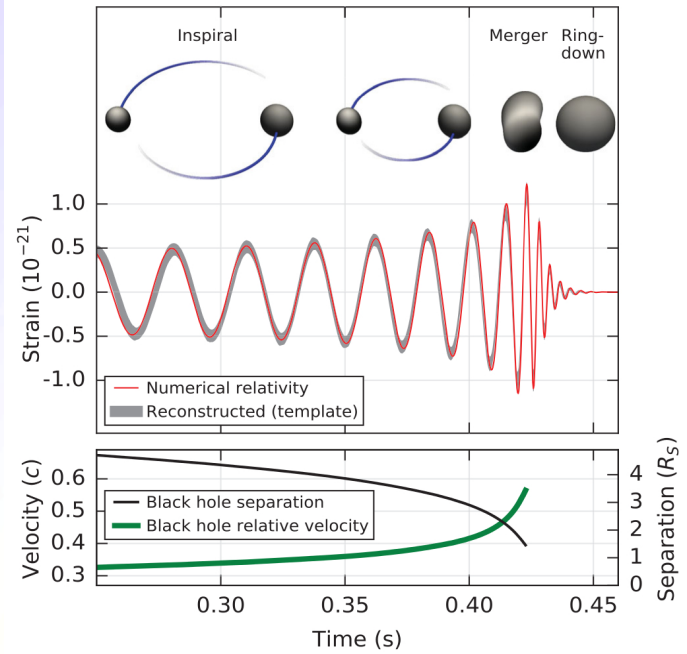

About the Internal Structure of Neutron Star Merger Products

1. Introduction
2. Static Properties of Compact Stars
3. Numerical Relativity and Relativistic Hydro-dynamics of Neutron Star Mergers
4. Properties of Hypermassive Neutron Stars
5. Outlook
6. Summary

Pulsars → Neutron Star Mergers

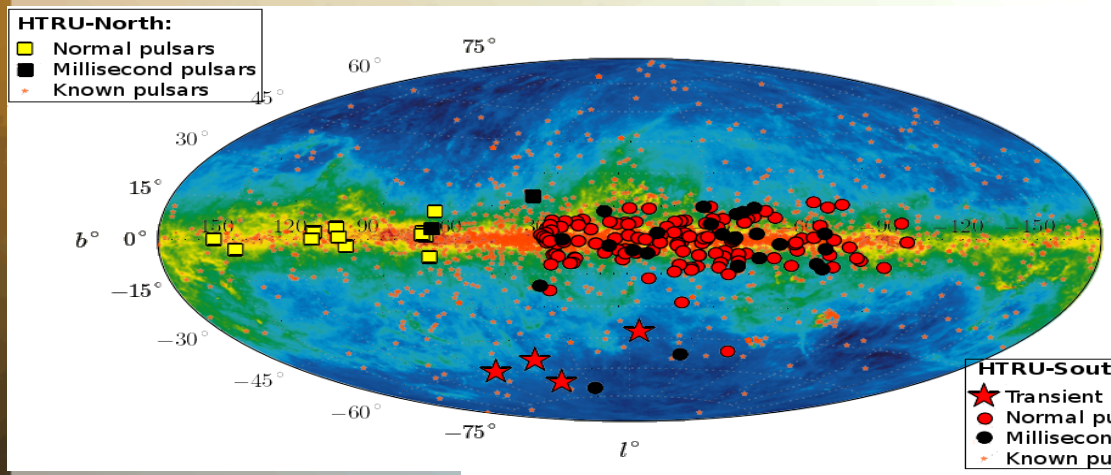

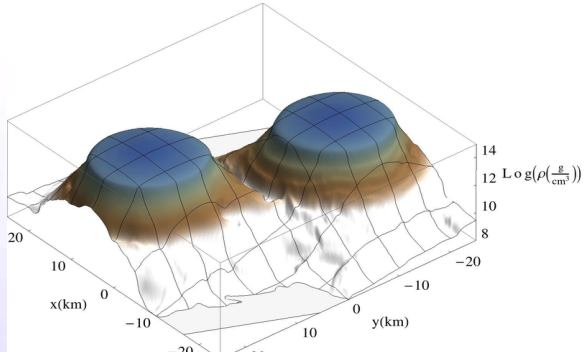

PSR B0531+21 (33.5 ms)
Crab Pulsar

PSR B1937+21 (1.56 ms)

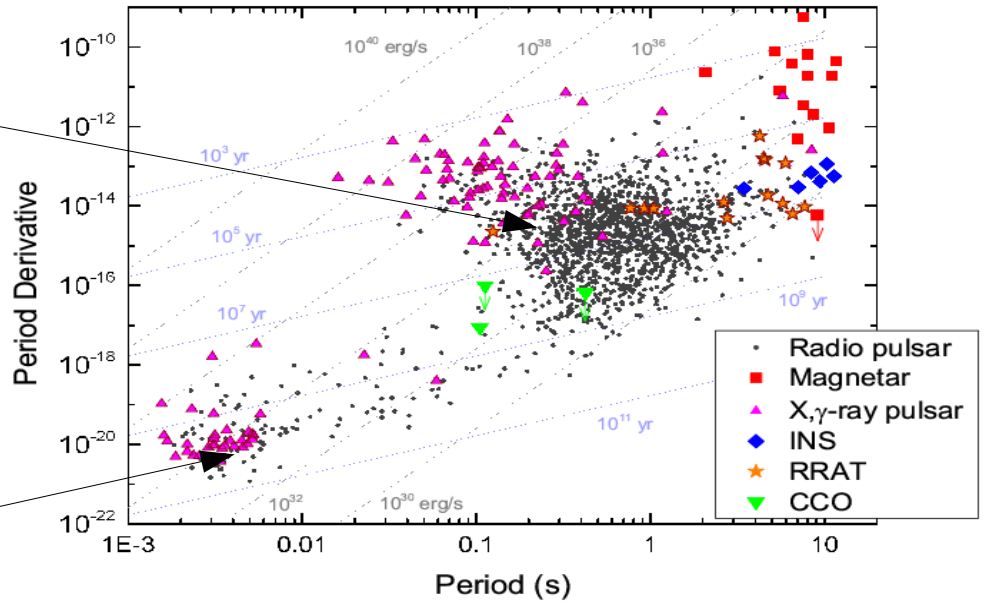

The emission of gravitational waves from merging neutron stars is at the verge of beeing detected by gravitational wave detectors

The Double Pulsar

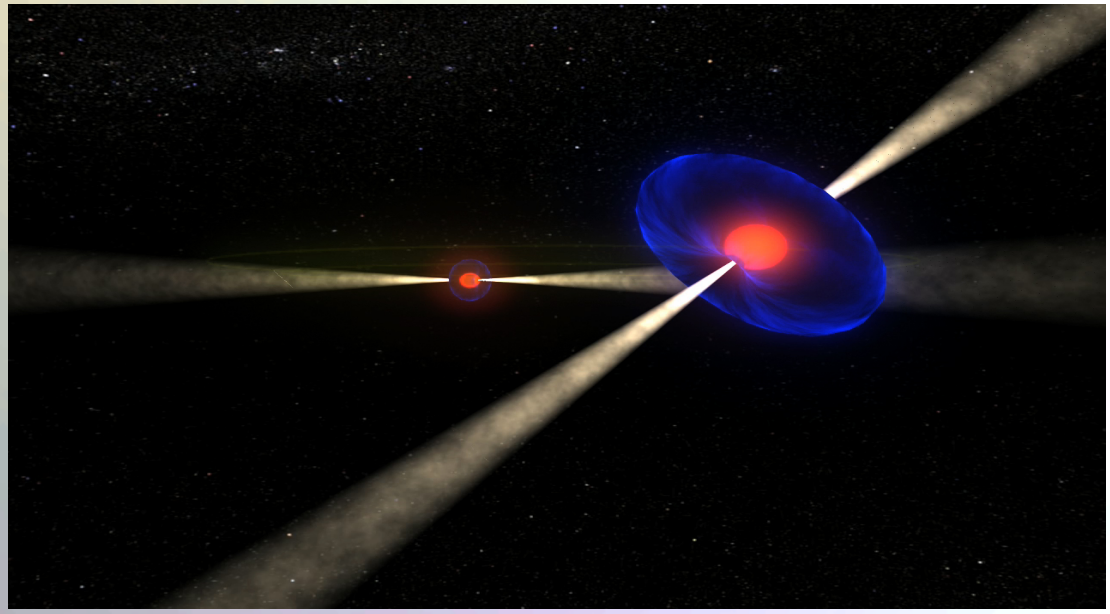

The **Double Pulsar** (PSR J0737-3039A/B), which was **discovered in 2003**, is an excellent system is for testing Einstein's theory of general relativity and alternative theories of gravity in the strong field regime (separated only by 800,000 km, orbital period of 147 minutes and a mean velocities of one million km/h). Additional: **Periodic eclipse** of one pulsar by the other, which is a direct consequence of the almost edge-on geometry of the orbit. Due to the emission of **gravitational waves**, the distance between the two neutron stars decreases with time and finally the two objects need to merge.

General Relativity and Quantum Cromodynamics

ART	Yang-Mills-Theories
$D_\beta v^\alpha = \partial_\beta\, v^\alpha + \Gamma^\alpha_{\sigma\beta}\, v^\sigma$	$D_{\beta a}{}^{b} = \partial_\beta\, 1_a{}^b + ig\, A_{\beta a}{}^b$
$R^\delta{}_{\mu\alpha\beta}\, v^\mu = [D_\alpha, D_\beta]\, v^\delta$ $R^\delta{}_{\mu\alpha\beta} = \Gamma^\delta_{\mu\alpha\|\beta} - \Gamma^\delta_{\mu\beta\|\alpha}$ $+\Gamma^\delta_{\nu\beta}\Gamma^\nu_{\mu\alpha} + \Gamma^\delta_{\nu\alpha}\Gamma^\nu_{\mu\beta}$	$F_{\alpha\beta a}{}^{b} = \frac{1}{ig}\left[D_{\alpha a}{}^{c}, D_{\beta c}{}^{b}\right]$ $= A_{\beta a}{}^{b}{}_{\|\alpha} - A_{\alpha a}{}^{b}{}_{\|\beta}$ $+\frac{1}{ig}\left[A_{\alpha a}{}^{c}, A_{\beta c}{}^{b}\right]$
$\mathcal{L}_G = R + \underbrace{(c_1\, R_{\mu\nu}R^{\mu\nu} + ...)}_{\equiv 0 \text{ for ART}}$	$\mathcal{L}_{YM} = \frac{1}{4} F_{\mu\nu a}{}^{b}\, F^{\mu\nu}{}_{a}{}^{b}$

QuantumCromoDynamic:
$(SU(3)_{(c)}$- Color Yang-Mills-Gauge Theory)

$$D_{\beta A}{}^{B} = \partial_\beta\, 1_A{}^B + ig\, G_{\beta A}{}^B$$
$_A{}^B$ =red, green, blue

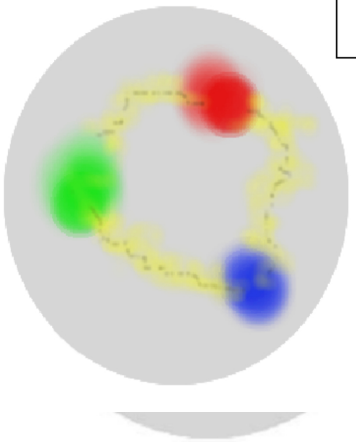

$$\psi^f_A = \begin{pmatrix} \psi^f_r \\ \psi^f_g \\ \psi^f_b \end{pmatrix}$$

Confinement
chiral symmetry, ...

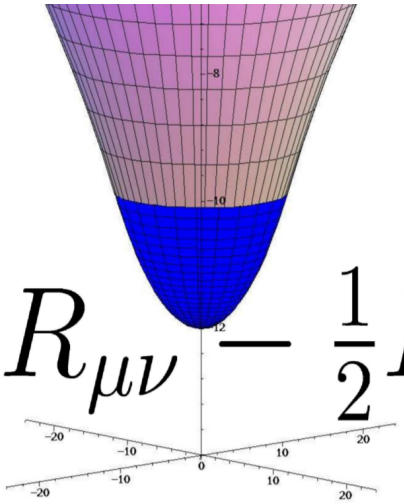

$$R_{\mu\nu} - \frac{1}{2} R\, g_{\mu\nu} = \frac{8\pi G}{c^4}\, T_{\mu\nu}$$

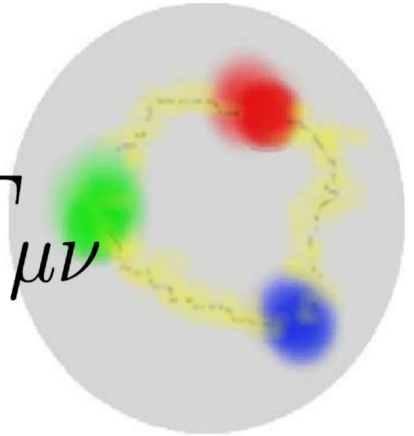

The QCD – Phase Transition and the Interior of a Hybrid Star

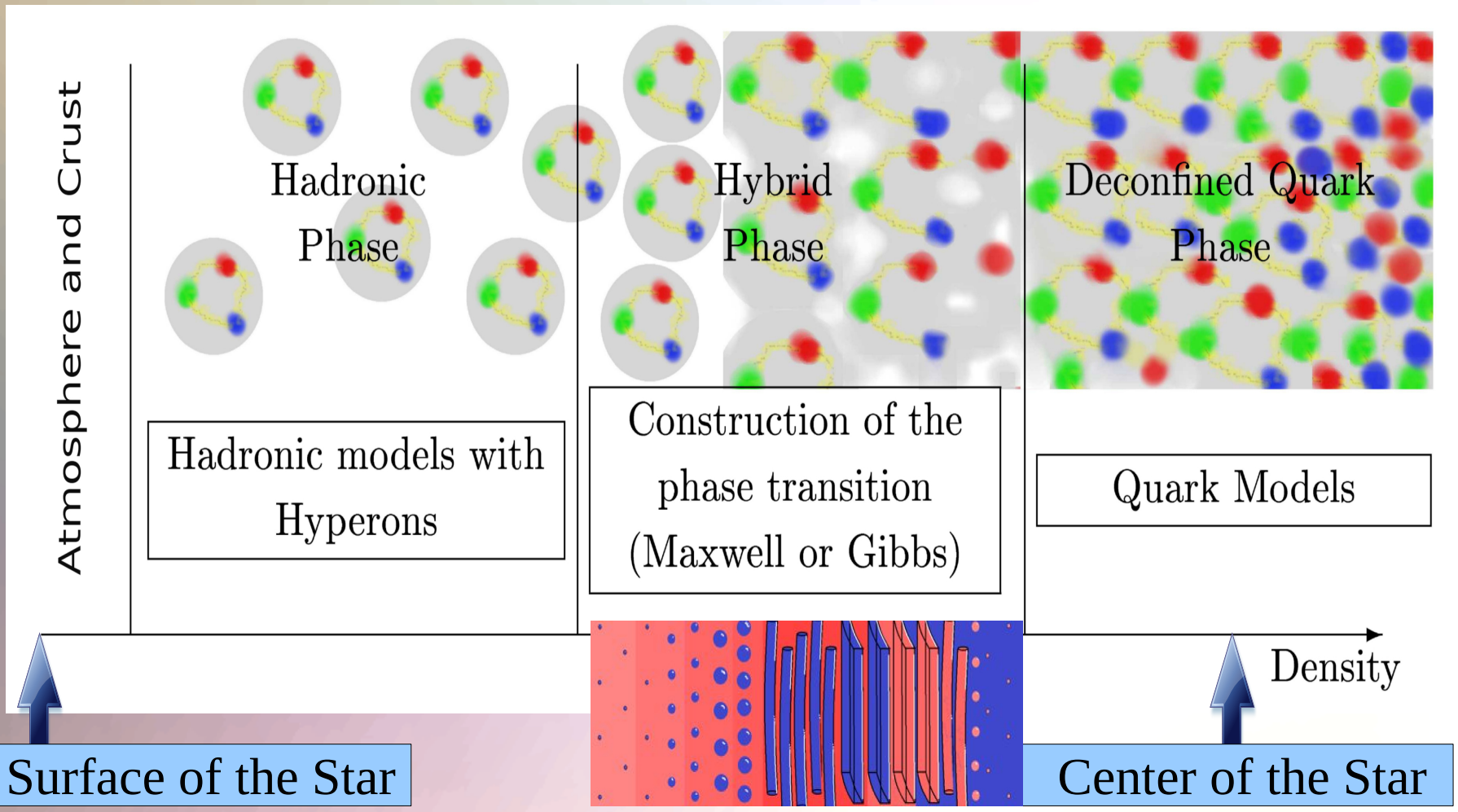

The Compact Star Zoo

Neutron stars with and without hyperons, quark stars and strange quark stars, hybrid stars with color superconducting quark matter, hybrid stars with Bose-Einstein condensates of antikaons, ...

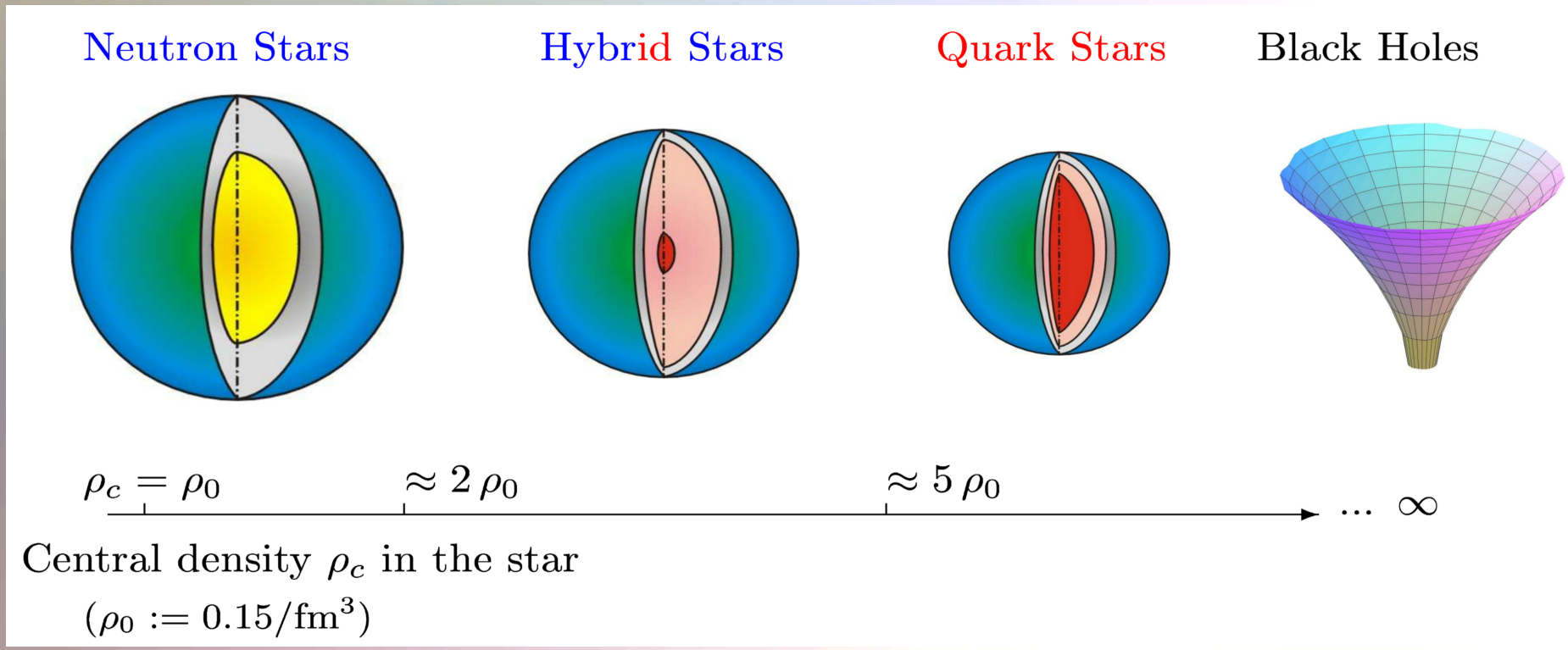

The Gibbs Construction

Hadronic and quark surface:

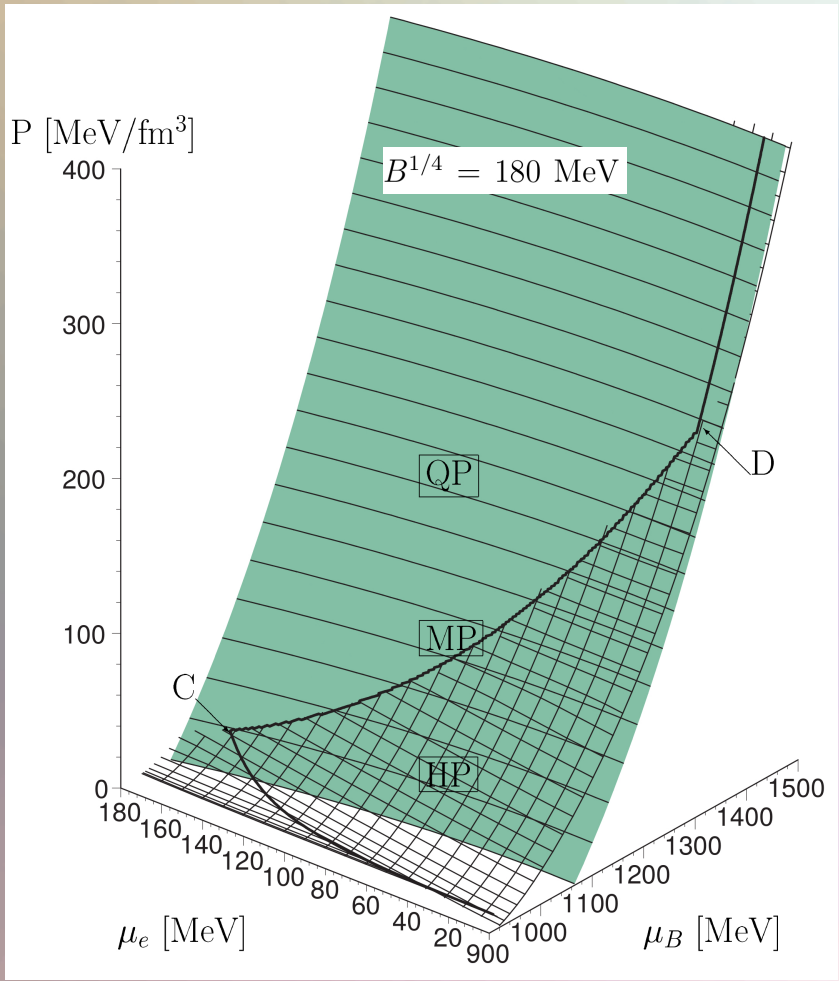

Particle composition:

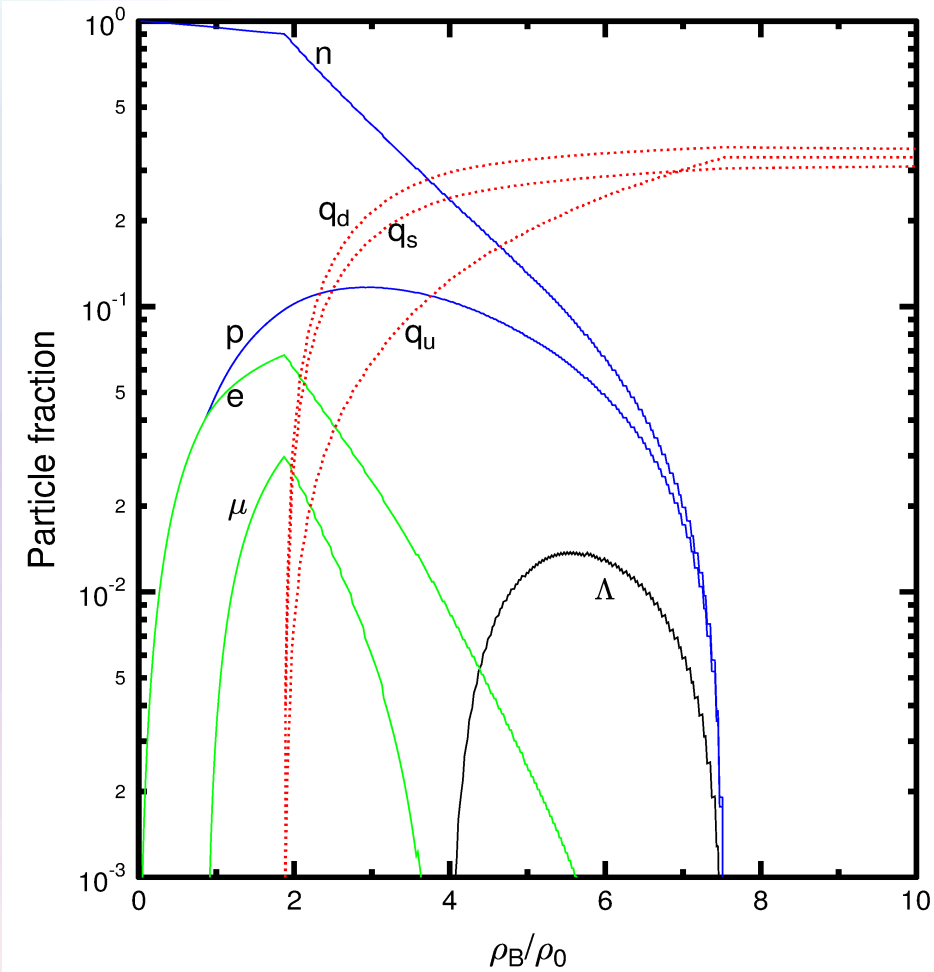

The Gibbs Construction

Hadronic and quark surface:

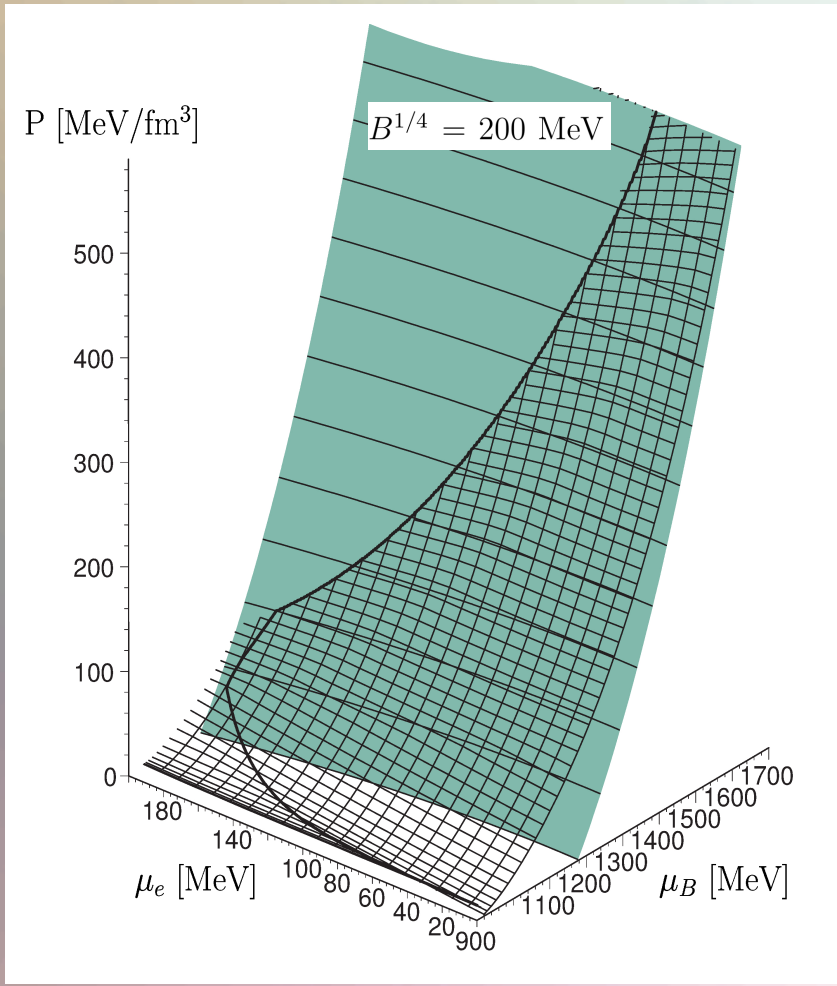

Particle composition:

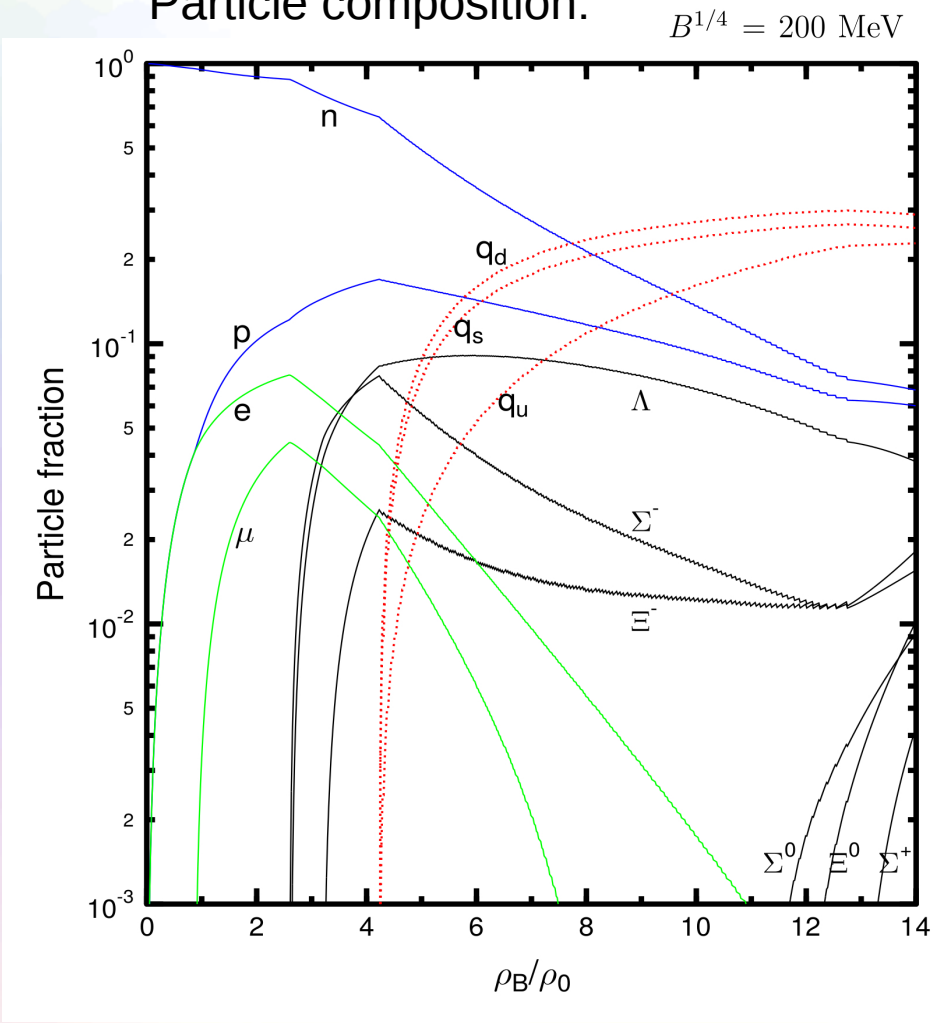

M. Hanauske, Dissertation, "Properties of Compact Stars within QCD-motivated Models"

Maxwell Construction

If the **surface tension is large** -> **mixed phase disappears** -> sharp boundary between the hadron and quark phase → **density jump** (see middle figure). **Twin star** properties can be found more easily when using a Maxwell construction (see left and right figure).
Accepted in PRD: *Stable hybrid stars within a SU(3) Quark-Meson-Model ;* A.Zacchi, M.Hanauske, J.Schaffner-Bielich (see arXiv:1510.00180)

Mass-Density relation

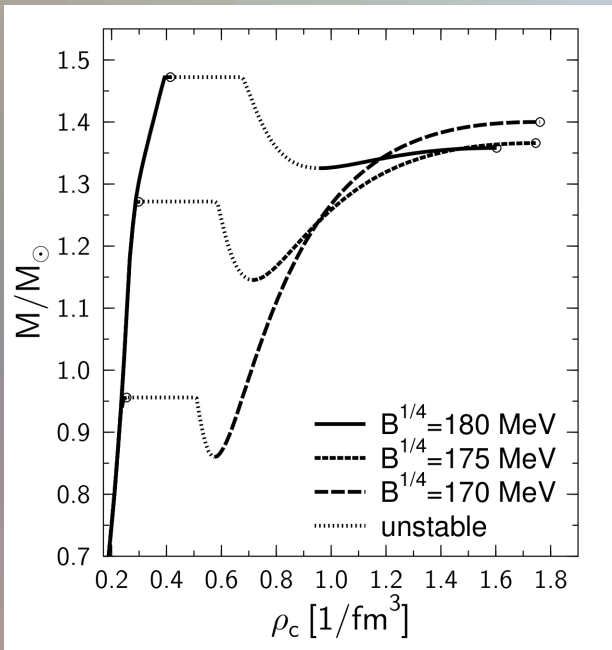

Energy-density profiles

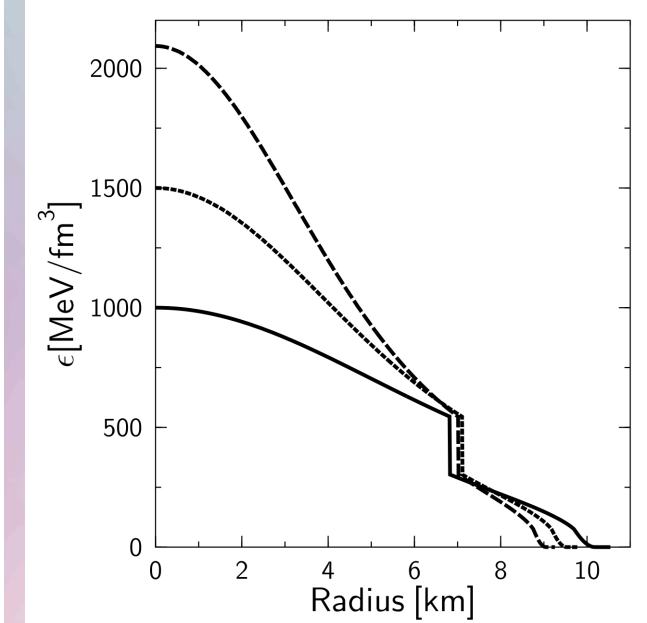

Radius-Mass relation

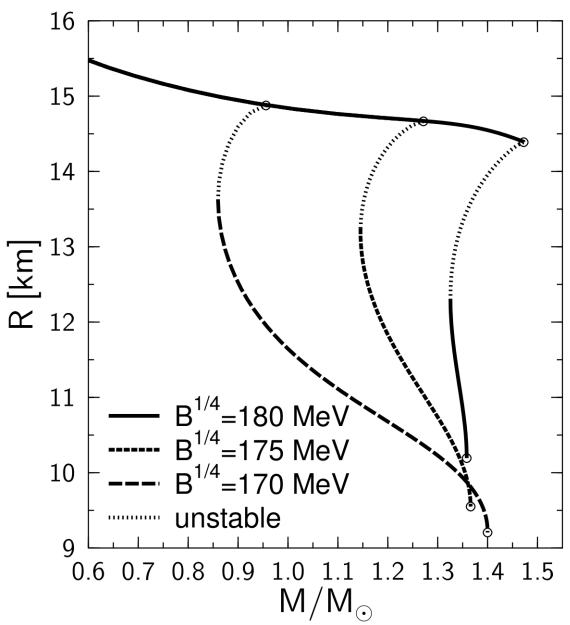

.N. Mishustin, M. Hanauske, A. Bhattacharyya, L.M. Satarov, H. Stöcker, and W. Greiner, “Catastrophic rearrangement of a compact star due to quark core formation”, Physics Letters B 552 (2003) p.1-8

The QCD- Phase Diagram

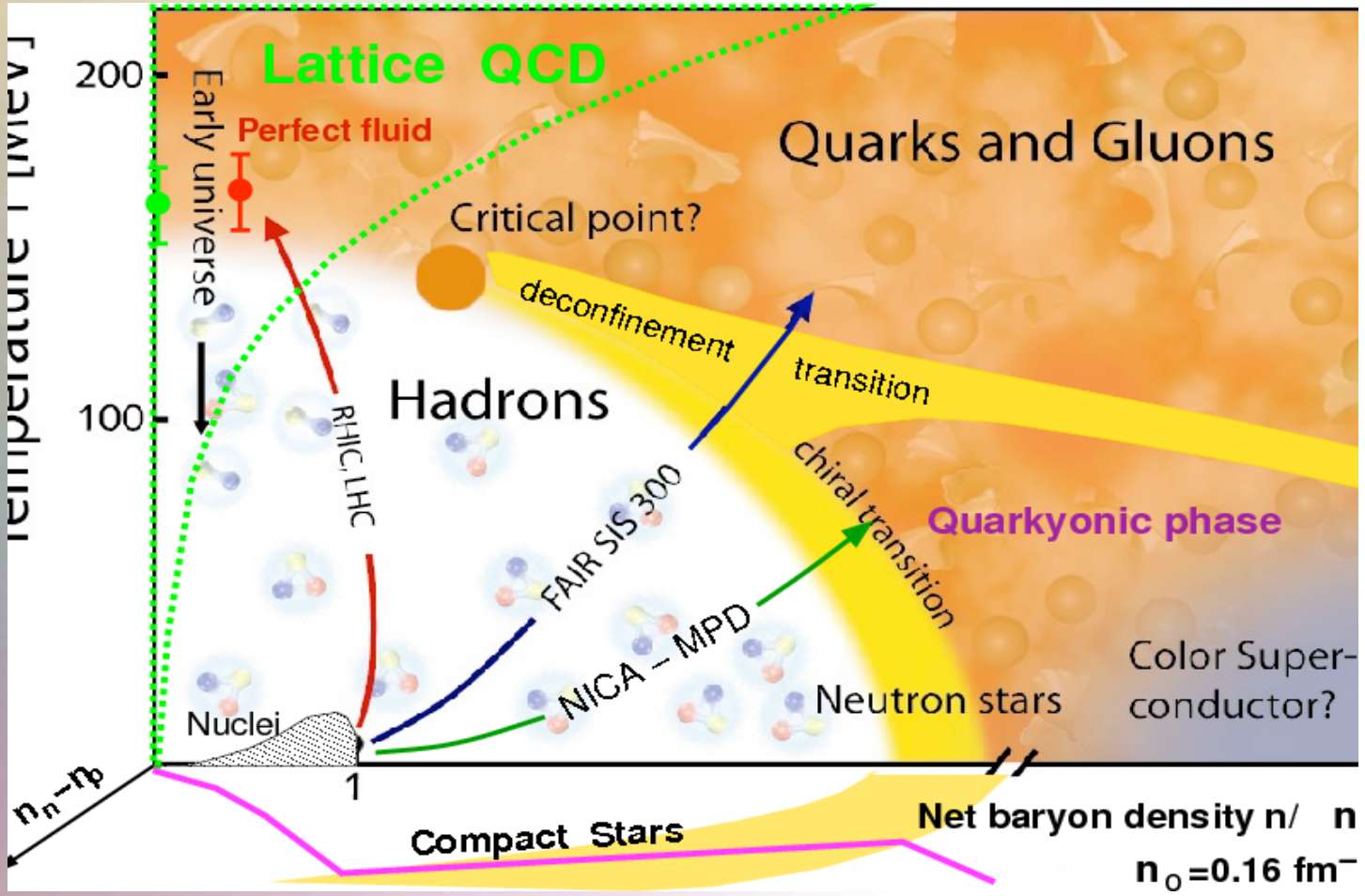

Image from http://inspirehep.net/record/823172/files/phd_qgp3D_quarkyonic2.png

Focus of the Talk

Research Questions:

- What happens when two neutron stars merge and how do the emitted gravitational waves look like?
- How does the interior of a neutron star merger product (NSMP) look like?
- How does the space-time structure of a NSMP look like?
- What makes the Hypermassive Neutron Stars (HMNS) to stabilize against gravitational collapse to a black hole?
- How does the rotation-profile of the differentially rotating HMNS look like?
- How to detect the QCD-phase transition with gravitational wave detectors?

Methodology:

- Based on a large number of full numerical-relativity simulations of merging neutron star binaries, the internal structure of the HMNS in the post-merger phase have been analysed.
- The simulations have been performed in full general relativity using the publicly available *Einstein-Toolkit* code together with the *Whisky* and *WhiskyTHC* code for the general-relativistic hydrodynamic equations.
- The HMNS properties have been analysed for a variety of different equation of states (EoS) and two initial neutron star mass values.

Neutron Star Mergers

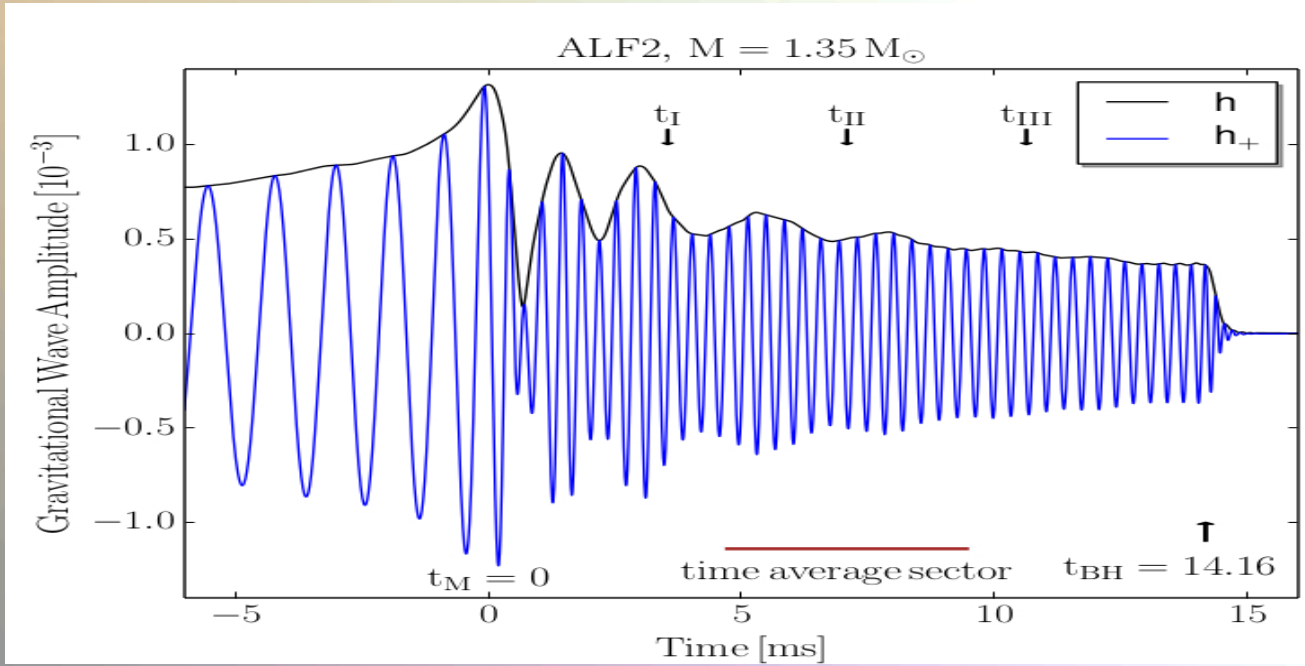

Gravitational wave emission
+
Gamma-ray burst

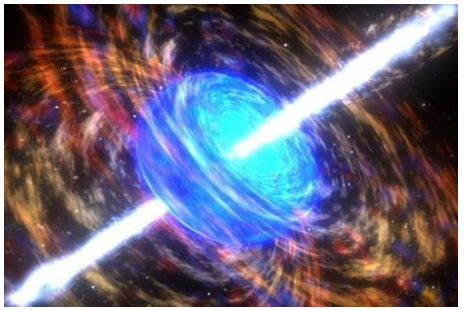

Inspiral phase	Merger and post-merger phase	Ringdown phase
NS + NS	HMNS	BH + Torus → BH

Spectral Properties of GWs

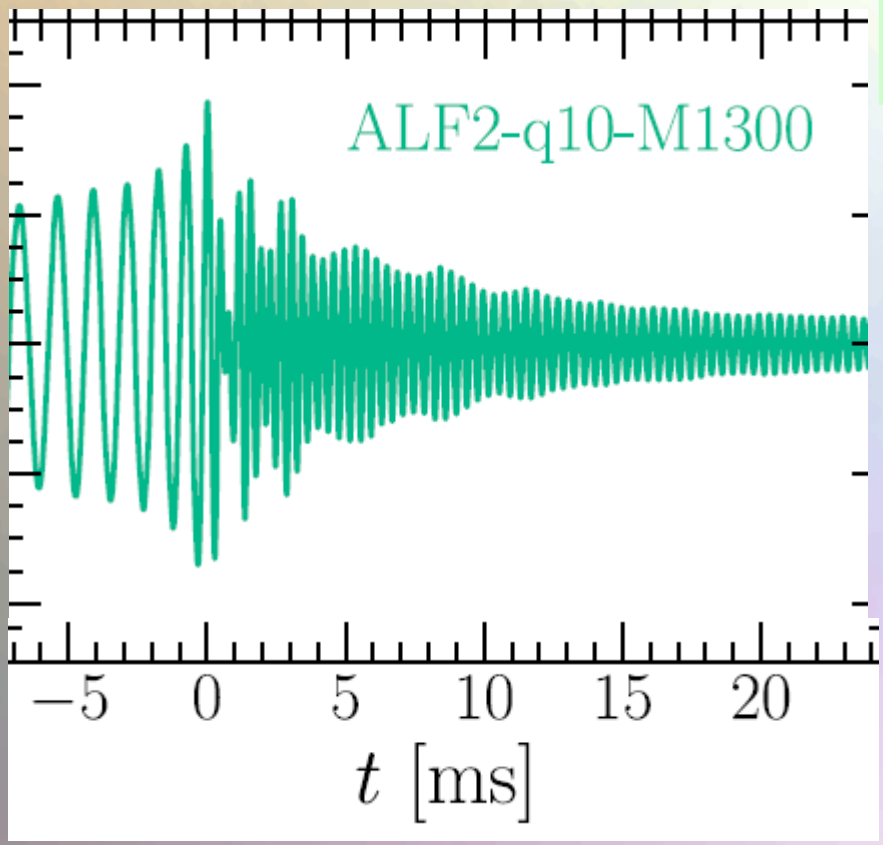

Full spectral profile
(thin curve)

Spectral profile
(t >3 ms)
(thick curve)

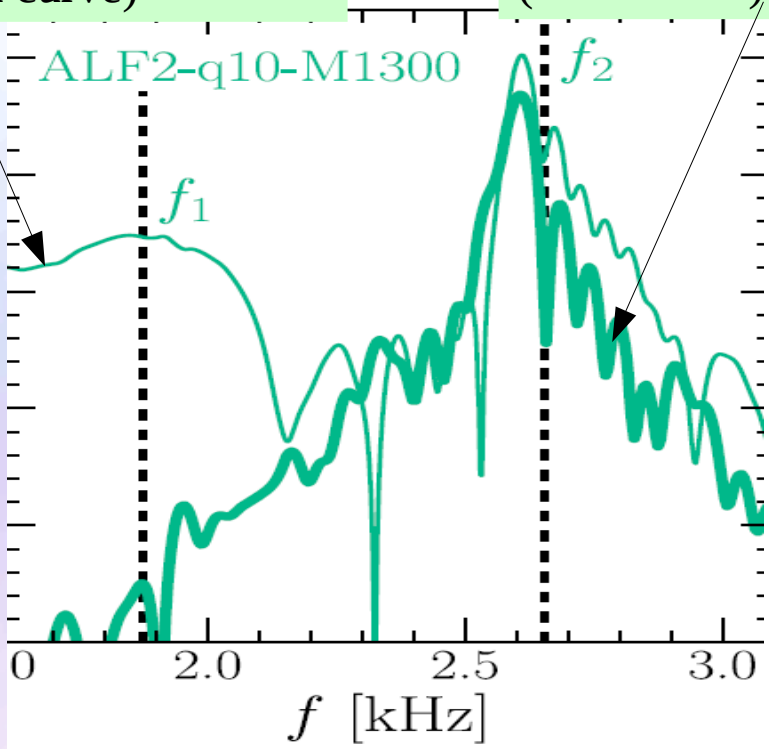

Two characteristic GW frequency peaks (f_1 and f_2); the origin of f_1 comes from t<3 ms. By measuring M, f_1 and f_2 one can set high constraints on the EoS.

"Spectral properties of the post-merger gravitational-wave signal from binary neutron stars", Kentaro Takami, Luciano Rezzolla, and Luca Baiotti, PHYSICAL REVIEW D 91, 064001 (2015)

GW-Spectrum for different EoSs

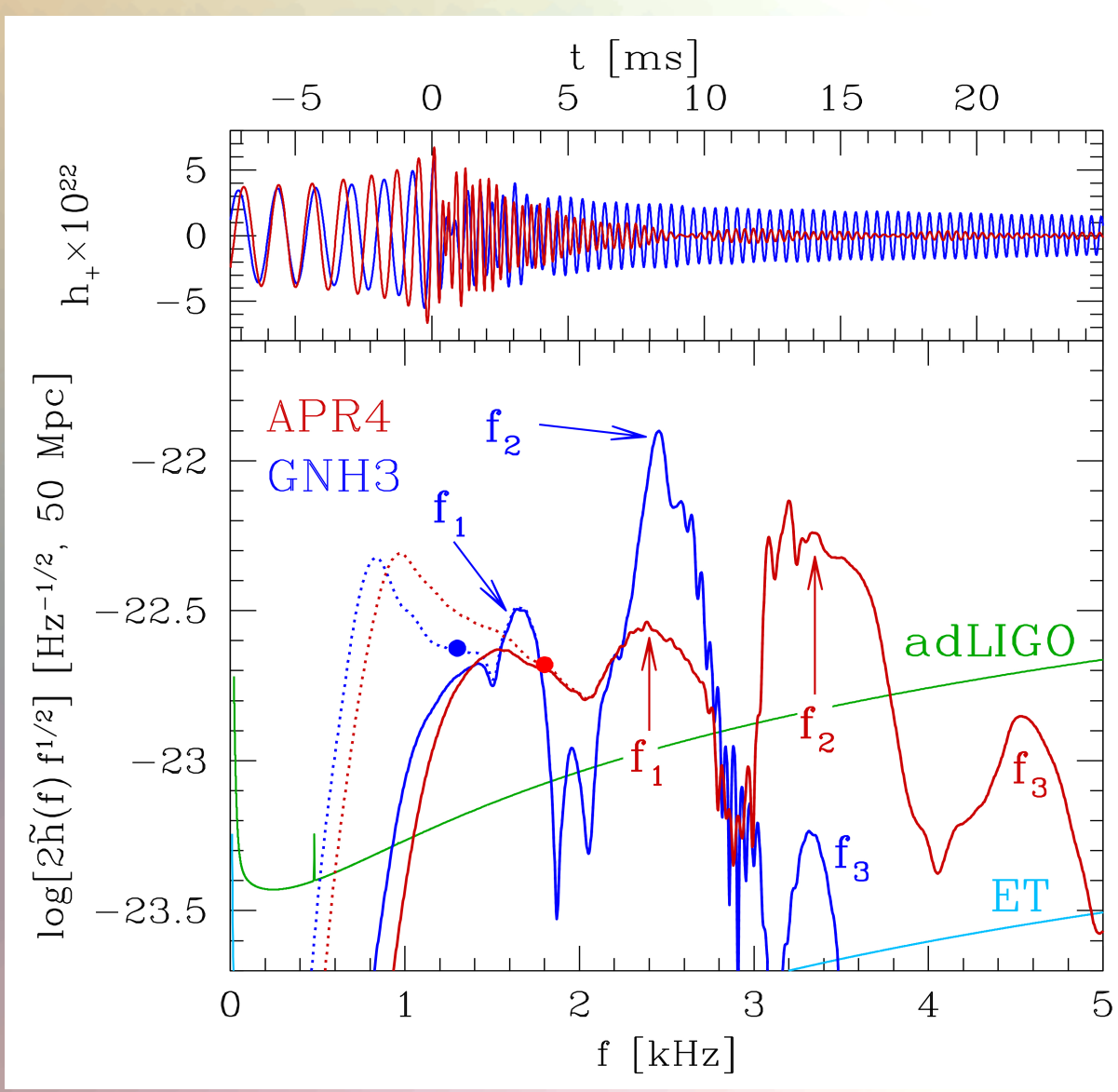

Two characteristic GW frequency peaks (f_1 and f_2); the origin of f_1 comes from t<3 ms. By measuring M, f_1 and f_2 one can set high constraints on the EoS.

See:
"Spectral properties of the post-merger gravitational-wave signal from binary neutron stars", Kentaro Takami, Luciano Rezzolla, and Luca Baiotti, PHYSICAL REVIEW D 91, 064001 (2015)

About the Internal Structure of Neutron Star Merger Products

1. Introduction
2. Static Properties of Compact Stars
3. **Numerical Relativity and Relativistic Hydrodynamics of Neutron Star Mergers**
4. Properties of Hypermassive Neutron Stars
5. Outlook
6. Summary

Relativistic Hydrodynamics and Numerical General Relativity

To solve the Einstein- and Hydrodynamical equation numerically, their mathematical structure has to be reformulated.

$$R_{\mu\nu} - \frac{1}{2} g_{\mu\nu} R = 8\pi T_{\mu\nu}$$

$$\nabla_\mu (\rho u^\mu) = 0\,,$$
$$\nabla_\nu T^{\mu\nu} = 0\,.$$

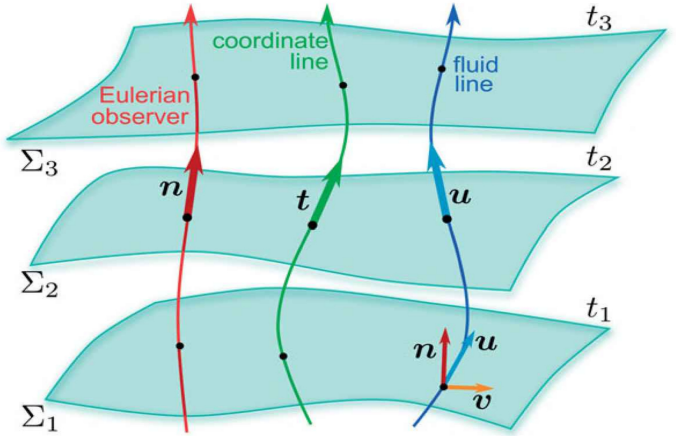

(3+1) decomposition of spacetime

$$g_{\mu\nu} = \begin{pmatrix} -\alpha^2 + \beta_i \beta^i & \beta_i \\ \beta_i & \gamma_{ij} \end{pmatrix}$$

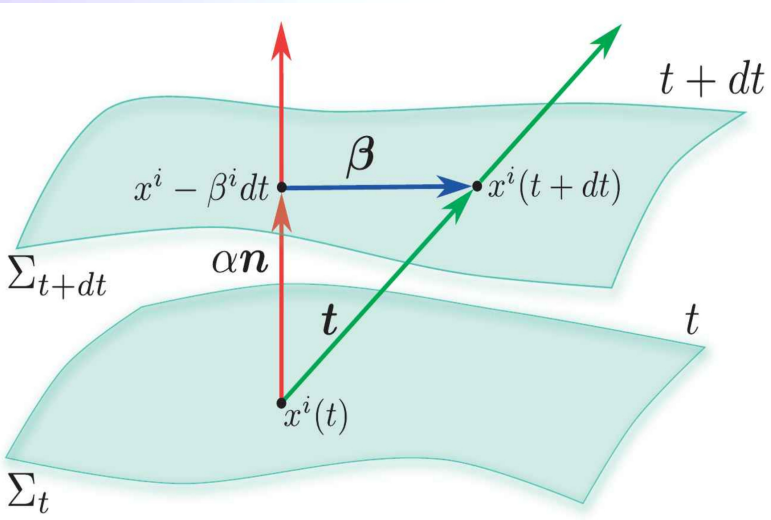

Lapse function α :

$$d\tau^2 = \alpha^2(t, x^j) dt^2$$

Shift vector β^i:

$$x^i_{t+dt} = x^i_t - \beta^i(t, x^j) dt$$

All figures and equations from: Luciano Rezzolla, Olindo Zanotti: Relativistic Hydrodynamics, Oxford Univ. Press, Oxford (2013)

The Frame-Dragging Effect

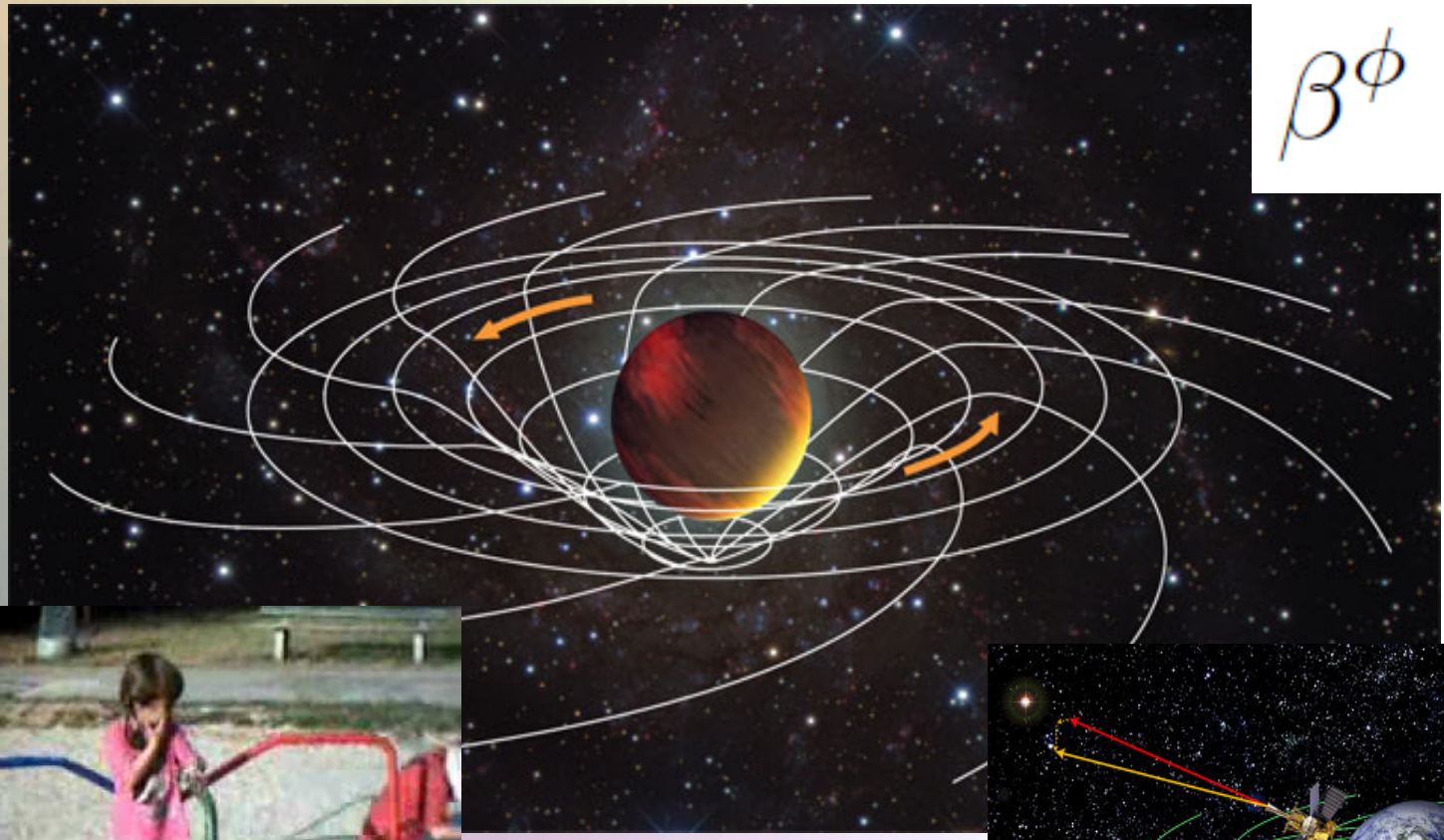

β^{ϕ}

Experiments

LARES

Gravity Probe B

merry-go-round

$$g_{\mu\nu} = \begin{pmatrix} -\alpha^2 + \beta_i\beta^i & \beta_i \\ \beta_i & \gamma_{ij} \end{pmatrix}$$

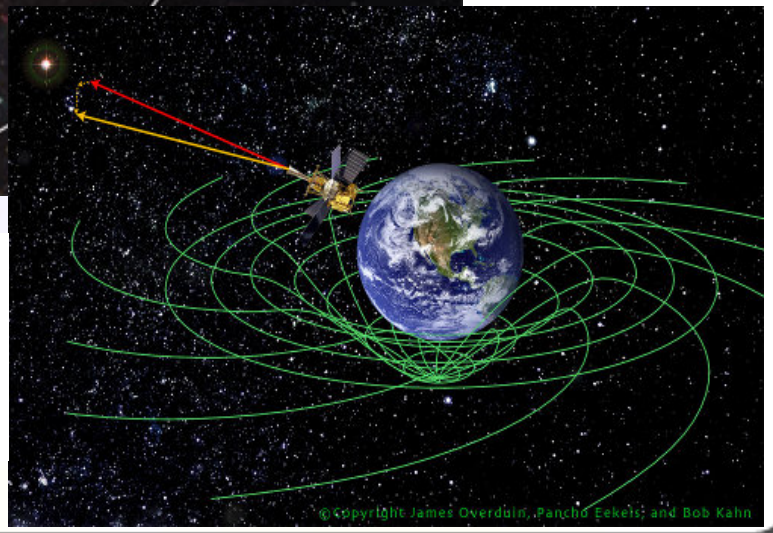

The Angular Velocity in the (3+1)-Split

$$\Omega(x,y,z,t) = \Omega = \frac{d\phi}{dt} = \frac{dx^\phi}{dt} = \qquad \text{with:} \quad x^\mu = (t, r, \phi, \theta)$$

$$= \frac{dx^\phi}{dt} = \frac{\frac{dx^\phi}{d\tau}}{\frac{dt}{d\tau}} = \frac{u^\phi}{u^t} \quad (1) \text{ with:} \quad u^\mu = \frac{dx^\mu}{d\tau}$$

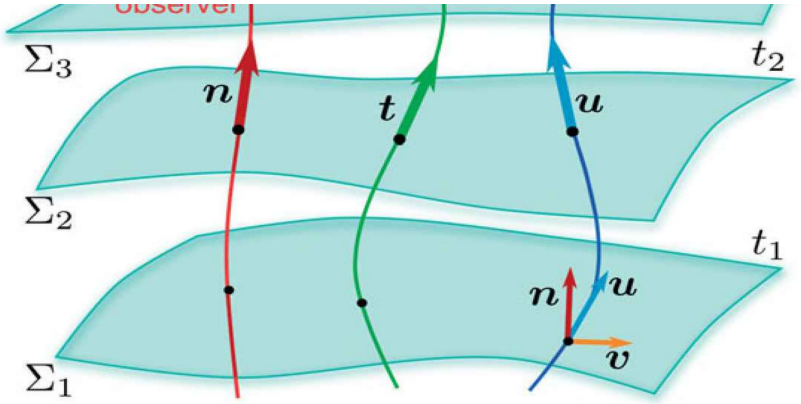

The angular velocity in the (3+1)-Split is a combination of the lapse function, the phi-component of the shift vector and the 3-velocity **v** of the fluid (spatial projection of the 4-velocity **u**)

$$v^i = \frac{\gamma^i_\mu u^\mu}{-n_\mu u^\mu} = \frac{1}{\alpha}\left(\frac{u^i}{u^t} - \beta^i\right) \qquad \text{with:} \quad i = 1,2,3 \text{ and } \mu = 0,1,2,3$$

$$\Leftrightarrow \quad \frac{u^i}{u^t} = \alpha v^i - \beta^i \qquad \text{Insert in (1)} \Rightarrow$$

$$\boxed{\Omega = \frac{d\phi}{dt} = \frac{u^\phi}{u^t} = \alpha v^\phi - \beta^\phi}$$

The ADM equations

The ADM (Arnowitt, Deser, Misner) equations come from a reformulation of the Einstein equation using the (3+1) decomposition of spacetime.

$$\partial_t \gamma_{ij} = -2\alpha K_{ij} + \mathcal{L}_{\boldsymbol{\beta}} \gamma_{ij} = -2\alpha K_{ij} + D_i \beta_j + D_j \beta_i$$

$$\partial_t K_{ij} = - D_i D_j \alpha + \beta^k \partial_k K_{ij} + K_{ik} \partial_j \beta^k + K_{kj} \partial_i \beta^k + \alpha \left({}^{(3)}R_{ij} + K K_{ij} - 2 K_{ik} K^k{}_j \right) + 4\pi\alpha \left[\gamma_{ij} (S - E) - 2 S_{ij} \right]$$

Time evolving part of ADM

$$D_j (K^{ij} - \gamma^{ij} K) = 8\pi S^i$$

$${}^{(3)}R + K^2 - K_{ij} K^{ij} = 16\pi E$$

Constraints on each hypersurface

Three dimensional covariant derivative

$$D_\nu := \gamma^\mu{}_\nu \nabla_\mu = (\delta^\mu_\nu + n_\nu n^\mu) \nabla_\mu$$

Three dimensional Riemann tensor

$${}^{(3)}R^\mu{}_{\nu\kappa\sigma} = \partial_\kappa {}^{(3)}\Gamma^\mu_{\nu\sigma} - \partial_\sigma {}^{(3)}\Gamma^\mu_{\nu\kappa} + {}^{(3)}\Gamma^\mu_{\lambda\kappa} {}^{(3)}\Gamma^\lambda_{\nu\sigma} - {}^{(3)}\Gamma^\mu_{\lambda\sigma} {}^{(3)}\Gamma^\lambda_{\nu\kappa}$$

$${}^{(3)}\Gamma^\alpha_{\beta\gamma} = \frac{1}{2} \gamma^{\alpha\delta} \left(\partial_\beta \gamma_{\gamma\delta} + \partial_\gamma \gamma_{\delta\beta} - \partial_\delta \gamma_{\beta\gamma} \right)$$

Spatial and normal projections of the energy-momentum tensor:

$$S_{\mu\nu} := \gamma^\alpha{}_\mu \gamma^\beta{}_\nu T_{\alpha\beta} ,$$
$$S_\mu := -\gamma^\alpha{}_\mu n^\beta T_{\alpha\beta} ,$$
$$S := S^\mu{}_\mu ,$$
$$E := n^\alpha n^\beta T_{\alpha\beta} ,$$

Extrinsic Curvature:

$$K_{\mu\nu} := -\gamma^\lambda{}_\mu \nabla_\lambda n_\nu = -\frac{1}{2} \mathcal{L}_{\boldsymbol{n}} \gamma_{ij}$$

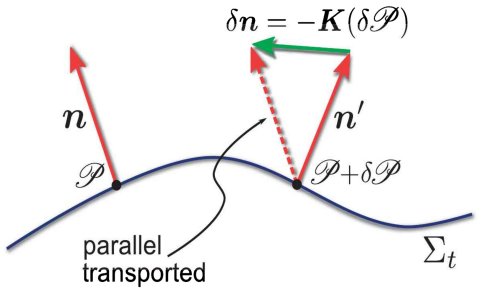

All figures and equations from: Luciano Rezzolla, Olindo Zanotti: Relativistic Hydrodynamics, Oxford Univ. Press, Oxford (2013)

About the Internal Structure of Neutron Star Merger Products

1. Introduction
2. Static Properties of Compact Stars
3. Numerical Relativity and Relativistic Hydro-dynamics of Neutron Star Mergers
4. Properties of Hypermassive Neutron Stars
   - Thermally hybrid EoS
   - Fully temperature dependent EoS
5. Outlook
6. Summary

Numerical Relativity and Relativistic Hydrodynamics

Five different EoS : **ALF2**, APR4, GNH3, H4 and Sly, approximated by piecewise polytopes. Two different masses: M=1.25 and M=1.35

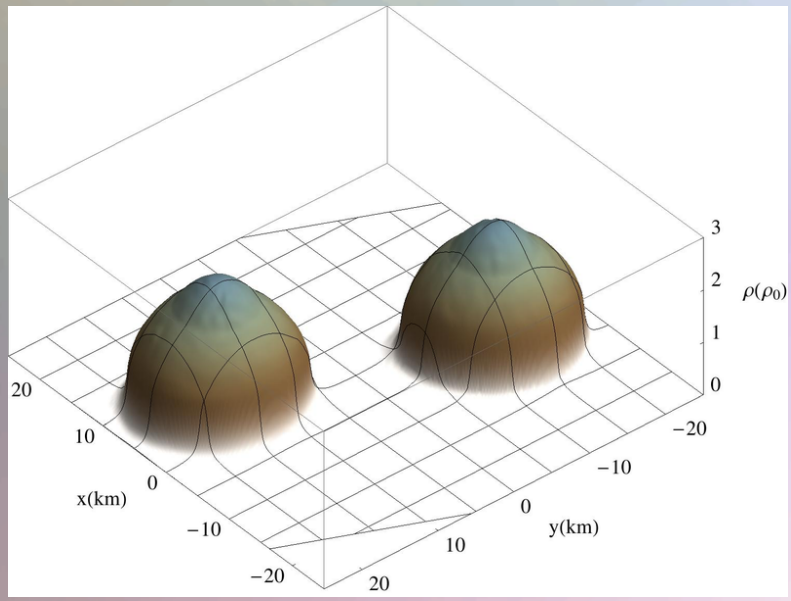

Simulations were done by Kentaro Takami

BSSNOK conformal traceless formulation of the ADM equations. 3+1 Valencia formulation and high resolution shock capturing methods for the hydrodynamic evolution. Simulations have been performed in full general relativity using the WHISKY code for the general-relativistic hydrodynamic equations. No Spin, no magnetic field, no neutrino leakage.

<u>Grid Structure</u>

Adaptive mesh refinement (six ref. levels)

Grid resolution: (from 221 m to 7.1 km)

Outer Boundary: 759 km

Initial separation of stellar cores: 45 km

The Equation of States

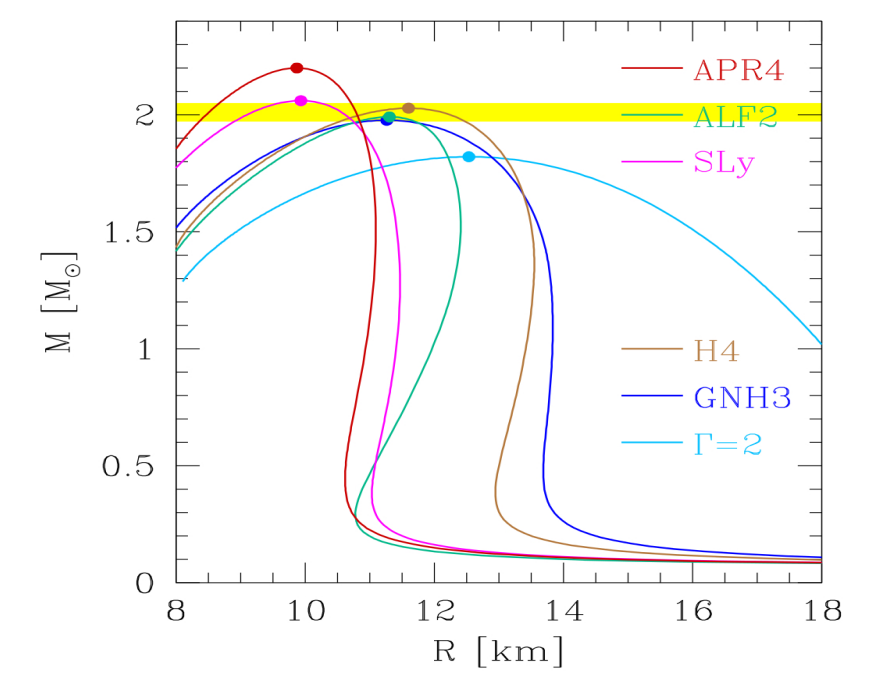

[1] A. Akmal, V. R. Pandharipande, and D. G. Ravenhall, Phys. Rev. C 58, 1804 (1998)

[2] F. Douchin and P. Haensel, Astron. Astrophys. 380, 151 (2001)

[3] N. K. Glendenning, Astrophys. J. 293, 470 (1985)

[4] N. K. Glendenning and S. A. Moszkowski, Phys. Rev. Lett. 67, 2414 (1991)

[5] M. Alford, M. Braby, M. Paris, and S. Reddy, Astrophys. J. 629, 969 (2005)

APR4 [1] and **SLy** [2] belong to the class of variational method EOSs (neutrons, protons, electrons and muons). **GNH3** [3] and **H4** [4] are relativistic mean-field models (neutrons, protons, electrons, muons and hyperons).

ALF2 [5] is a model for hybrid stars; it has implemented a phase transition to color-flavor-locked quark matter. Assuming a moderate surface tension, Gibbs-construction used (mixed phase from $3\rho_0$ up to $7.8\rho_0$). Pasta phase is expected to be present in the mixed phase (tiny, positively charged quark matter droplets → later rods and slabs (spaghetti and lasagne).

Thermal Contribution to the EoSs

Cold part of the EoS is adequate to describe neutron-star matter prior to the merger. After contact, when the HMNS is formed, large shocks will however increase the temperature. The total pressure p and the specific internal energy ε are therefore composed of a cold nuclear-physics part p_c (APR4, SLY, GNH3, H4 and ALF2) and an thermal ideal fluid component p_{th}:

$$p = p_{\rm c} + p_{\rm th}\,, \quad \epsilon = \epsilon_{\rm c} + \epsilon_{\rm th}$$

Where the thermal, ideal fluid part is given by (Γ_{th} =2):

$$p_{\rm th} = \rho\epsilon_{\rm th}\left(\Gamma_{\rm th} - 1\right)\,, \quad \epsilon_{\rm th} = \epsilon - \epsilon_{\rm c}$$

Cold part of the EoSs is approximated by piecewise polytropes (i=1..4) :

$$p_{\rm c} = K_i\rho^{\Gamma_i}\,, \quad \epsilon_{\rm c} = \epsilon_i + K_i\frac{\rho^{\Gamma_i - 1}}{\Gamma_i - 1}$$

The HMNS Lifetime for different EoS M=1.35

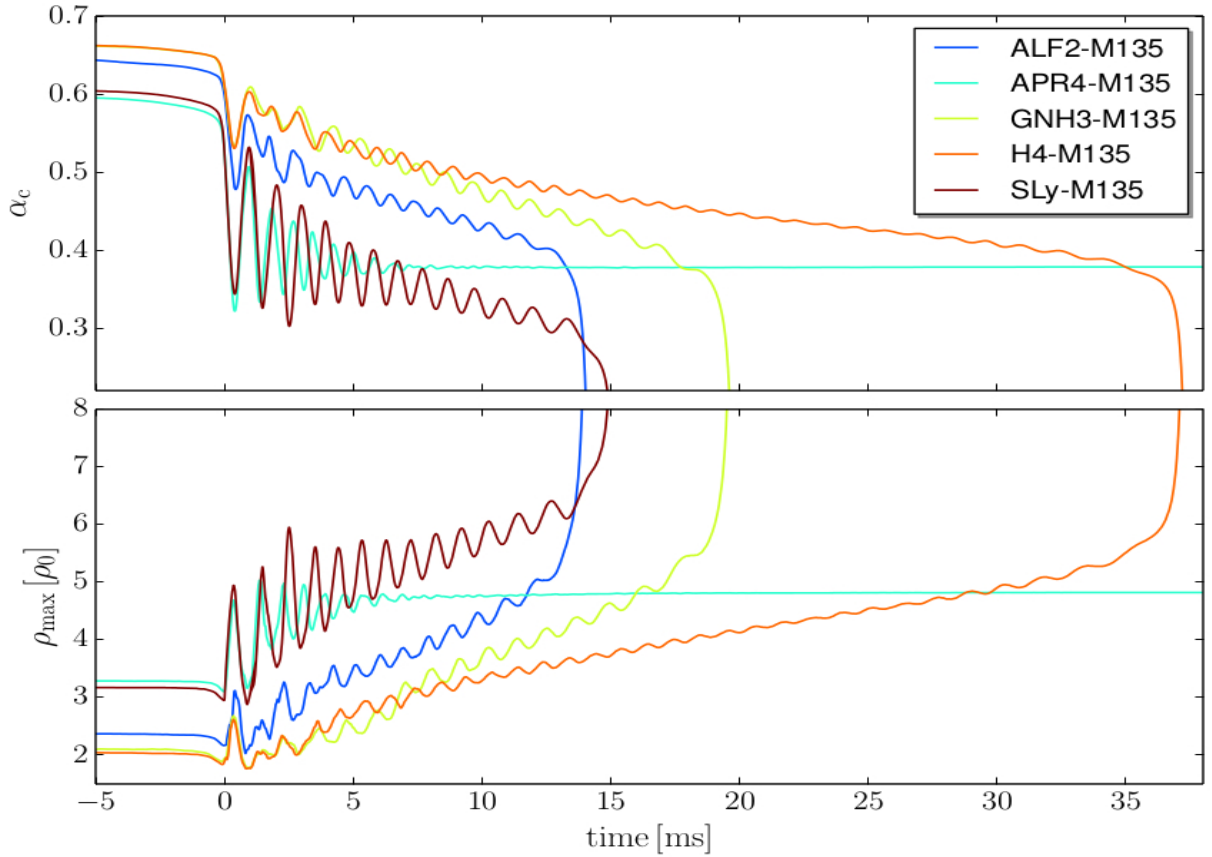

Central value of the lapse function α_c (upper panel) and maximum of the rest mass density ρ_{max} in units of ρ_0 (lower panel) versus time for the high mass simulations .

EoS: ALF2, M=1.35 Post-Merger Phase

Gravitational wave amplitude h_+ and |h| at a distance of 738 km

for the ALF2-M135 model

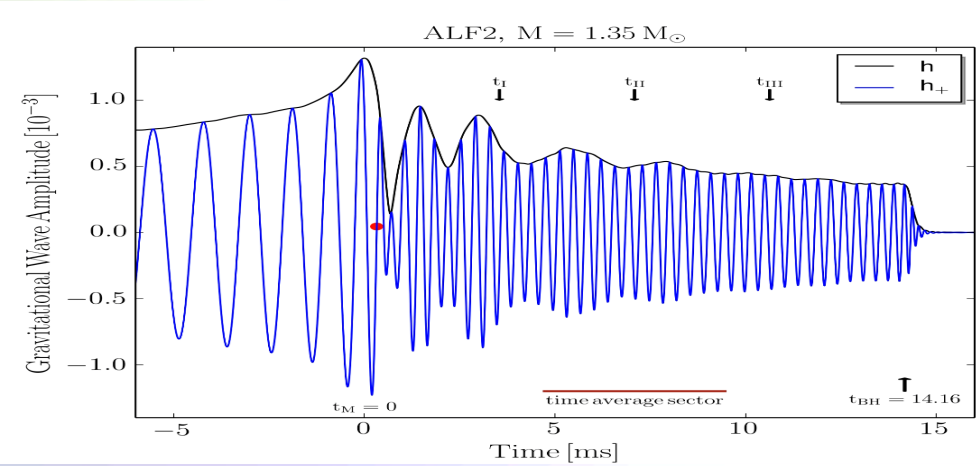

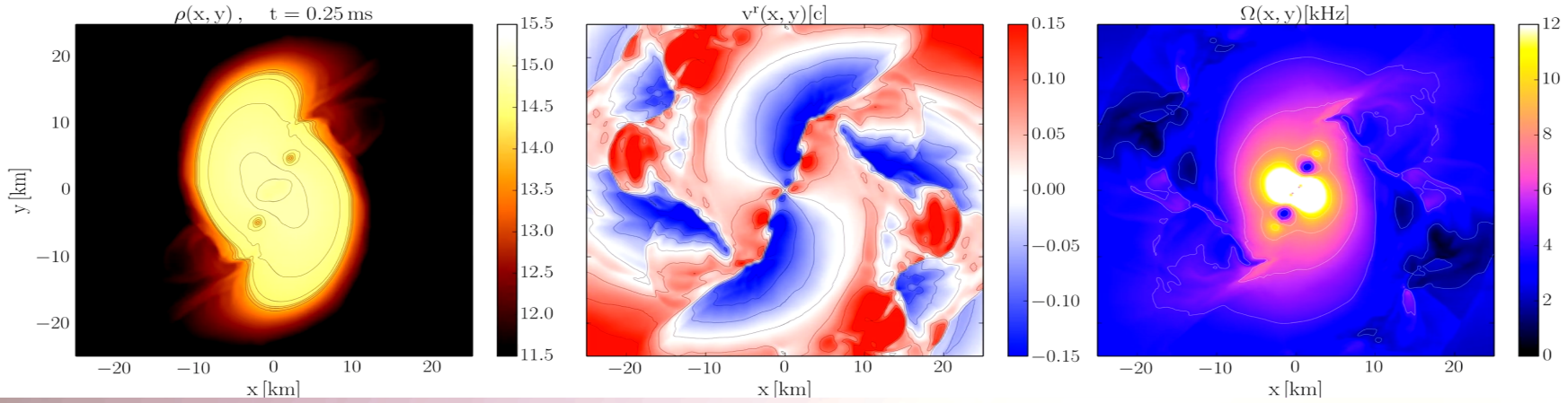

EoS: ALF2, M=1.35 Post-Merger Phase

$$\Omega(x,y,z,t)|_{z=0} =$$

$$\alpha(x,y,t) \quad \cdot \quad v^{\phi}(x,y,t) \quad - \quad \beta^{\phi}(x,y,t)$$

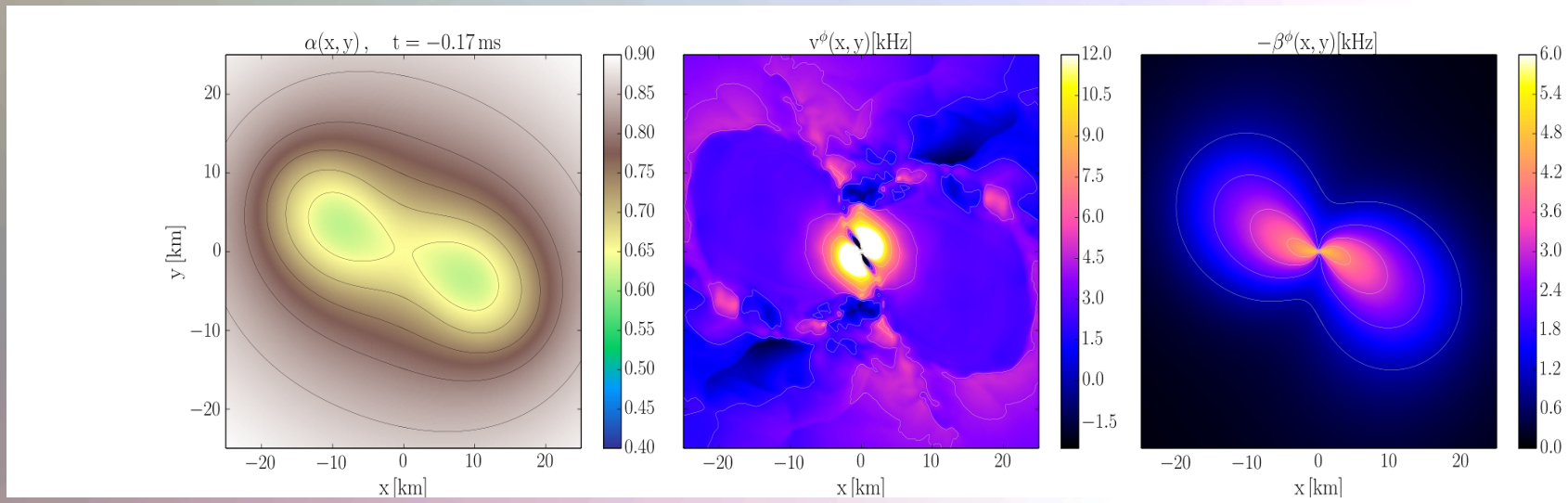

The angular velocity Ω is consisting of a lapse (α) corrected part of the angular component of the three velocity v^i (i = x, y, z) minus a frame dragging related part which is mathematically described by the φ-component of the shift vector β^i.

EoS: ALF2, M=1.35 Post-Merger Phase

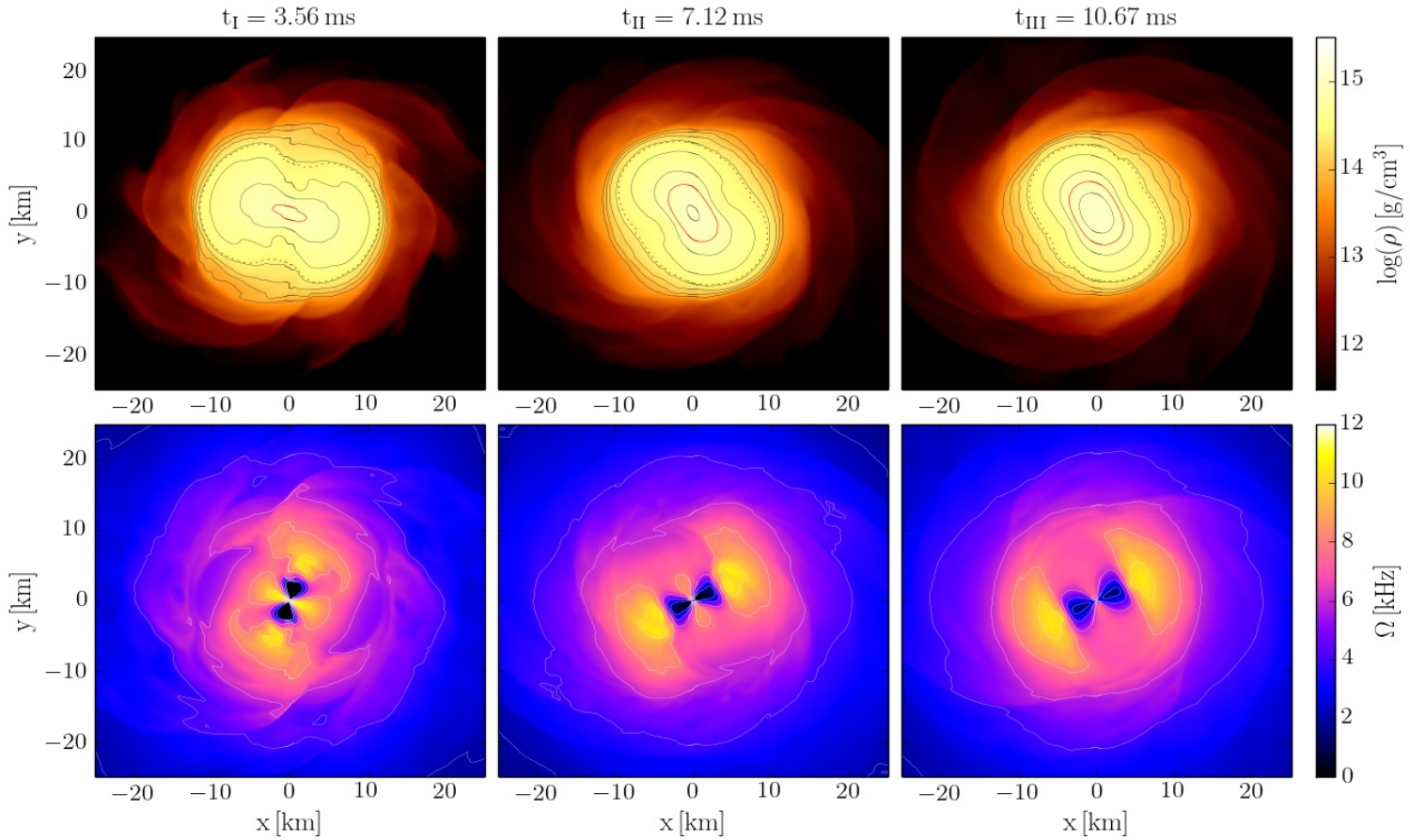

Logarithm of the rest mass density Log(ρ) [g/cm^3] (upper row) and fluid angular velocity Ω [kHz] (lower row) in the xy-plane at three different post-merger times.

The HMNS Lifetime for different EoS M=1.25

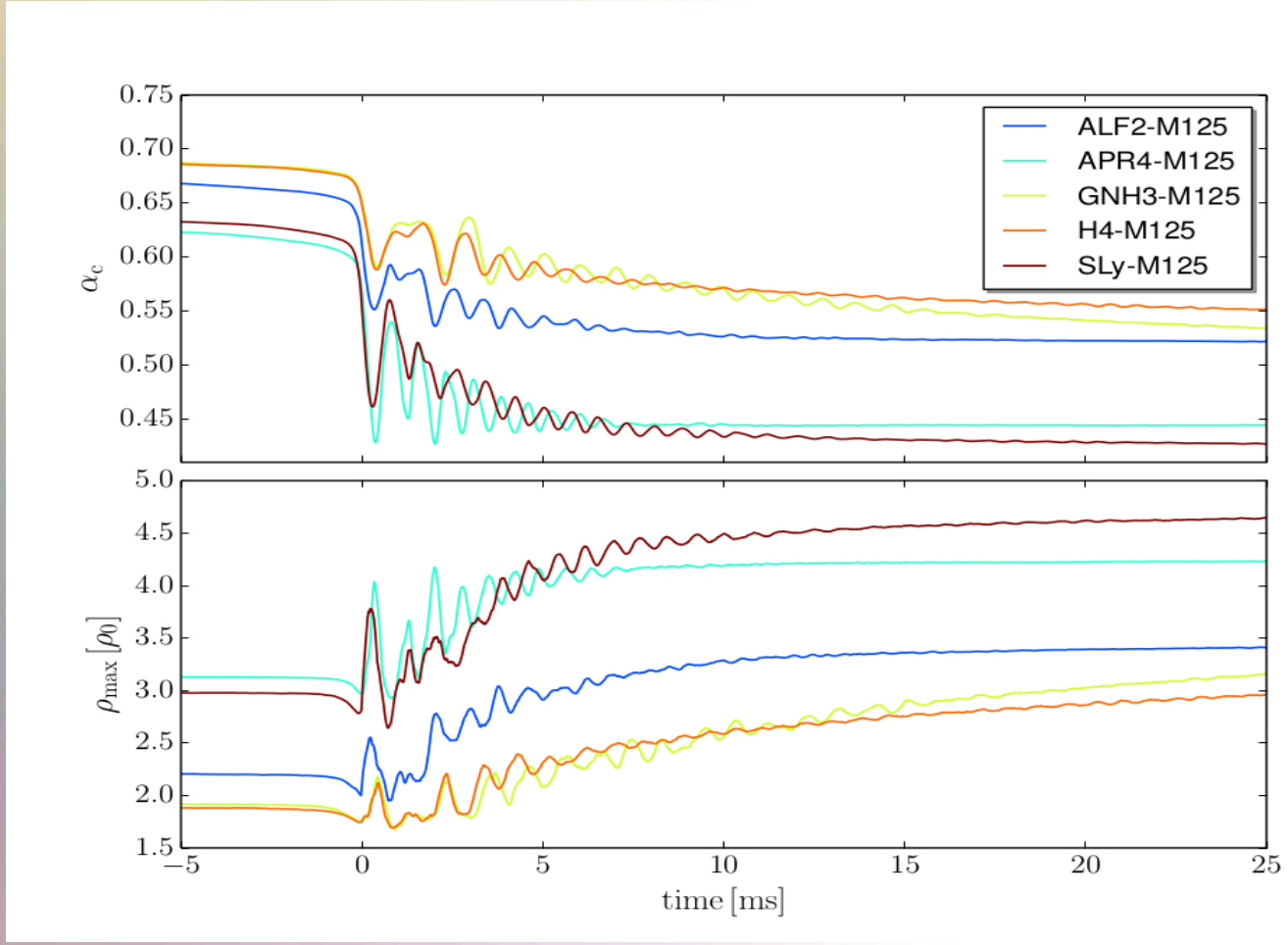

Central value of the lapse function α_c (upper panel) and maximum of the rest mass density ρ_{max} in units of ρ_0 (lower panel) versus time for the low mass simulations .

EoS: ALF2, M=1.25 Post Merger Phase

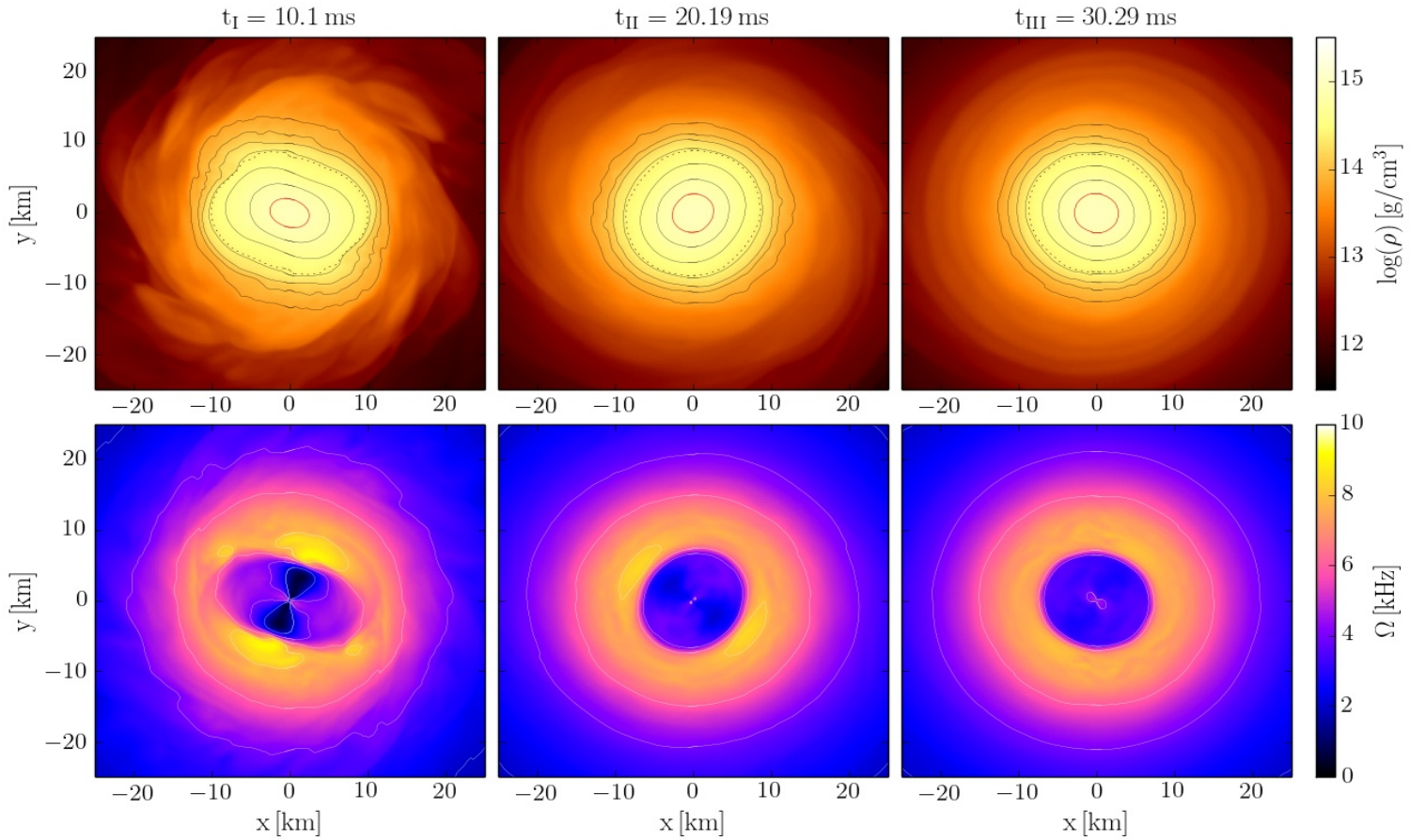

Logarithm of the rest mass density Log(ρ) [g/cm^3] (upper row) and fluid angular velocity Ω [kHz] (lower row) in the xy-plane at three different post-merger times.

Temperature dependent EoS (LS220)

To verify our results, a microphysical temperature- and composition-dependent equation of state (LS220, see Lattimer J. M., Swesty D. F., 1991, Nuclear Phys. A, 535, 331) has been used. The simulation where performed by **Luke Bovard**, who simulated the merging NS-NS-system (M=1.32) using the SuperMUC high-end supercomputer in Garching. The simulation took about 7 days using 1000 cores.

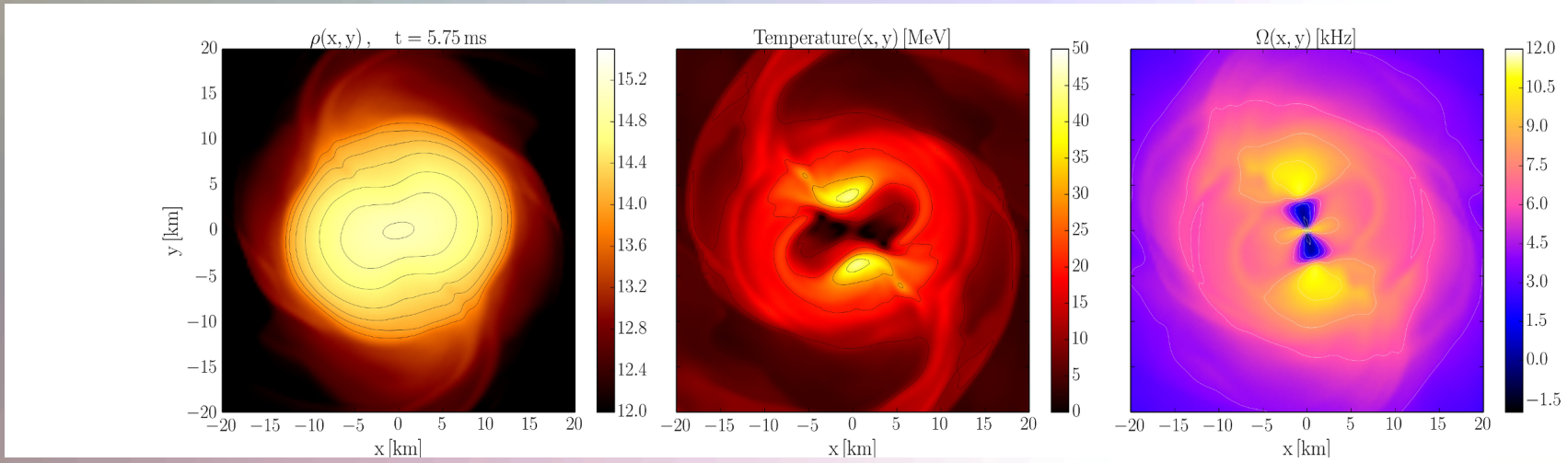

Logarithm of the rest mass density Log(ρ) [g/cm^3] (left), temperature T [Mev] (middle) and fluid angular velocity Ω [kHz] (right) in the xy-plane calculated with WhiskyTHC using the temperature-density dependent LS220-EoS.

Tracing the fluid cells t=[6,12] ms

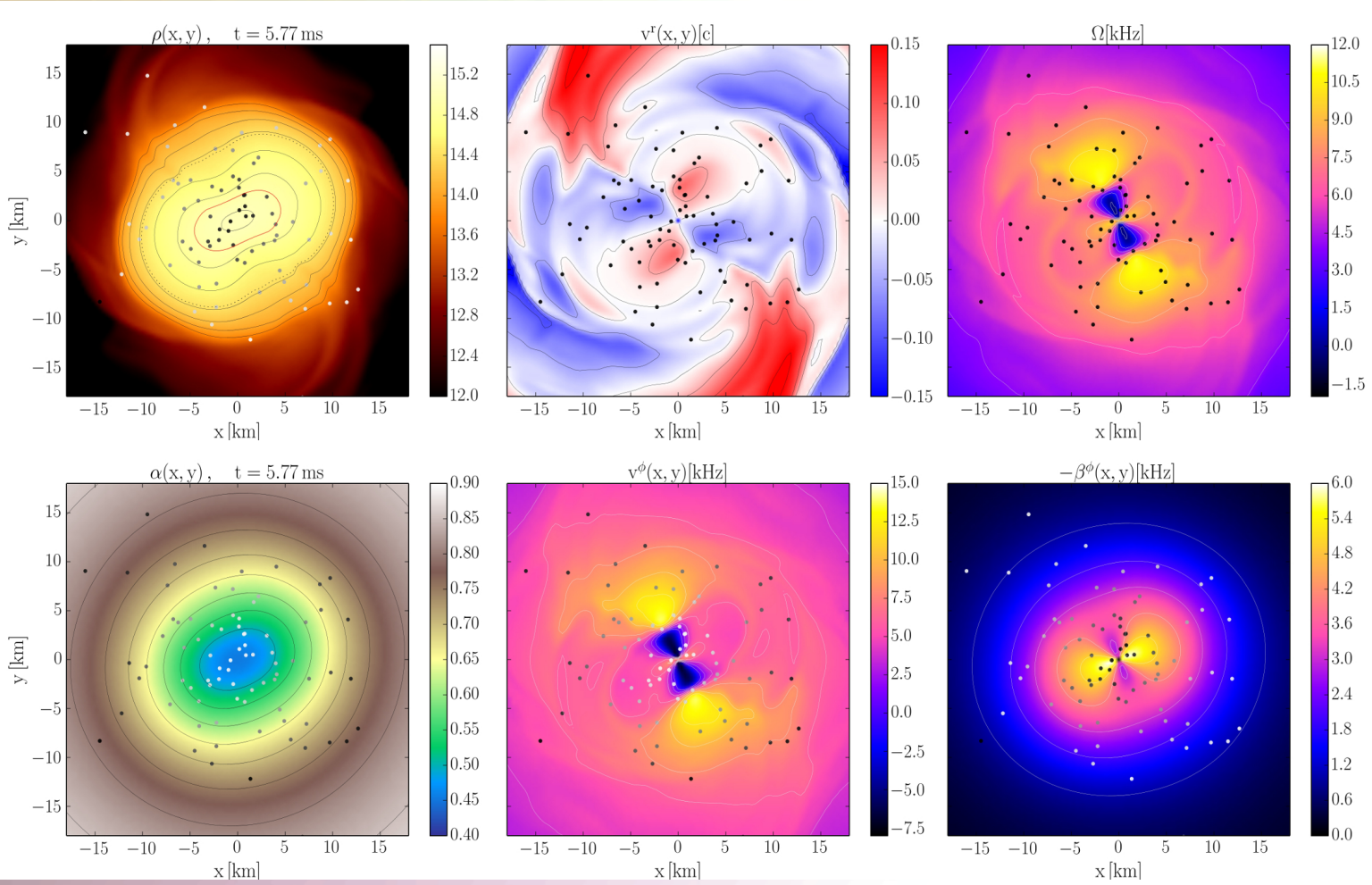

Logarithm of the rest mass density Log(ρ) [g/cm^3] (upper row), radial component of the 3-velocity v^i [c] (upper middle) and fluid angular velocity Ω [kHz] (upper right).
Lower row: Components of Ω (lapse α, velocity v^φ and shift β^φ)

Tracing the fluid cells t=[21,27] ms

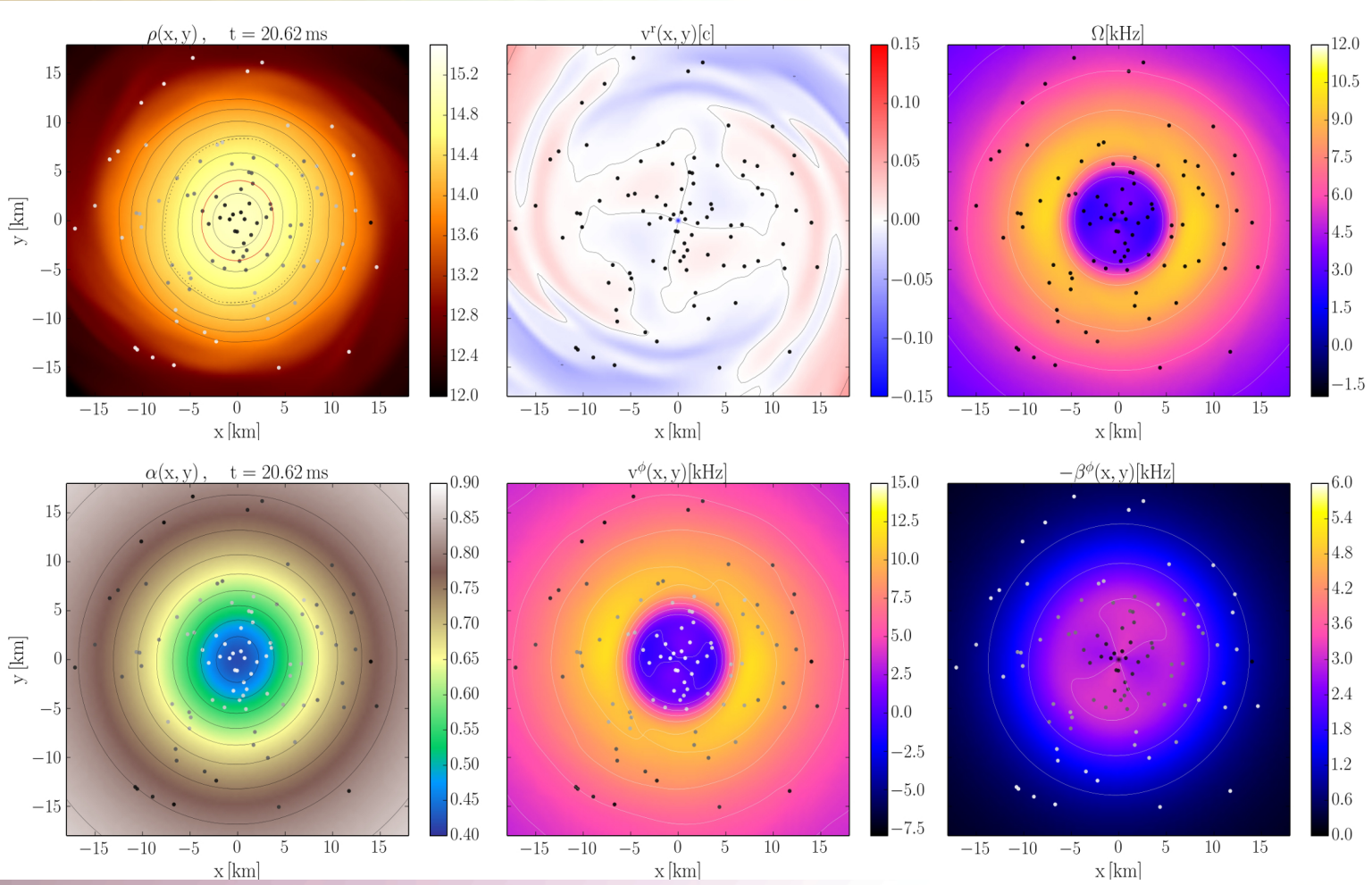

Logarithm of the rest mass density Log(ρ) [g/cm^3] (upper row), radial component of the 3-velocity v^i [c] (upper middle) and fluid angular velocity Ω [kHz] (upper right).
Lower row: Components of Ω (lapse α, velocity v^φ and shift β^φ)

Rotation Profile H4-EoS, M=1.35

Post Merger Phase

$$\Omega(x, y, z, t)|_{z=0} =$$

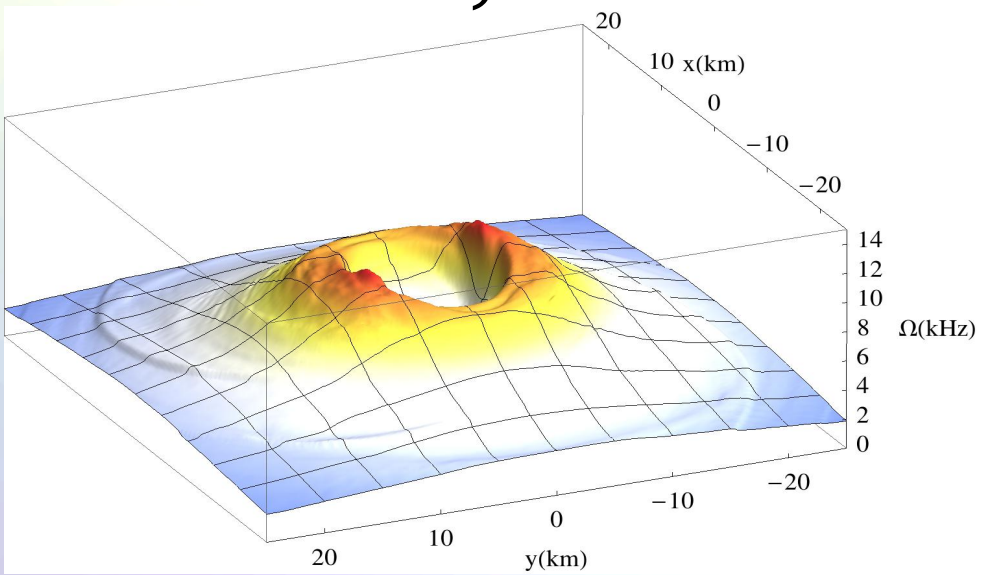

$$\Omega(r, \phi, z, t)|_{z=0} =$$

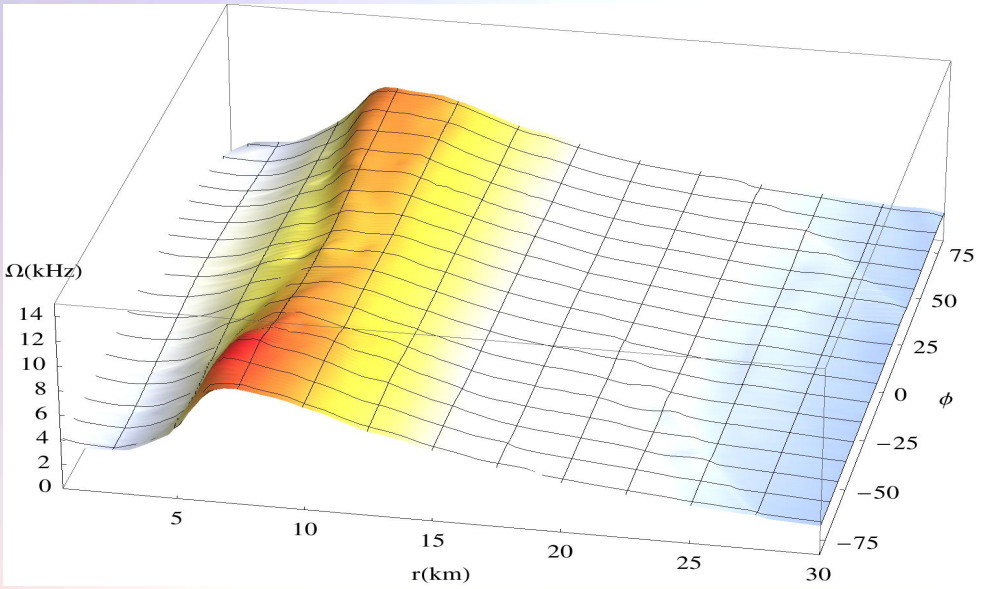

Φ-averaged Rotation Profile

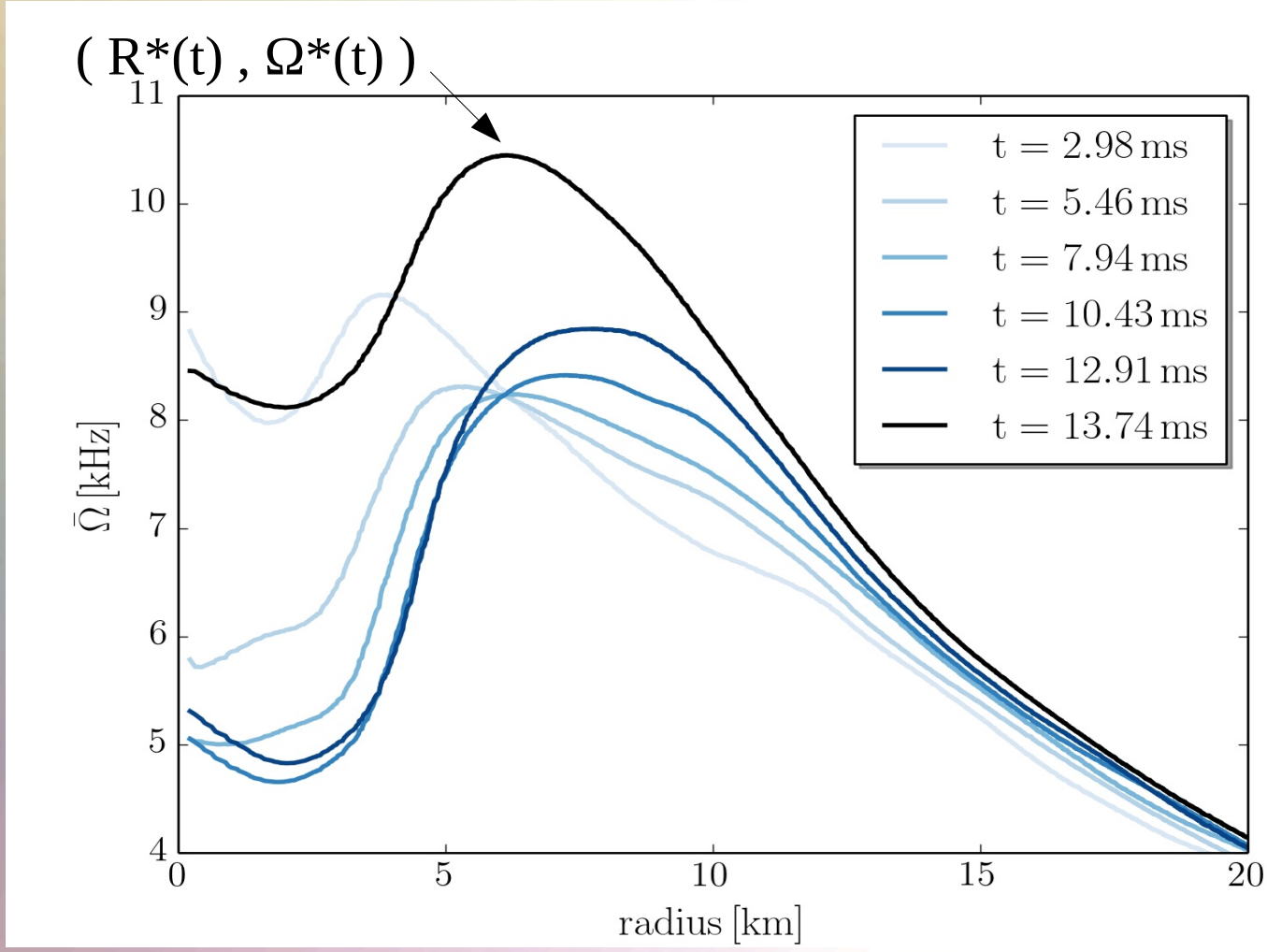

φ-averaged fluid angular velocity Ω in the equatorial plane for the ALF2-M135 model at different time segments (time average with Δt = 1 ms).

ALF2-M135: Ω* and R* vs. time

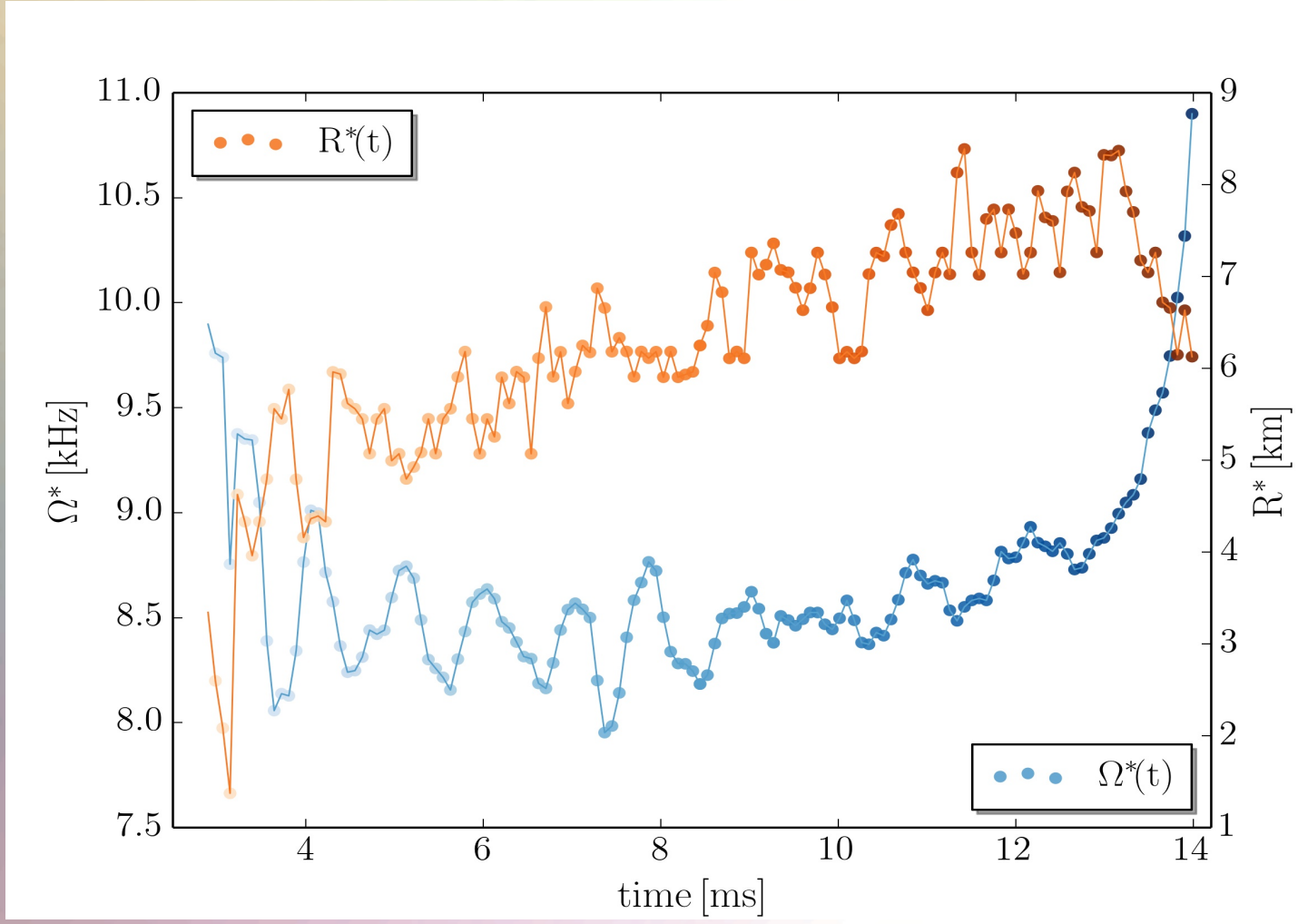

Maximum value of the rotation profile Ω* (blue points) and its radial position R* (orange points) calculated within the ALF2-M135 model as a function of time.

ALF2-M125: Ω* and R* vs. time

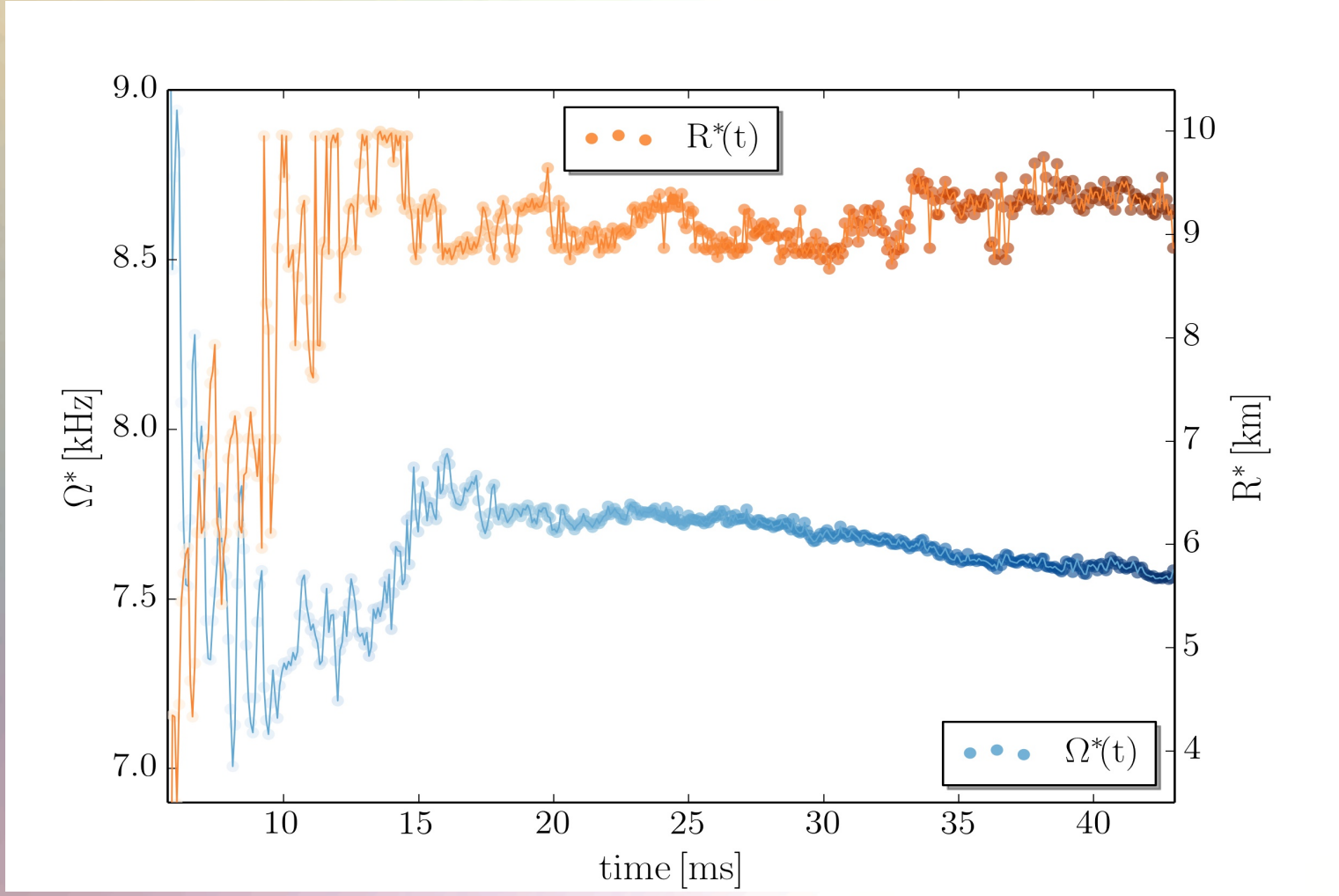

Maximum value of the rotation profile Ω* (blue points) and its radial position R* (orange points) calculated within the ALF2-M125 model as a function of time.

Averaging Procedure for Ω

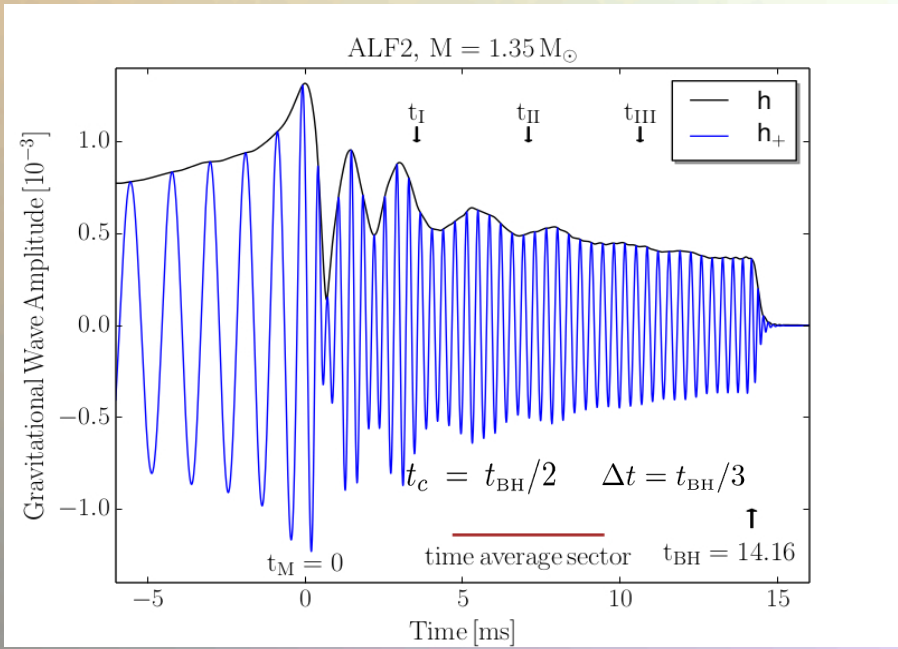

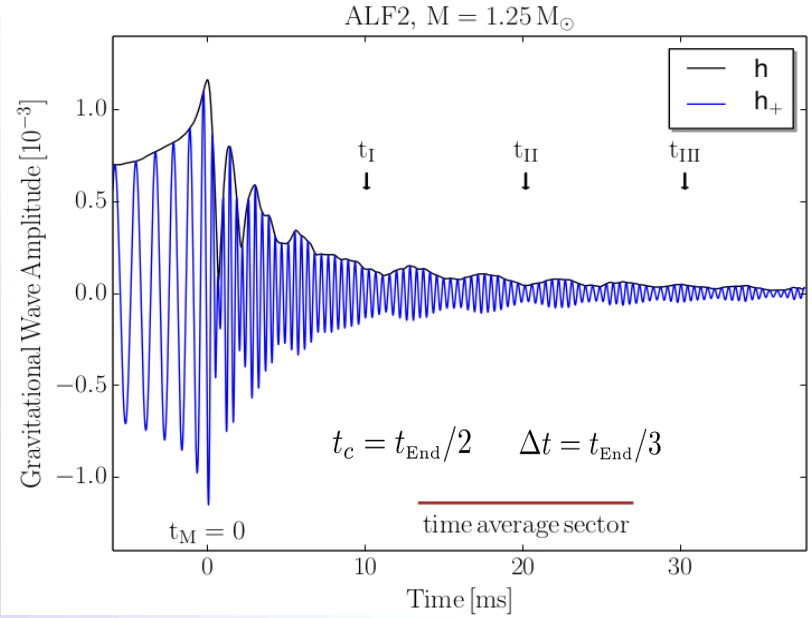

In order to compare the structure of the rotation profiles between the different EOSs, a certain time averaging procedure has been used:

$$\bar{\Omega}(r, t_c) = \int_{t_c - \Delta t/2}^{t_c + \Delta t/2} \int_{-\pi}^{\pi} \Omega(r, \phi, t') \; d\phi \, dt'$$

Time-averaged rotation profiles

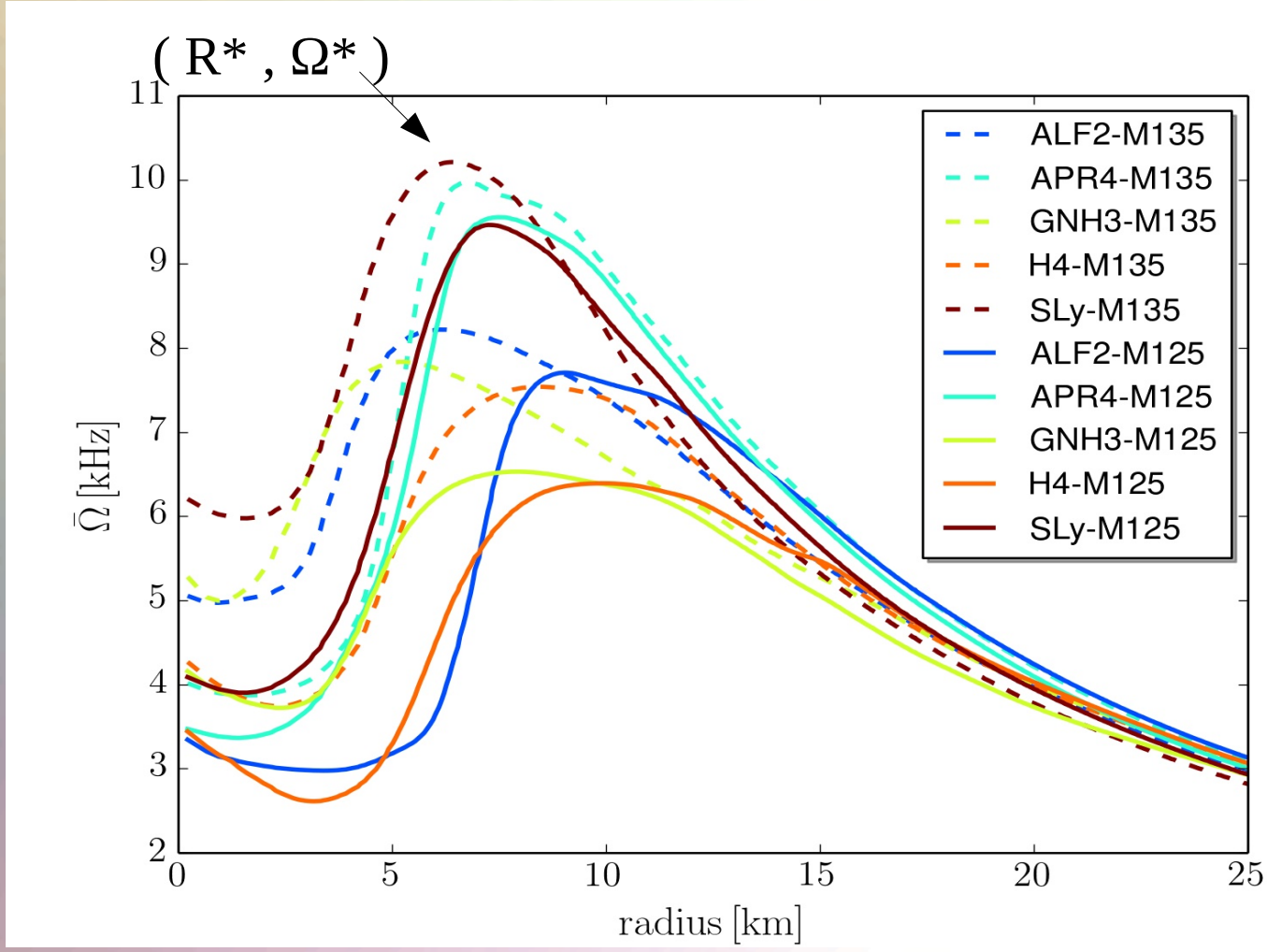

Soft EoSs:
Sly
APR4

Stiff EoSs:
GNH3
H4

Time-averaged rotation profiles for different EoS
Low mass runs (solid curves), high mass runs (dashed curves).

Ω* versus Compactness

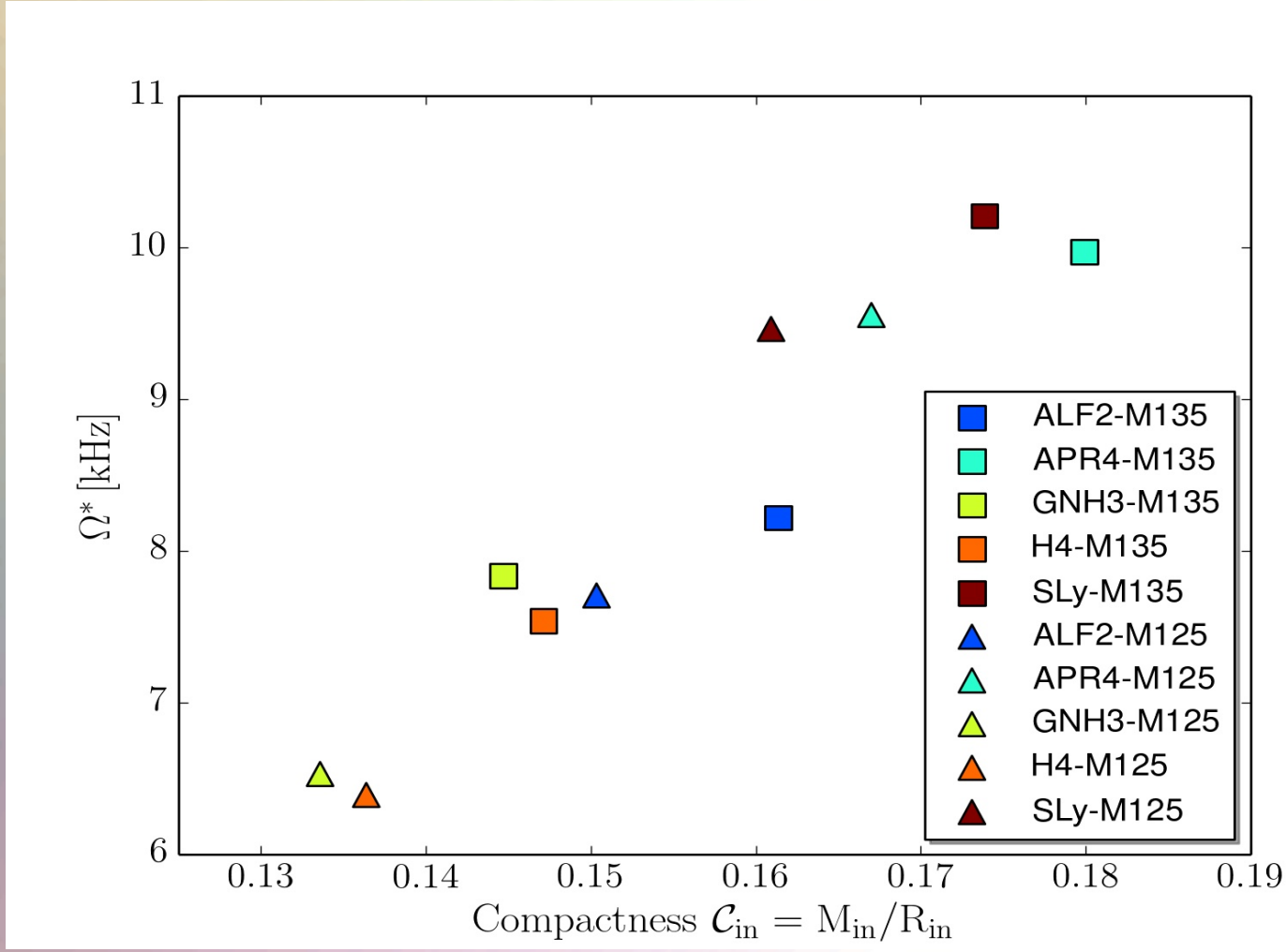

Maximum value Ω* [kHz] of the time-averaged rotation profiles versus the compactness of the initial star.

GW-Spectrum for different EoSs

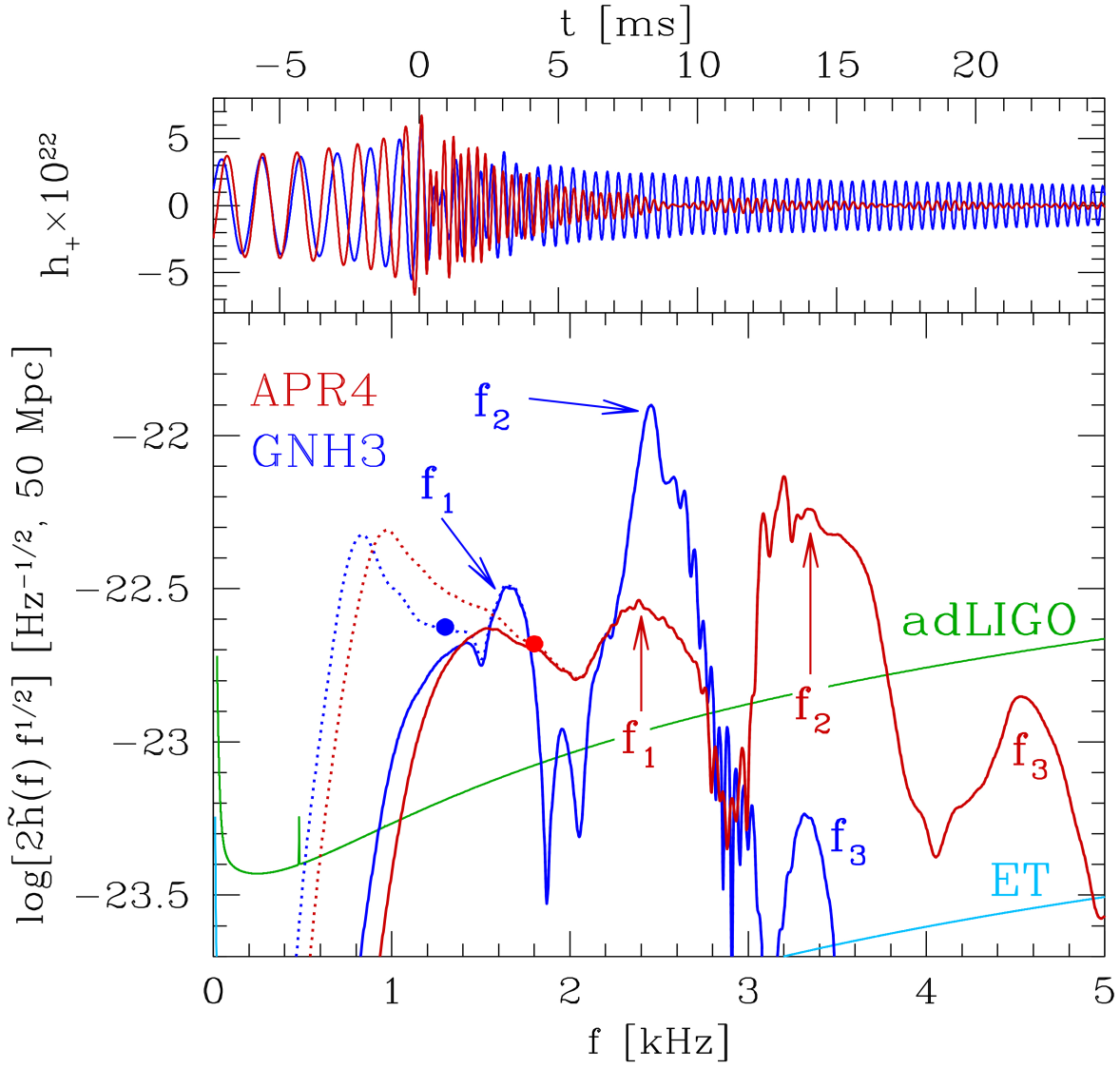

Two characteristic GW frequency peaks (f1 and f2); the origin of f1 comes from t<3 ms. By measuring M, f1 and f2 one can set high constraints on the EoS.

See:
"Spectral properties of the post-merger gravitational-wave signal from binary neutron stars", Kentaro Takami, Luciano Rezzolla, and Luca Baiotti, PHYSICAL REVIEW D 91, 064001 (2015)

Ω* versus GW-frequency Ω_2

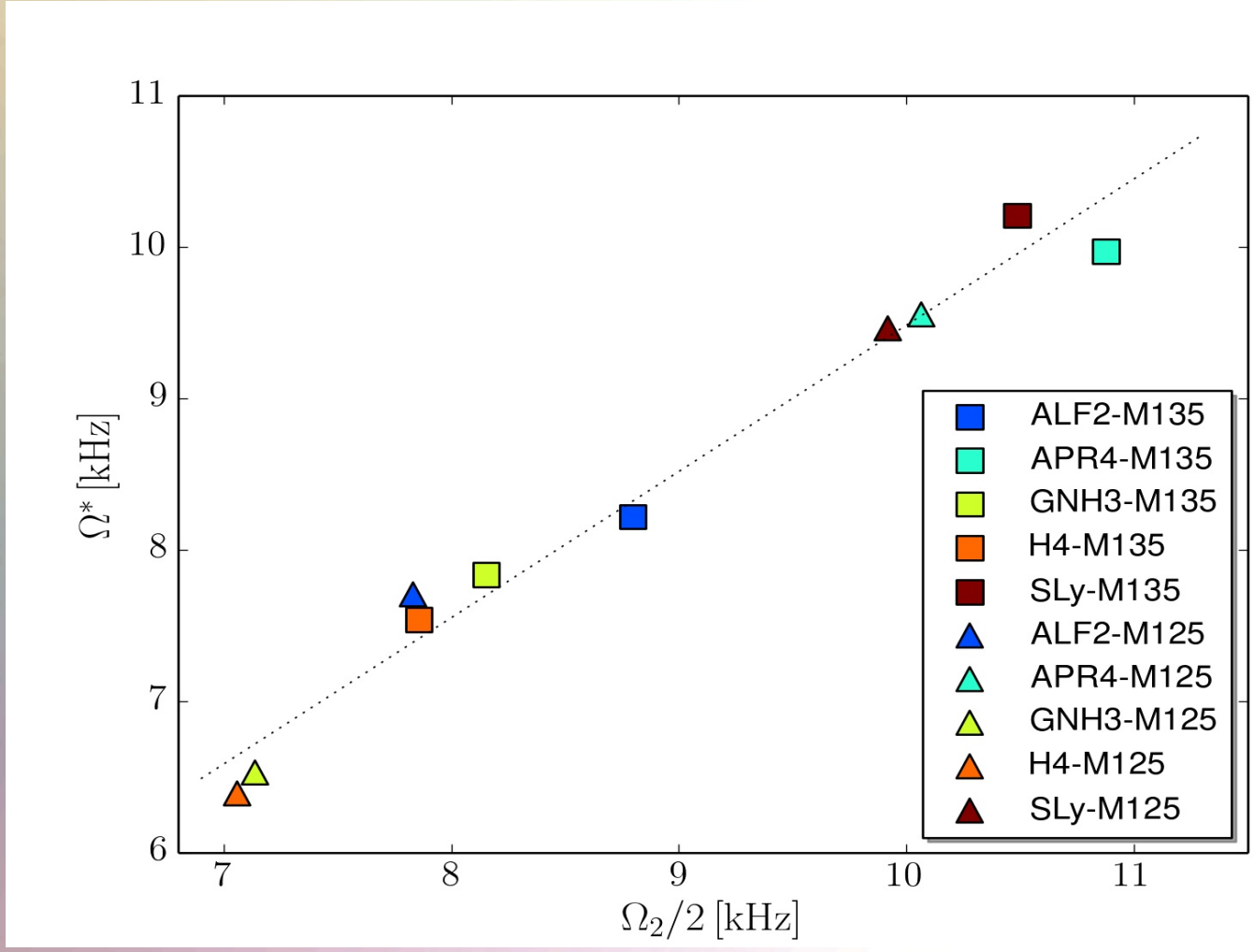

Maximum value Ω* [kHz] of the time-averaged rotation profiles versus the gravitational wave frequency-peak Ω_2 [kHz].

Ejected Mass

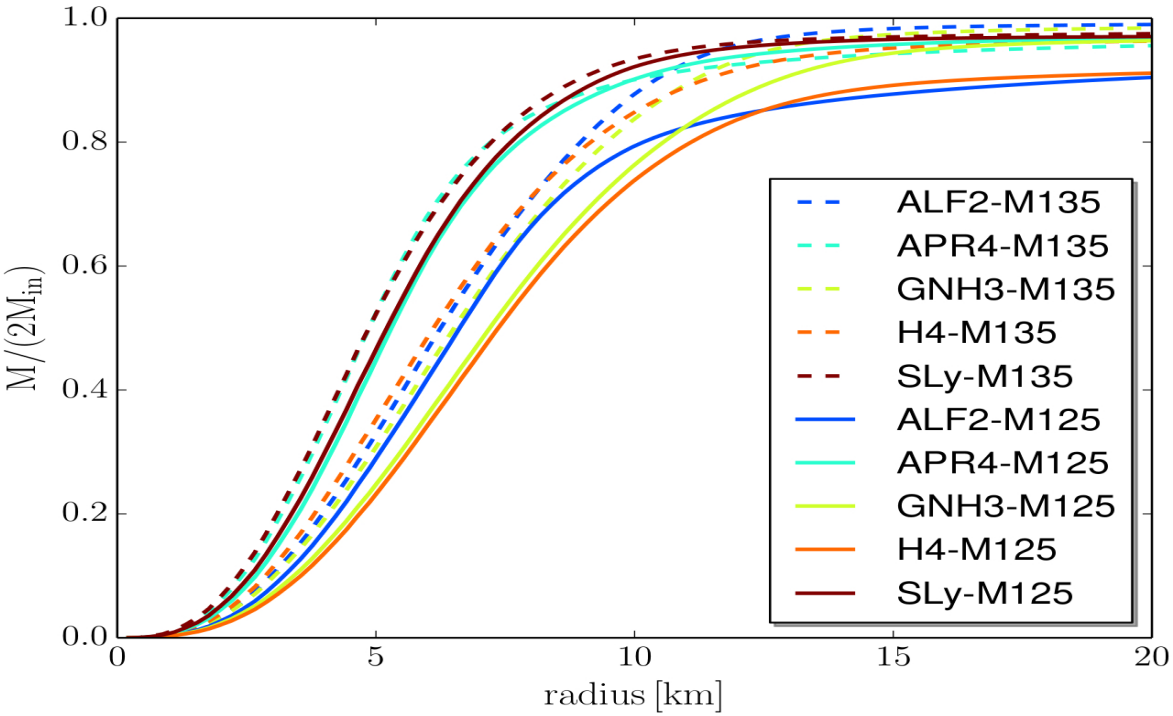

$$M_{\rm b}(r) = \int_0^{2\pi}\int_0^{\pi}\int_0^{r} \sqrt{\gamma}\, W \rho\, \tilde{r}^2 \sin(\theta)\, d\tilde{r} d\theta d\phi$$

$$\textbf{with:} \qquad W = \alpha\, u^t = \frac{1}{\sqrt{1 - v^i v_i}} \quad ,$$

Total rest mass M_b divided by the total rest mass of the system ($2M_{in}$) as a function of the radial distance [km].

ALF2-M135: Hoop Conjecture

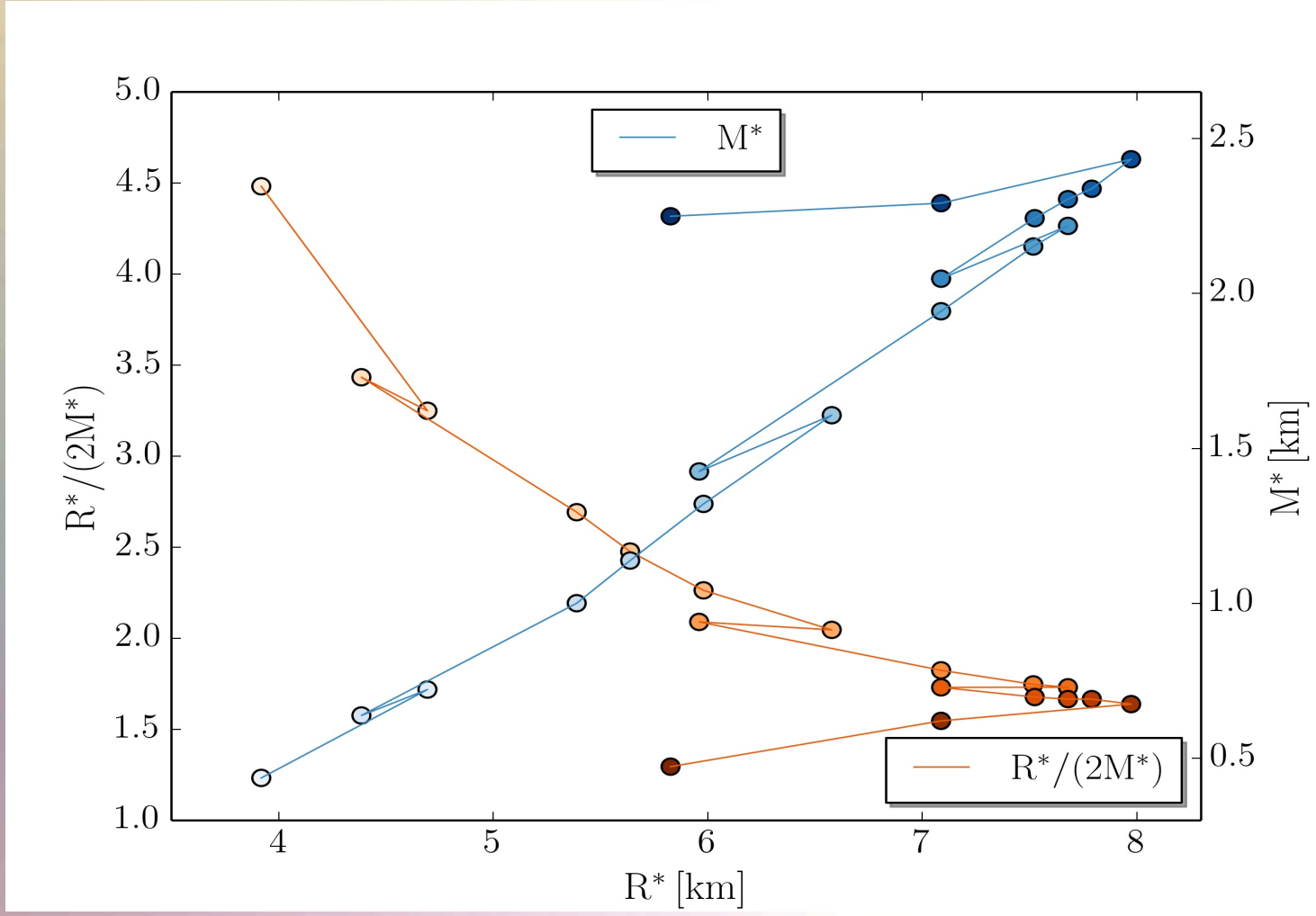

Mass M* which is inside a sphere of r < R* as a function of R*.

R*/(2M*) versus Compactness

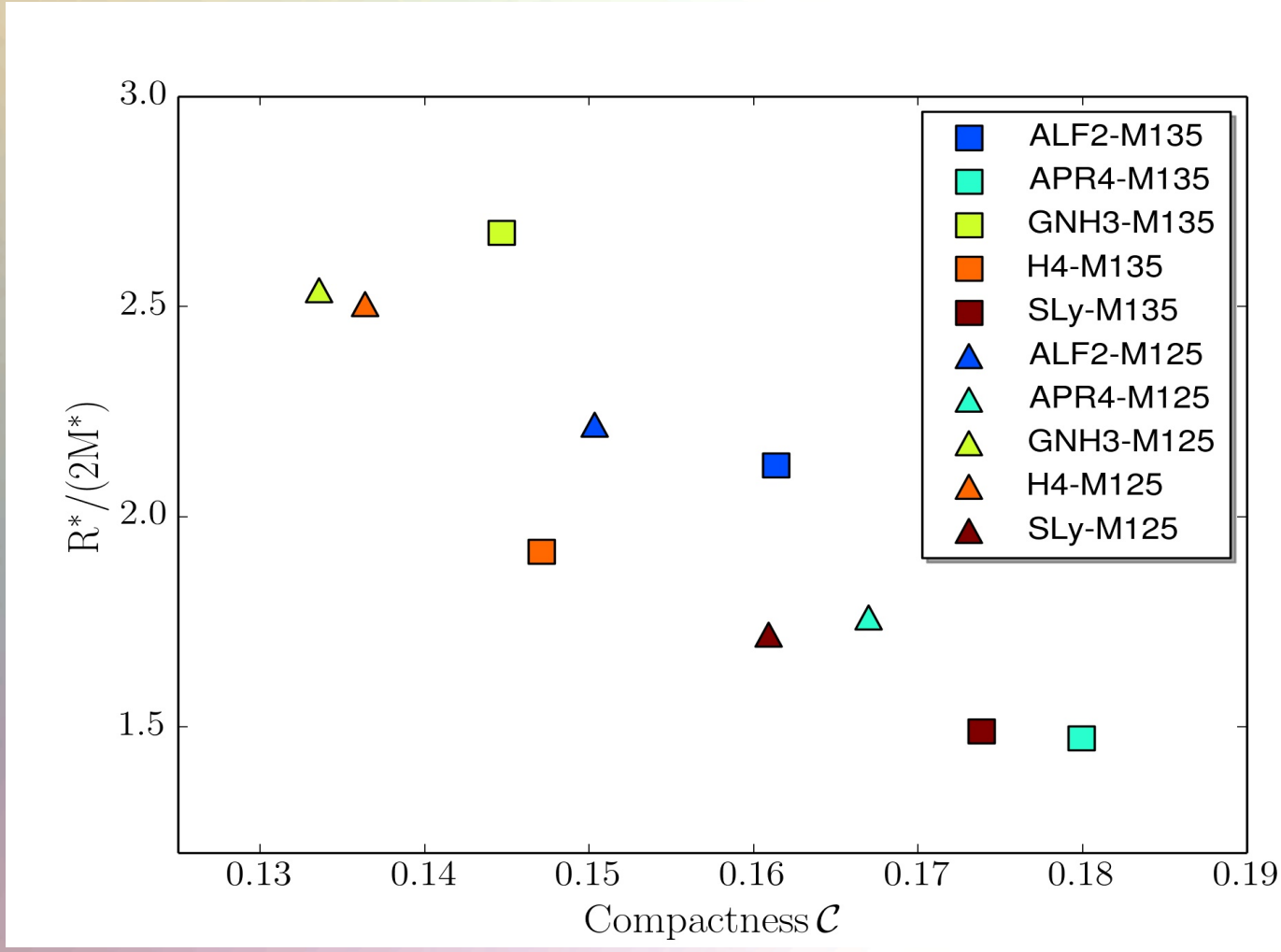

R*/(2M*) as a function of compactness of the initial star for the time-averaged rotation profiles.

Circular Motion around a Kerr-BH

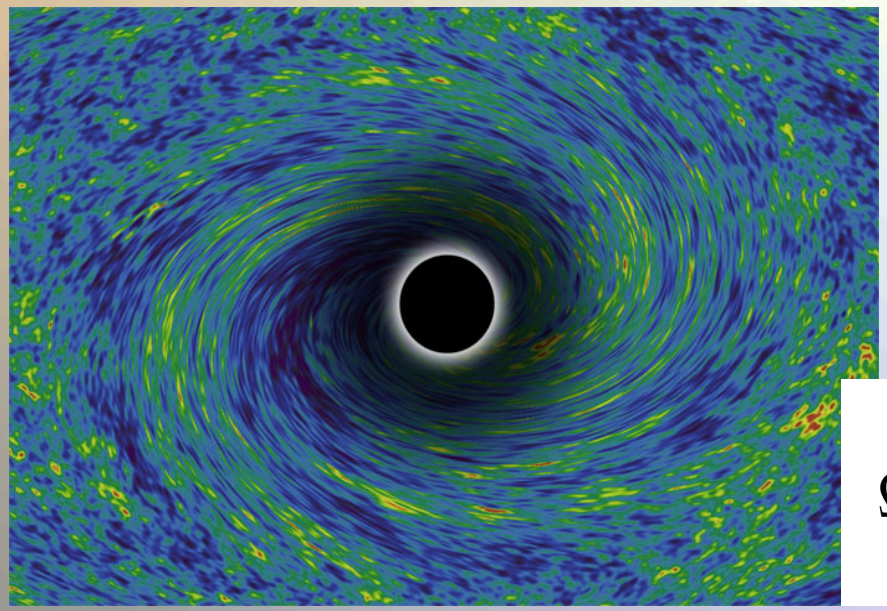

A non-interacting fluid (a test-particle) in stable, co-rotating circular motion around a rotating **Kerr black hole** (Mass M and angular momentum J)has a certain Keplerian angular velocity:

$$\Omega_{\mathrm{Kep}}(r) = \frac{\sqrt{M}}{\sqrt{r^3} + a\sqrt{M}} \quad \text{with: } a := \frac{J}{M}$$

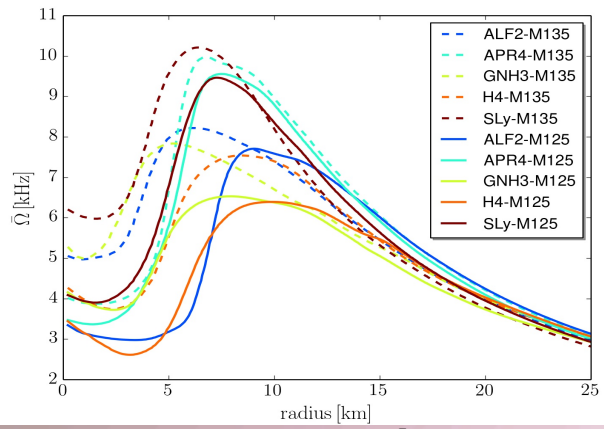

Keplerian Rotation

$$\chi := \left(\Omega_{\mathrm{Kep}}(r)\sqrt{r^3}\right)^2 = \frac{M}{\left(1 + \frac{a\sqrt{M}}{\sqrt{r^3}}\right)^2}$$

$$\underbrace{\cong}_{\text{for } r>>M} M\left(1 - 2\frac{a\sqrt{M}}{\sqrt{r^3}} + 3\frac{a^2 M}{r^3} - \mathcal{O}\left(\frac{1}{\sqrt{r^9}}\right)\right)$$

Keplerian limit of Ω

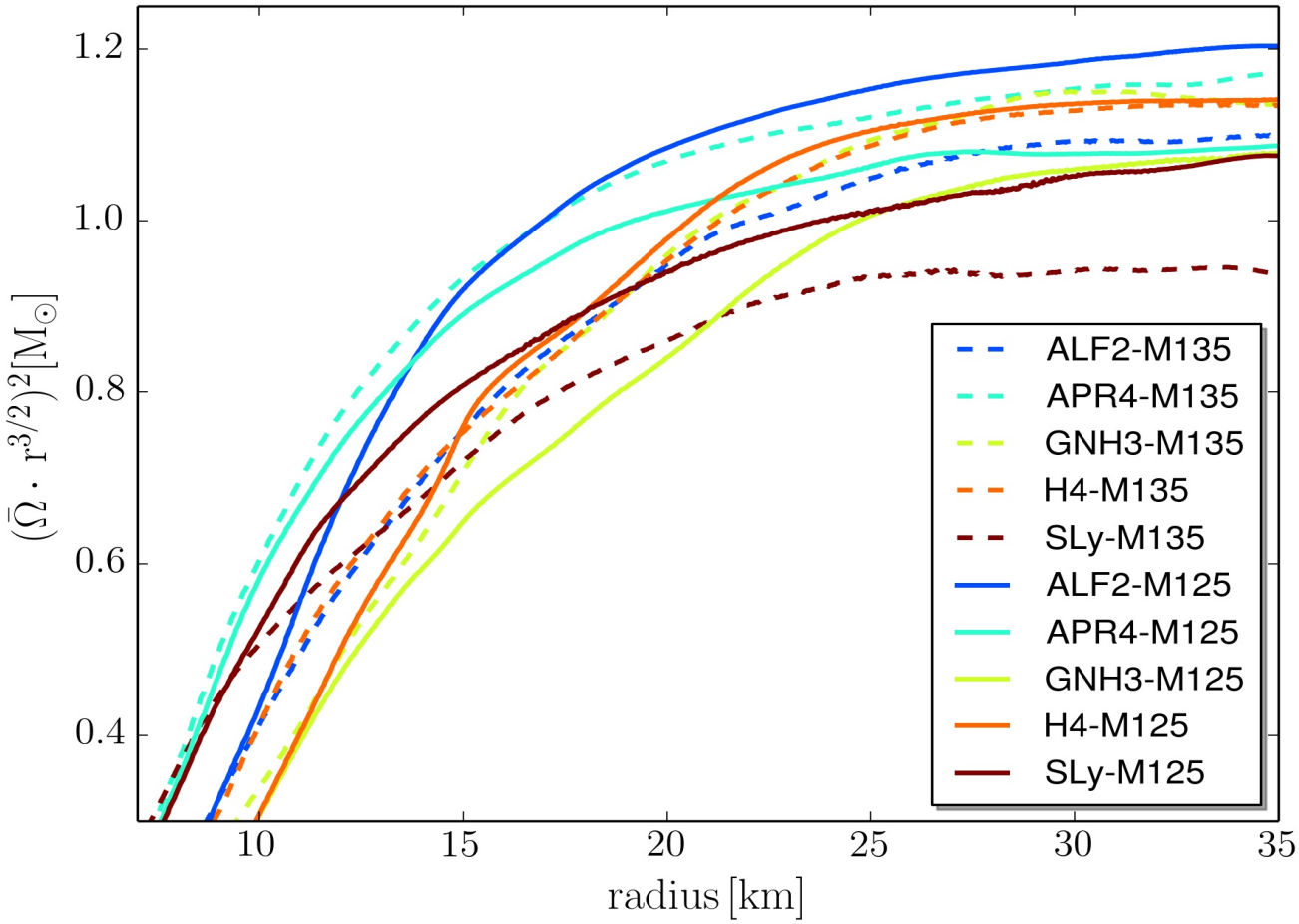

$\chi := \bar{\Omega}^2 r^3$ as a function of the radial distance r.

Keplerian limit of Ω

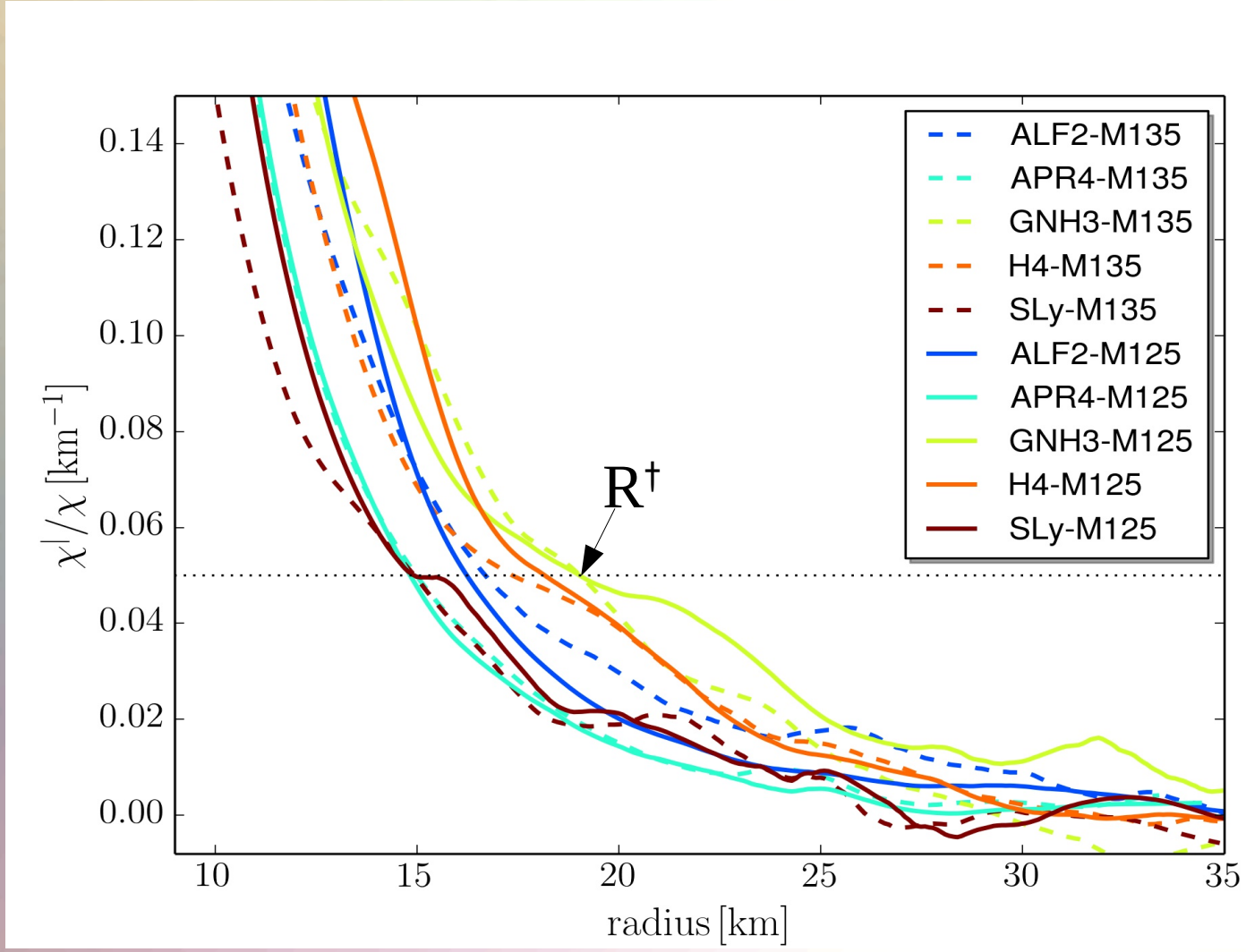

Mass fraction outside $R^{\dagger}$

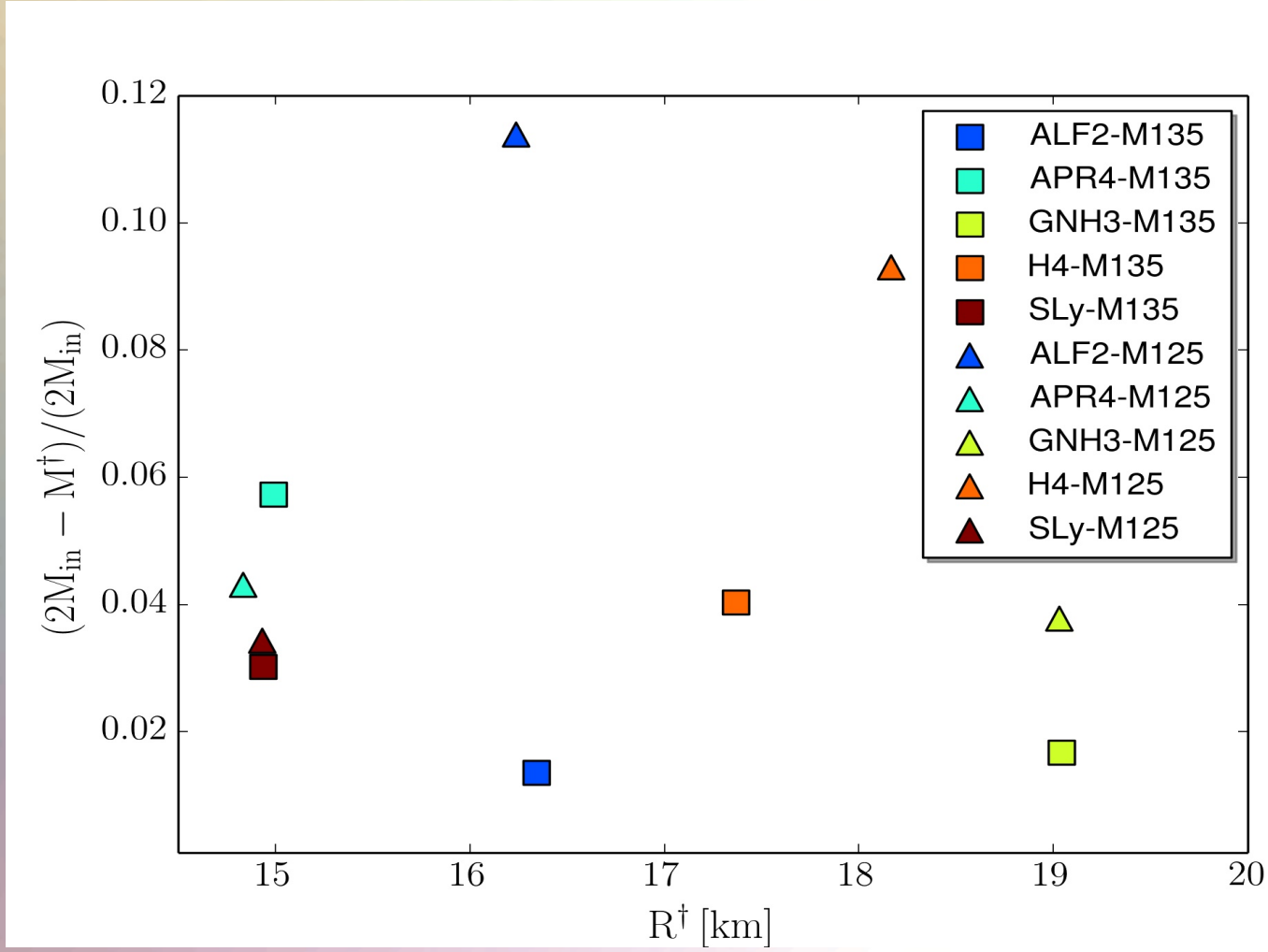

Fraction of mass which is outside $R^{\dagger}$ as a function of $R^{\dagger}$.

Eccentric Binaries

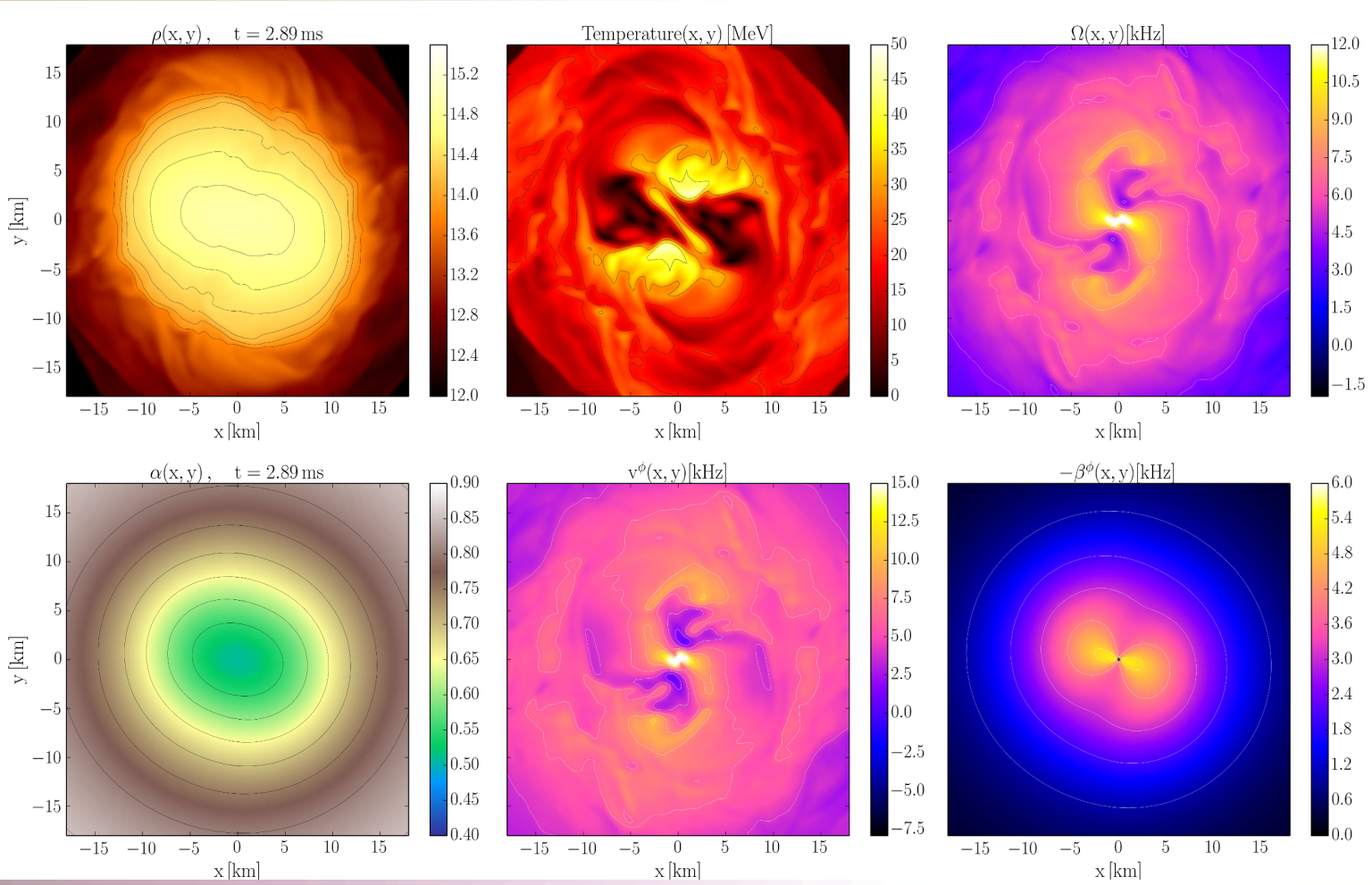

The simulation where performed by **Jens Pappenfort**, who simulated the eccentric merging NS-NS-system using WhiskyTHC + neutrino leakage.

Remote from the Equatorial Plane

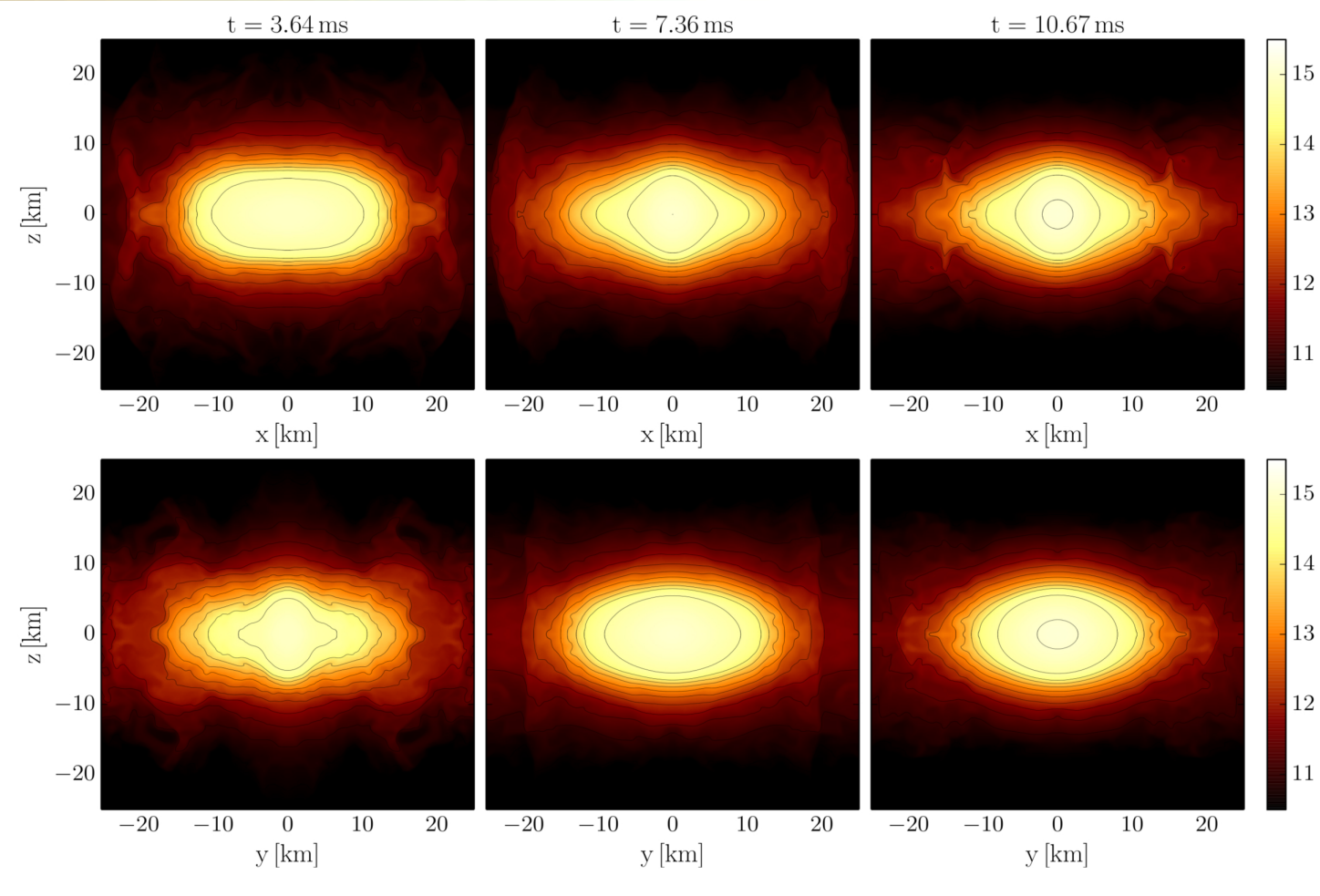

Logarithm of the rest mass density Log(ρ) [g/cm^3] in the zx- and zy-plane for three different times (ALF2, M=1.35).

Remote from the Equatorial Plane

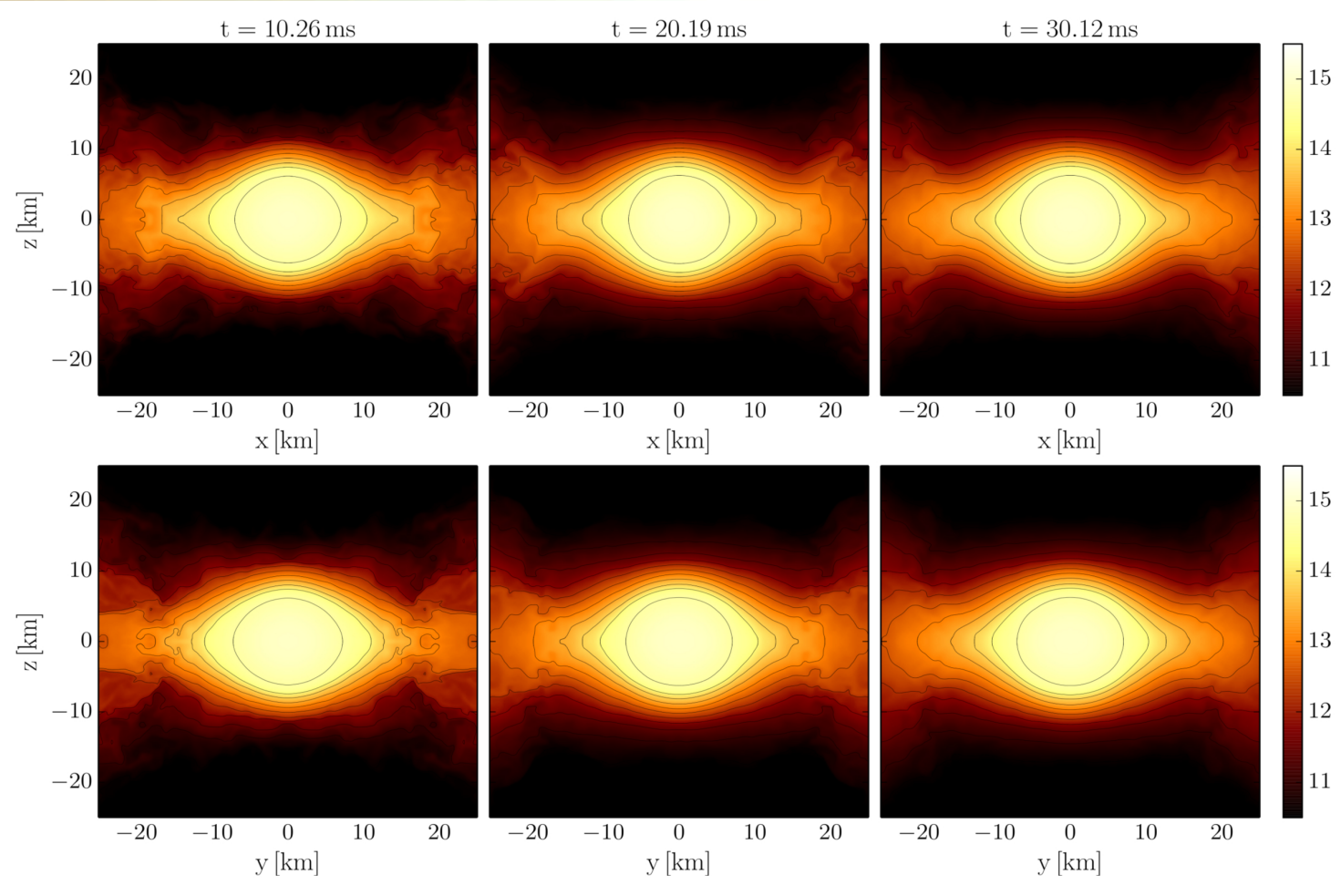

Logarithm of the rest mass density Log(ρ) [g/cm^3] in the zx- and zy-plane for three different times (ALF2, M=1.25).

Outlook

The construction of an realistic EoS, which includes a hadron-quark phase transition, depends on the underlying effective model of the hadron and quark interaction. GW-spectrum (f_1 and f_2) will change dramatically →
QCD phase transition (if strong) will be detectable with gravitational waves.

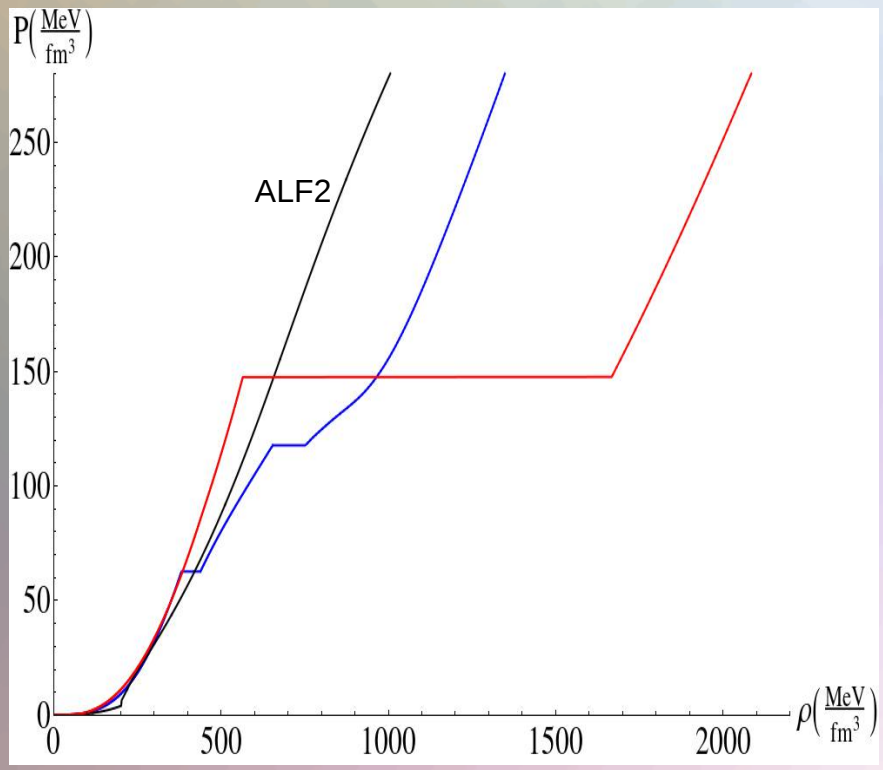

Selection of current EoS

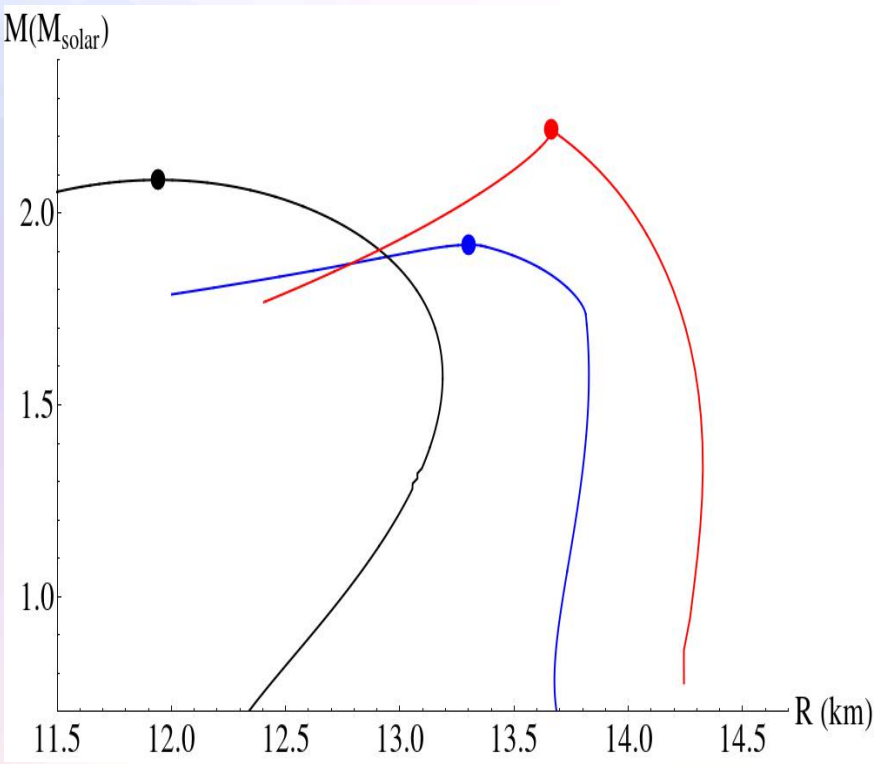

Star properties (Mass vs. Radius). Points correspond to the corresponding maximum mass of the EoS.

Summary

1. The differential rotation profiles of the hypermassive neutron stars (HMNS) in the merger, post-merger and black hole formation phase have been analysed.
2. The HMNS rotation profiles show a structural uniqueness in respect to a variation of the EoS and initial neutron star mass.
3. The maximum value of the rotation curves Ω^* strongly correlates with the Ω_2 gravitational wave frequency peak.
4. The internal fluid motion inside a HMNS could create a periodical quark-hadron phase transition scenario accompanied by a neutrino- and short gamma-ray bursts.

In Preparation:

Rotational properties of hypermassive neutron stars from binary mergers

Kentaro Takami, Matthias Hanauske, Luciano Rezzolla, Filippo Galeazzi, Bruno Mundim, Luke Bovard and José A. Font

End

- ….Additional, backup-slides follow

Gauge Conditions

On each spatial hypersurface, four additional degrees of freedom need to be specified: A *slicing condition* for the lapse function and a *spatial shift condition* for the shift vector need to be formulated to close the system. In an optimal gauge condition, singularities should be avoided and numerical calculations should be less time consuming.

Bona-Massó family of slicing conditions: $\partial_t \alpha - \beta^k \partial_k \alpha = -f(\alpha)\, \alpha^2 (K - K_0)$

"1+log" slicing condition: $f = 2/\alpha$ where $f(\alpha) > 0$ and $K_0 \coloneqq K(t = 0)$

"Gamma-Driver" shift condition:

$$\partial_t \beta^i - \beta^j \partial_j \beta^i = \frac{3}{4} B^i,$$

$$\partial_t B^i - \beta^j \partial_j B^i = \partial_t \tilde{\Gamma}^i - \beta^j \partial_j \tilde{\Gamma}^i - \eta B^i$$

Summary

- The transition from confined hadronic matter to deconfined quark matter is called the Hadron-Quark Phase Transition
- Depending on the value of the hadron-quark surface tension, the Maxwell- or Gibbs-phase transition construction should be used
- The star's density profile has a huge density jump (Riemann problem) at the phase transition boundary, if a Maxwell construction is used
- Realistic numerical simulations of collapsing neutron stars or neutron star mergers should use an EoS with a hadron quark phase transition
- Realistic rotation profile in hyper massive neutron stars indicate that the maximum of the rotation curve come along with the hadron quark phase transition boundary (mixed phase if Gibbs is used)
- The decisive amount of matter which is trapped behind the event horizon when a black hole is formed (in an merger or collapsing scenario of neutron stars) is deconfined quark matter

The Gibbs Construction

Hadronic and quark surface:

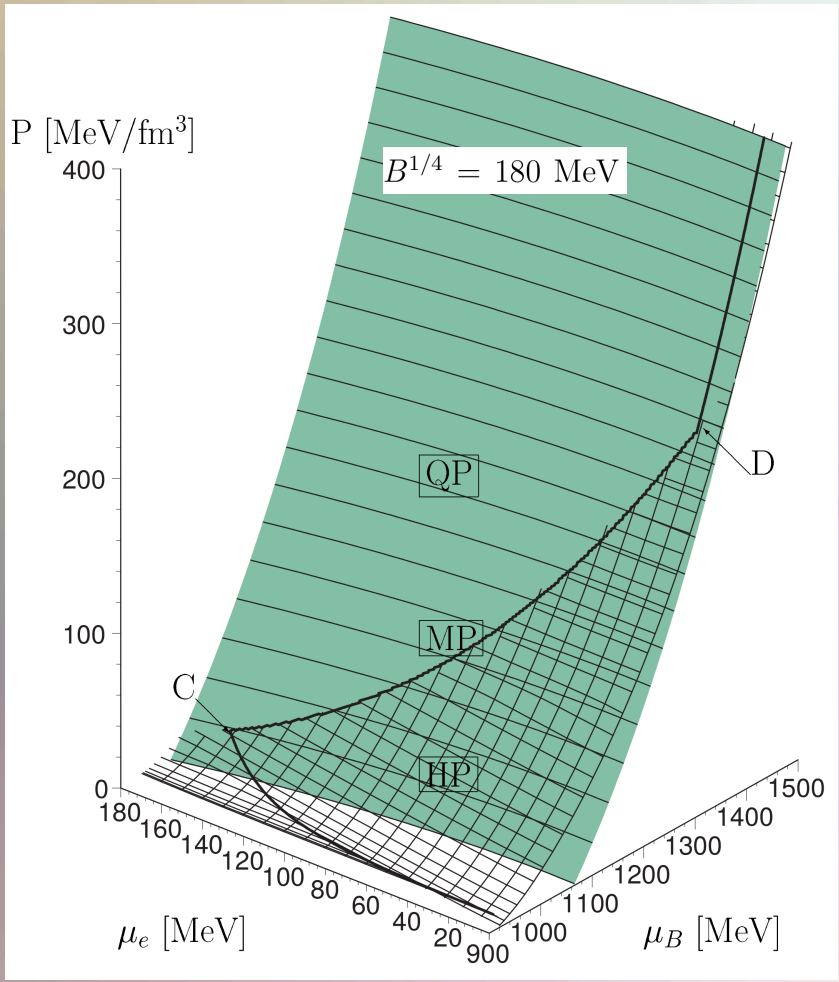

Charge neutrality condition is only globally realized

$$\rho_e := (1-\chi)\rho_e^H(\mu_B,\mu_e) + \chi\rho_e^Q(\mu_B,\mu_e) = 0\,.$$

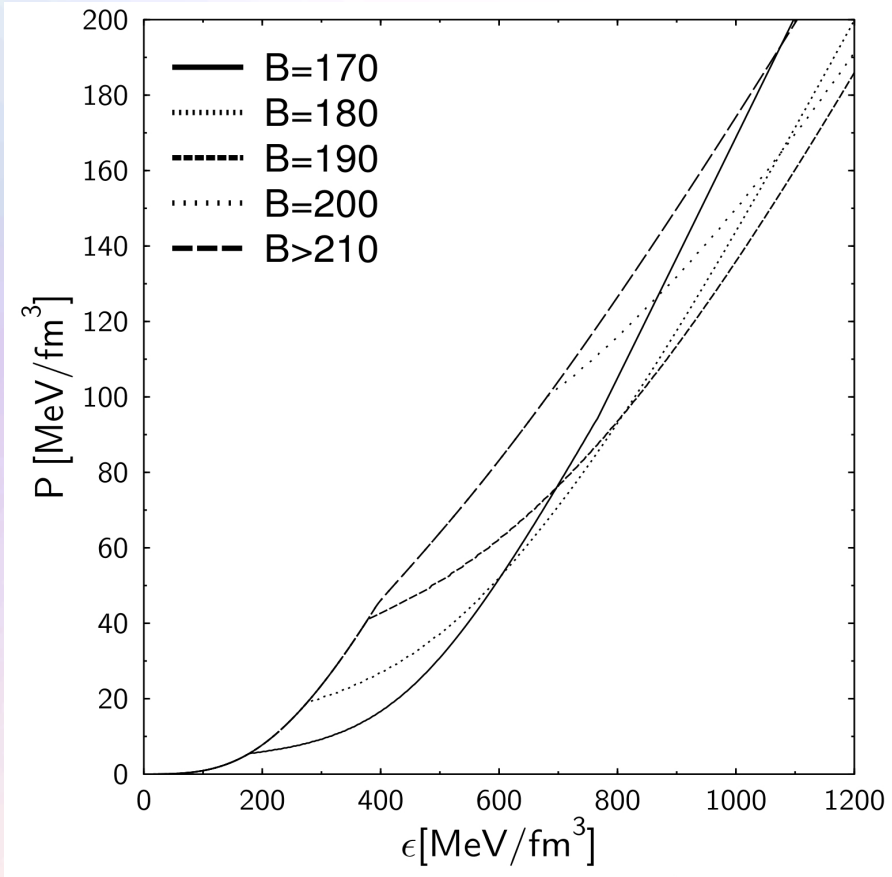

The Maxwell Construction

If the surface tension is large -> mixed phase disappears

-> sharp boundary between the hadron and quark phase
->Maxwell construction should be used

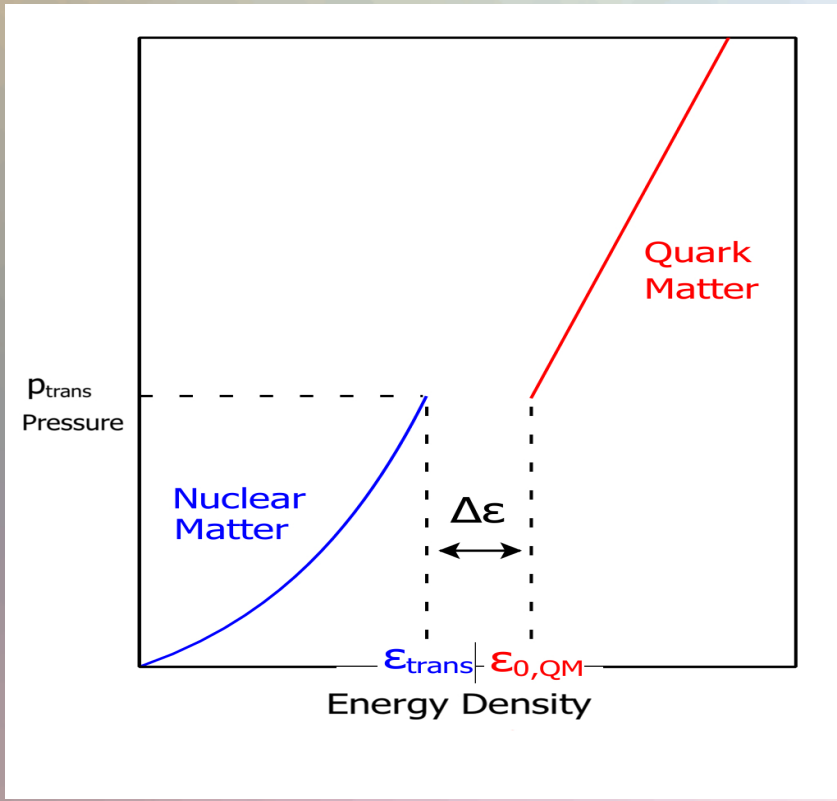

Image from M.G. Alford, S. Han, and M. Prakash, Phys. Rev. D 88, 083013 (2013)

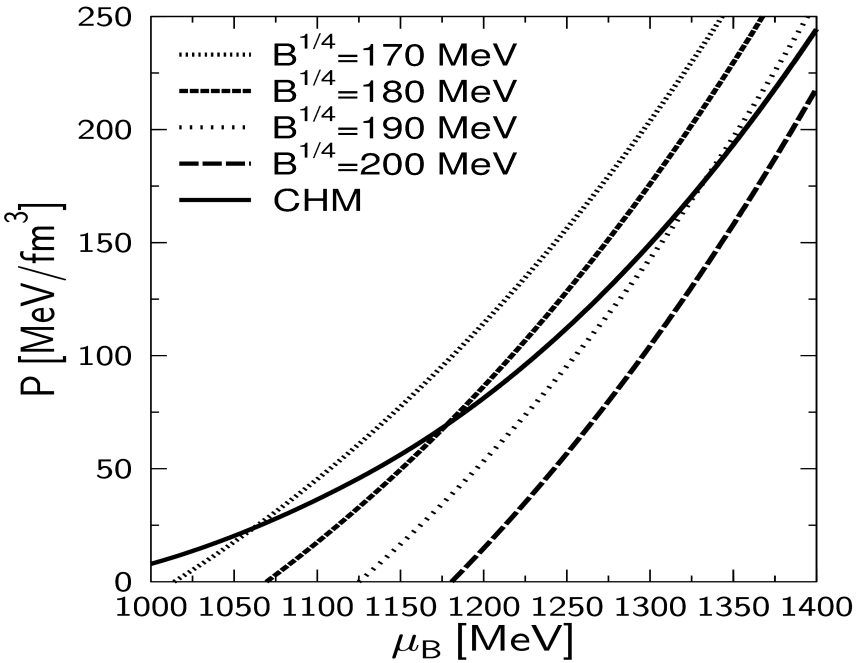

Pressure and baryon chemical potential stays constant, while the density and the charge chemical potential jump discontinuously during the phase transition.

Summary

- The transition from confined hadronic matter to deconfined quark matter is called the Hadron-Quark Phase Transition
- Depending on the value of the hadron-quark surface tension, the Maxwell- or Gibbs-phase transition construction should be used
- The star's density profile has a huge density jump (Riemann problem) at the phase transition boundary, if a Maxwell construction is used
- Realistic numerical simulations of collapsing neutron stars or neutron star mergers should use an EoS with a hadron quark phase transition
- Realistic rotation profile in hyper massive neutron stars indicate that the maximum of the rotation curve come along with the hadron quark phase transition boundary (mixed phase if Gibbs is used)
- The decisive amount of matter which is trapped behind the event horizon when a black hole is formed (in an merger or collapsing scenario of neutron stars) is deconfined quark matter

Current Projects

- The twin star collapse
  (Collaborators: A.Zacchi, J.Schaffner-Bielich and L.Rezzolla)
- Oscillations of hybrid and quark stars within different models of the phase transition
  (Collaborators: A.Brillante, I.Mishustin, A.Sedrakian and L.Rezzolla)
- Hybrid and quark star merger calculations with temperature dependent equation of states
  (Collaborators: S. Schramm, B.Franzon, F.Galeazzi and L.Rezzolla)
- Differential rotation profiles of hypermassive hybrid stars and the effect Maxwell- vs. Gibbs-construction
  (Collaborators: K.Takami, F.Galeazzi, B.Mundim, L.Bovard and L.Rezzolla)
- Collapse scenario and black hole formation in the context of the hadron-quark phase transition

Current Projects

- The twin star collapse
  (Collaborators: A.Zacchi, J.Schaffner-Bielich and L.Rezzolla)
- Oscillations of hybrid and quark stars within different models of the hadron-quark phase transition
  (Collaborators: A.Brillante, I.Mishustin, A.Sedrakian and L.Rezzolla)
- Hybrid and quark star merger calculations with temperature dependent equation of states
  (Collaborators: S. Schramm, B.Franzon, F.Galeazzi and L.Rezzolla)
- Differential rotation profiles of hypermassive hybrid stars and the effect Maxwell- vs. Gibbs-construction
  (Collaborators: K.Takami, F.Galeazzi, B.Mundim, L.Bovard and L.Rezzolla)
- Collapse scenario and black hole formation in the context of the hadron-quark phase transition

The Twin Star Collapse

Usually it is assumed that this loss of stability leads to the collapse into a black hole. However, realistic calculations open another possibility: the collapse into the twin star on the second sequence. A star from the first sequence which reaches the maximum mass (point A) will collapse to its twin star. The latter is the corresponding star on the second sequence, i.e. the one which has the same total baryon number (point B).

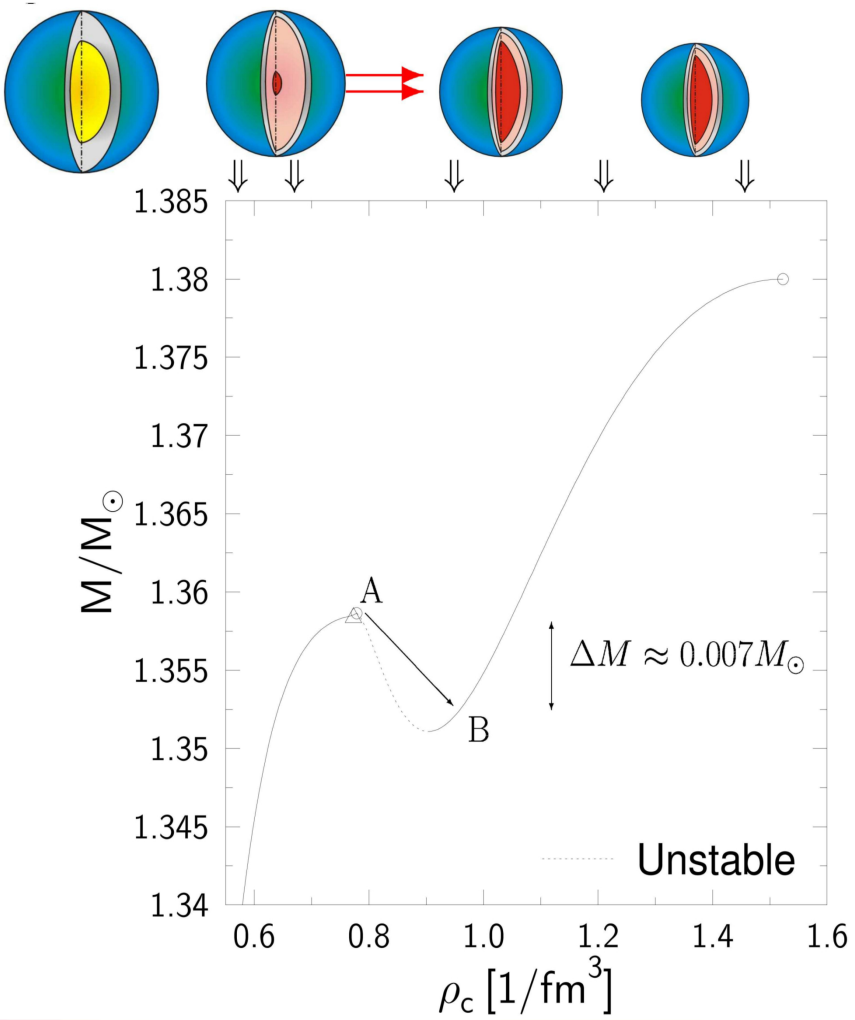

I.N. Mishustin, M. Hanauske, A. Bhattacharyya, L.M. Satarov, H. Stöcker, and W. Greiner, “Catastrophic rearrangement of a compact star due to quark core formation”, Physics Letters B 552 (2003) p.1-8

J. Schaffner-Bielich, M. Hanauske, H. Stöcker, and W. Greiner, Phys. Rev. Lett. 89, 171101 (2002)

S. Banik, M. Hanauske, D. Bandyopadhyay, and W. Greiner, Phys. Rev. D 70, 123004 (2004)

The Twin Star Collapse

Density profiles of the two twins

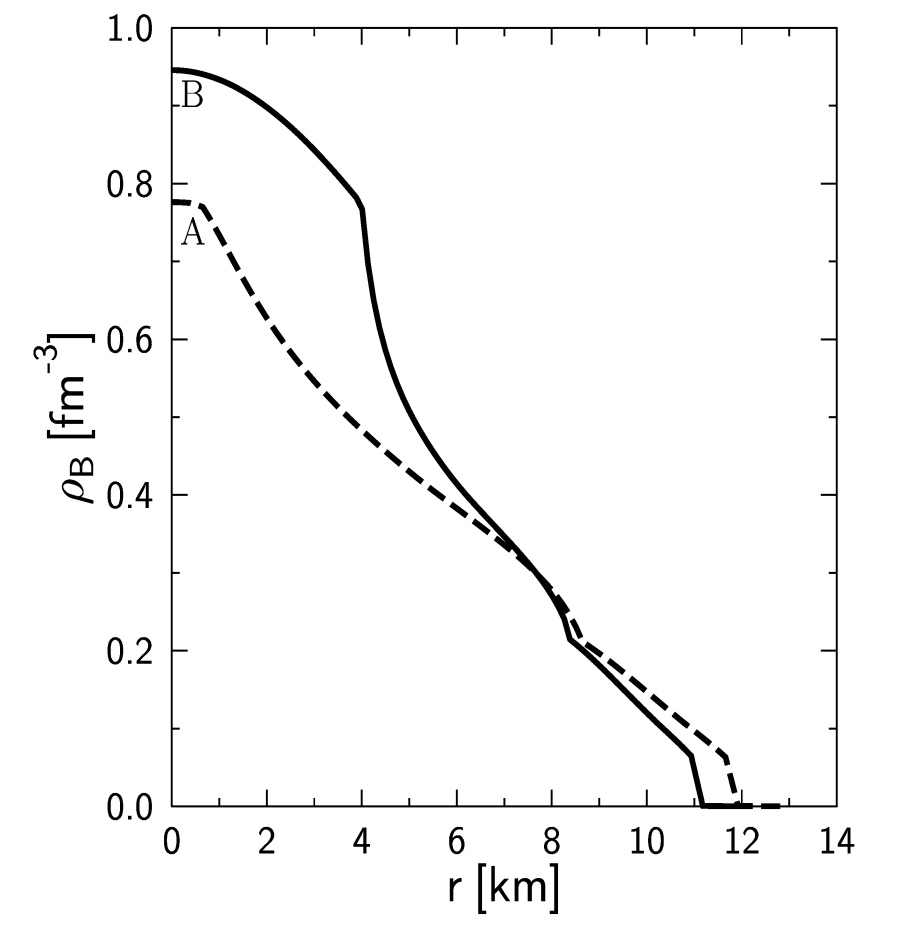

Conservation of total baryonic mass

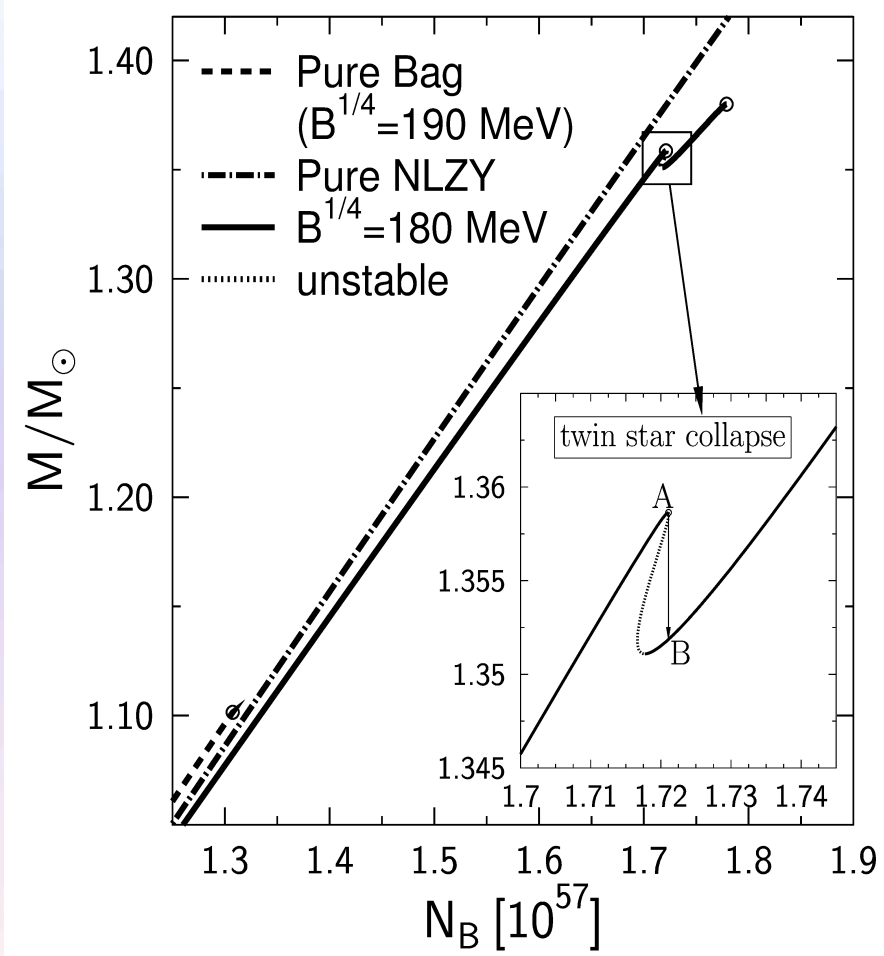

Summary

- The transition from confined hadronic matter to deconfined quark matter is called the Hadron-Quark Phase Transition
- Depending on the value of the hadron-quark surface tension, the Maxwell- or Gibbs-phase transition construction should be used
- The star's density profile has a huge density jump (Riemann problem) at the phase transition boundary, if a Maxwell construction is used
- In a narrow parameter window Twin Stars a possible: The collapse from a neutron to a hybrid quark star will emit a burst of gravitational waves, neutrinos and gamma rays
- Realistic numerical simulations of collapsing neutron stars or neutron star mergers should use an EoS with a hadron quark phase transition
- The decisive amount of matter which is trapped behind the event horizon when a black hole is formed (in an merger or collapsing scenario of neutron stars) is deconfined quark matter

Current Projects

- The twin star collapse
  (Collaborators: A.Zacchi, J.Schaffner-Bielich and L.Rezzolla)
- Oscillations of hybrid and quark stars within different models of the hadron-quark phase transition
  (Collaborators: A.Brillante, I.Mishustin, A.Sedrakian and L.Rezzolla)
- Hybrid and quark star merger calculations with temperature-dependent equation of states
  (Collaborators: S. Schramm, B.Franzon, F.Galeazzi and L.Rezzolla)
- Differential rotation profiles of hypermassive hybrid stars and the effect Maxwell- vs. Gibbs-construction
  (Collaborators: K.Takami, F.Galeazzi, B.Mundim, L.Bovard and L.Rezzolla)
- Collapse scenario and black hole formation in the context of the hadron-quark phase transition

Collapse Scenario of a Hybrid Star

The gravitational collapse of a hybrid star to a black hole is visualized on the right side within a space-time diagram of the Schwarzschild metric in advanced Eddington-Finkelstein coordinates.

The formation of the apparent and event horizon of the black hole confines the quark star macroscopically. Finally the colour charge of the deconfined free quarks cannot be observed from outside.

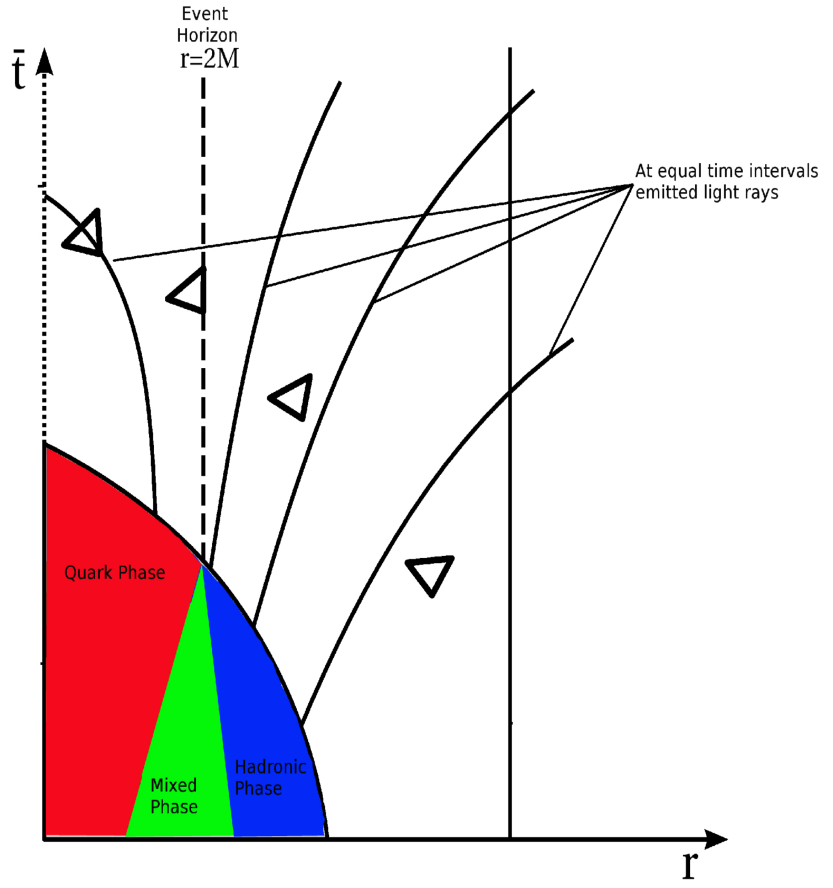

M. Hanauske, Dissertation: "Properties of Compact Stars within QCD-motivated Models" ;
University Library Publication 2004 (urn:nbn:de:hebis:30-0000005872)

The QCD- Phase Diagram

The QCD phase diagram at temperature T and net baryon density is displayed on the right side.

Some regions can be accessed by heavy ion collisions at different energies.

Matter of the early universe and in the interior of compact stars are also indicated within the diagram.

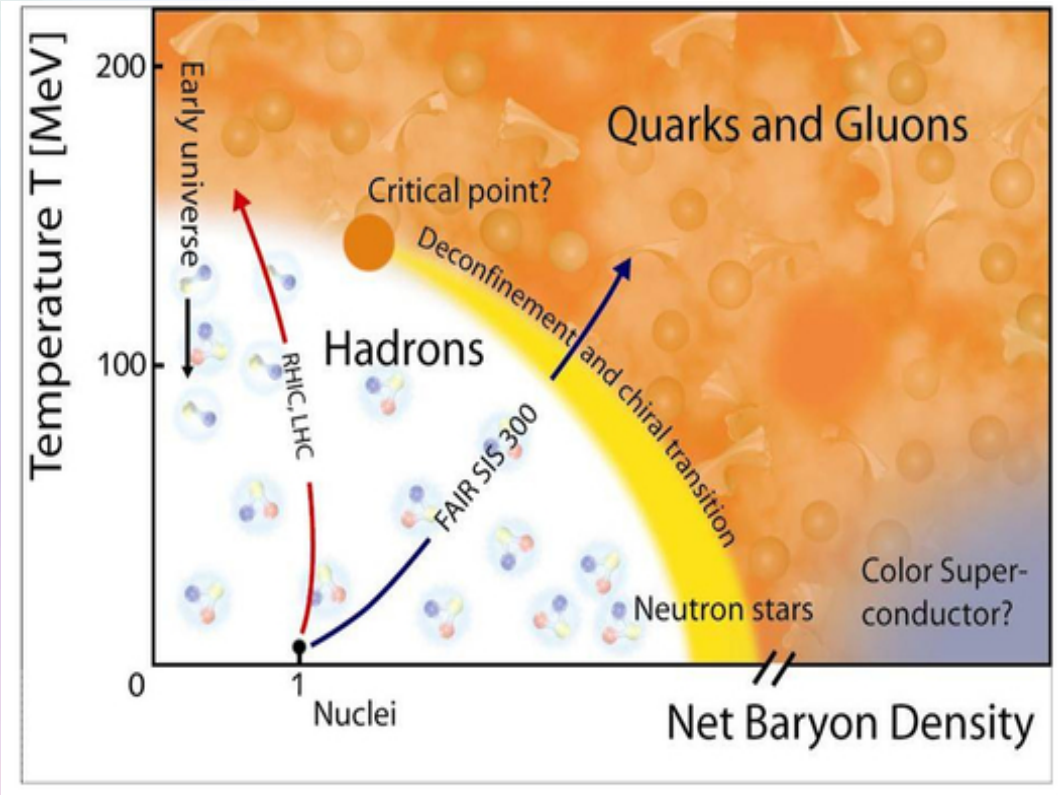

Image from
http://webarchiv.fz-juelich.de/nic/Publikationen/Broschuere/Elementarteilchenphysik/hadron.jpg

Neutron Stars (NS)

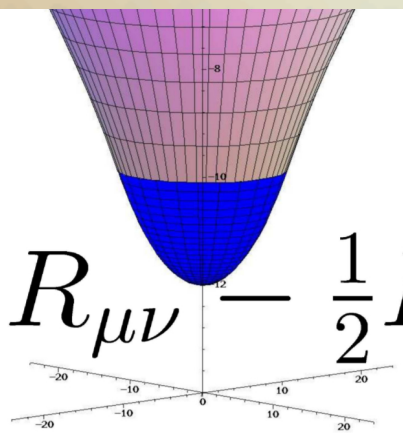

$$R_{\mu\nu} - \frac{1}{2} R\, g_{\mu\nu} = \frac{8\pi G}{c^4} T_{\mu\nu}$$

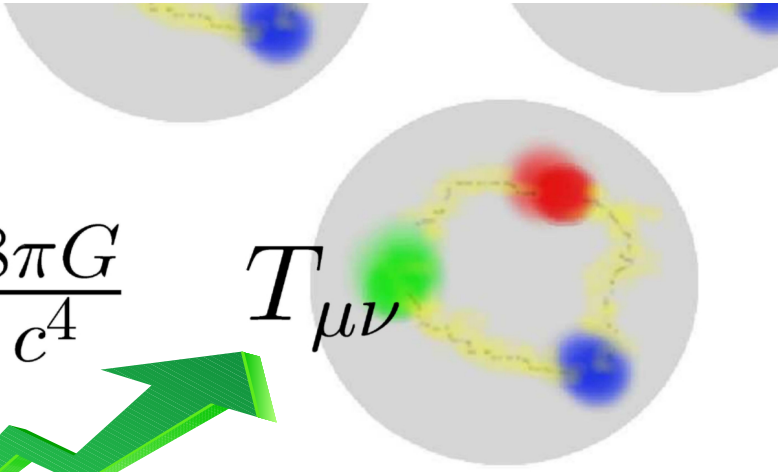

Relativistic Mean-Field Hadronic Models

$$\sum_B \quad (p, n, \Lambda, \Sigma^-, \Sigma^0, \Sigma^+, \Xi^-, \Xi^0)$$

$$\begin{aligned}\mathcal{L} &= \sum_B \overline{\psi}_B \left(i\partial\!\!\!/ - m_B\right)\psi_B + \frac{1}{2}\partial^\mu\sigma\partial_\mu\sigma - \frac{1}{2}m_\sigma^2\sigma^2 - \frac{a}{3}\sigma^3 - \frac{b}{4}\sigma^4 - \frac{1}{4}\omega^{\mu\nu}\omega_{\mu\nu} \\ &+\frac{1}{2}m_\omega^2\omega^\mu\omega_\mu - \frac{1}{4}\vec{\rho}^{\mu\nu}\vec{\rho}_{\mu\nu} + \frac{1}{2}m_\rho^2\vec{\rho}^\mu\vec{\rho}_\mu \quad + \sum_B \overline{\psi}_B \left(g_{\sigma B}\sigma + g_{\omega B}\omega^\mu\gamma_\mu + g_\rho\vec{\rho}^\mu\gamma_\mu\vec{\tau}_B\right)\psi_B\end{aligned}$$

$$\begin{aligned}\mathcal{L}^{YY} &= \frac{1}{2}\left(\partial^\mu\sigma^*\partial_\mu\sigma^* - m_{\sigma^*}^2\sigma^{*2}\right) - \frac{1}{4}\phi^{\mu\nu}\phi_{\mu\nu} + \frac{1}{2}m_\phi^2\phi^\mu\phi_\mu \\ &+\sum_Y \overline{\psi}_Y \left(g_{\sigma^*Y}\sigma^* + g_{\phi Y}\phi^\mu\gamma_\mu\right)\psi_Y \quad ,\end{aligned}$$

$$\mathcal{L}_{\rm lep} = \sum_{l=e,\mu} \overline{\psi}_l[i\gamma_\mu\partial^\mu - m_l]\psi_l$$

Composition of Neutron Star Matter

Neutron star matter conditions:

1) Charge Neutrality
2) β-equilibrium
3) Strangeness production

$$n \;\Leftrightarrow\; p + e + \tilde{\nu}_e$$

Λ-Hyperon $\quad n + n \leftrightarrow n + \Lambda + K^0 \quad \mu_\Lambda = \mu_n$

Σ^--Hyperon $\quad n + n \leftrightarrow n + \Sigma^- + K^+ \quad \mu_{\Sigma^-} = \mu_n + \mu_e$

Chemical potentials and single particle energies of hyperons in dependence of the baryonic density.

$$E_i(k) \;=\; E_i^*(k) + g_{i\omega}\omega_0 + g_{i\phi}\phi_0 + g_{i\rho}I_{3i}\rho_0$$

$$E_i^*(k) = \sqrt{k_i^2 + m_i^{*2}} \qquad \mu_i \;=\; b_i\mu_n - q_i\mu_e$$

M. Hanauske, D. Zschiesche, S. Pal, S. Schramm, H. Stöcker, and W. Greiner, Astrophys. J. 537, 958 (2000)

Particle composition vs baryonic density

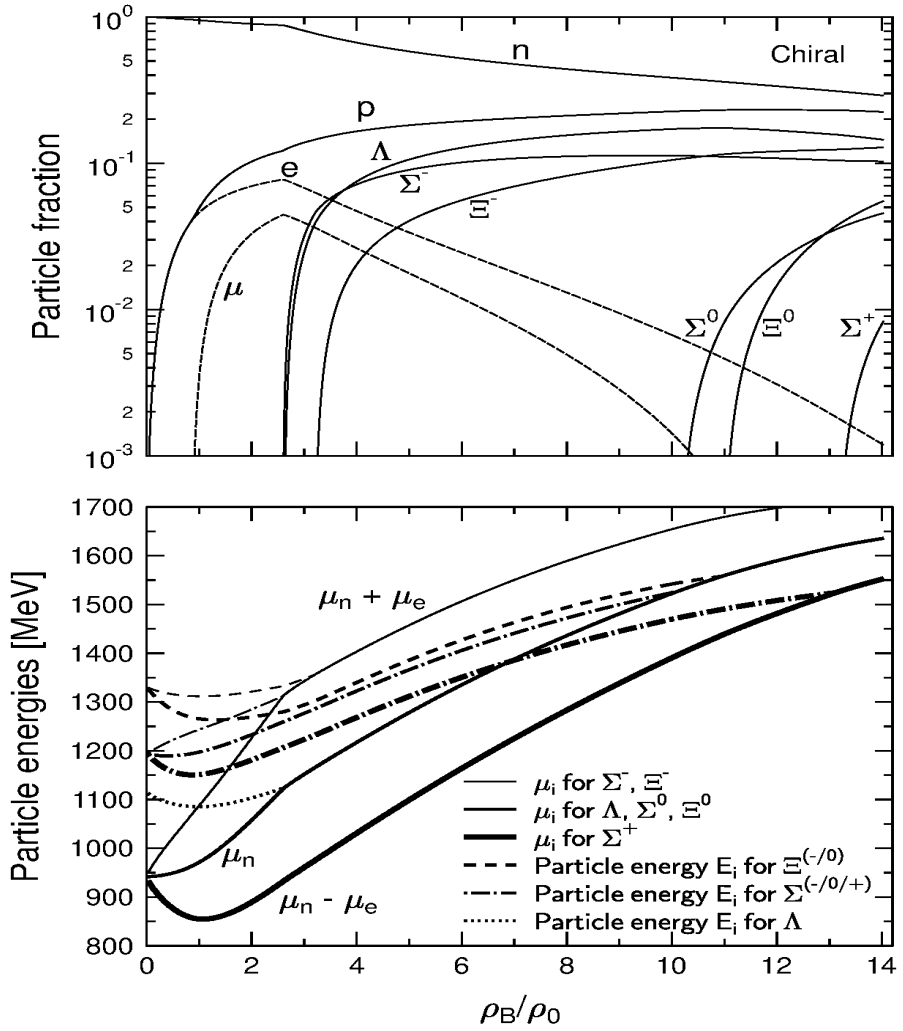

Neutron Star Properties

The neutron star radius as a function of its mass. A low, middle and high density star is displayed within the figure. Additionally the onset of hyperonic particles is visualized.

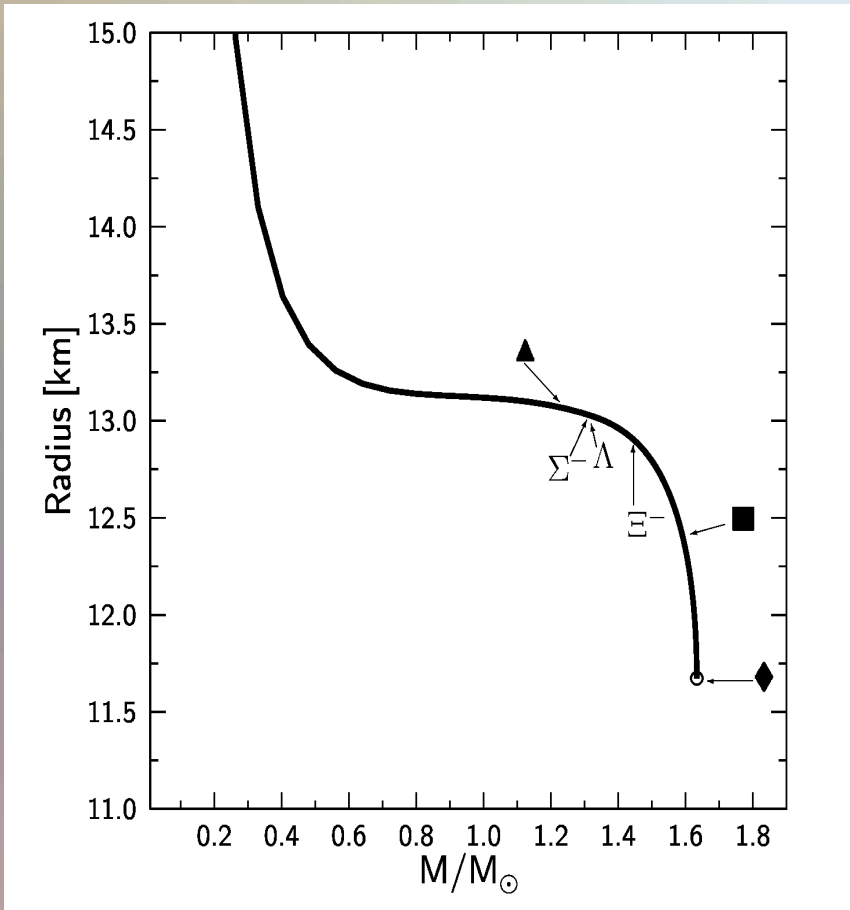

Energy density profiles of three neutron stars with different central densities and masses. The low density stars do not contain any hyperons, whereas the other two stars do have hyperons in their inner core.

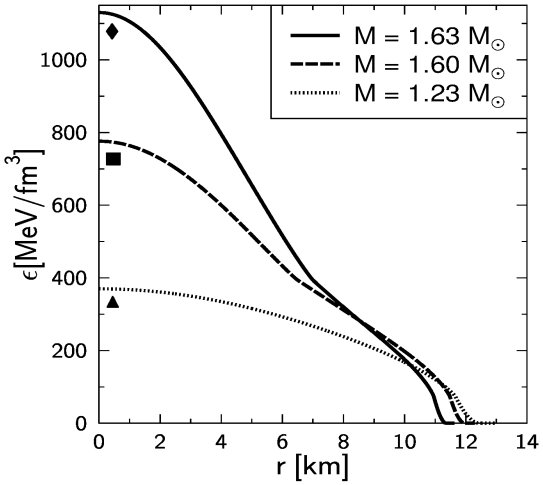

Time-time component of the metric tensor as a function of the radial coordinate. The solid line corresponds to the inner TOV-solution, whereas the doted curve depicts the outer Schwarzschild part.

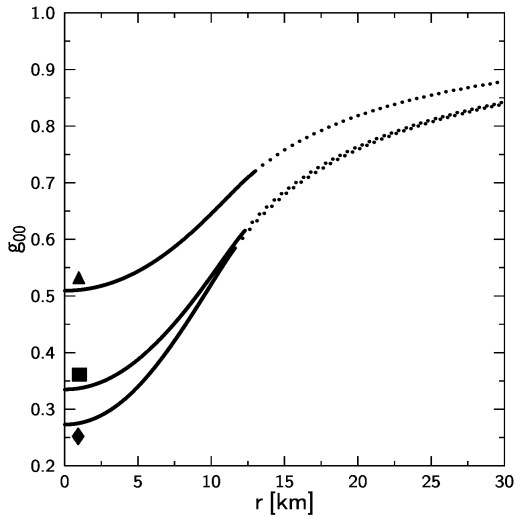

Hybrid Stars

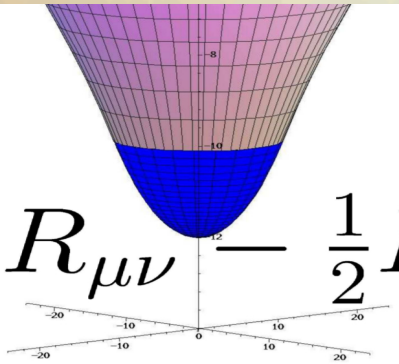

$$R_{\mu\nu} - \frac{1}{2} R\, g_{\mu\nu} = \frac{8\pi G}{c^4} T_{\mu\nu}$$

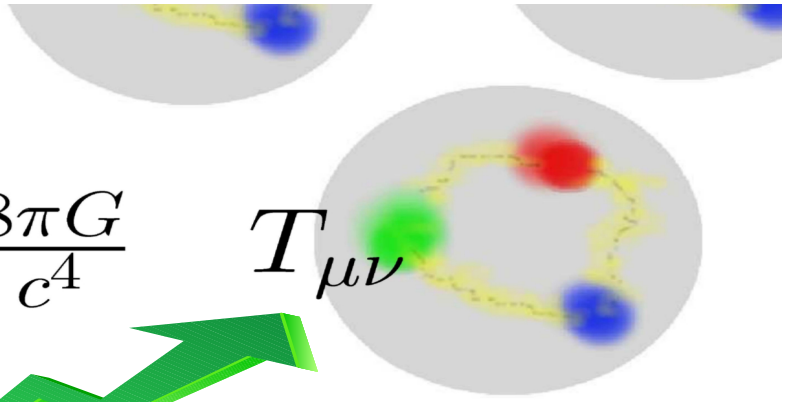

Hadronic Model + Quark Model (eg. NJL model or MIT-Bag model)

Lagrangian density of the NJL model

$$\begin{aligned}
\mathcal{L} = & \underbrace{\overline{\psi}\left(i\partial\!\!\!/ - \hat{m}_0\right)\psi}_{\text{Kinetische und Massenbeiträge}} + \underbrace{G_S \sum_{j=0}^{8}\left[\left(\overline{\psi}\,\frac{\lambda_j}{2}\,\psi\right)^2 + \left(\overline{\psi}\,\frac{i\gamma_5\lambda_j}{2}\,\psi\right)^2\right]}_{\text{Skalare Wechselwirkung}} \\
& \underbrace{- G_V \sum_{j=0}^{8}\left[\left(\overline{\psi}\,\gamma_\mu\frac{\lambda_j}{2}\,\psi\right)^2 + \left(\overline{\psi}\,\gamma_\mu\frac{\gamma_5\lambda_j}{2}\,\psi\right)^2\right]}_{\text{Vektorielle Wechselwirkung}} \qquad \psi \equiv \psi^f_{Aa} \\
& \underbrace{- K\left[\det{}_f\left(\overline{\psi}\left(1-\gamma_5\right)\psi\right) + \det{}_f\left(\overline{\psi}\left(1+\gamma_5\right)\psi\right)\right]}_{\text{Flavour Mischterme}} + \underbrace{\mathcal{L}_L}_{\text{Leptonische Beiträge}}
\end{aligned}$$

MIT-Bag model

$$\epsilon^Q = \sum_{f=u,d,s} \frac{\nu_f}{2\pi^2} \int_0^{k_F^f} k^2 \sqrt{m_f^2 + k^2}\, dk + B$$

$$P^Q = \sum_{f=u,d,s} \frac{\nu_f}{6\pi^2} \int_0^{k_F^f} \frac{k^4}{\sqrt{m_f^2 + k^2}}\, dk - B\,,$$

Hybrid Star Properties

In contrast to the Gibbs construction, the star's density profile within the Maxwell construction (see right figure) will have a huge density jump at the phase transition boundary. Twin star properties can be found more easily when using a Maxwell construction.

Mass-Density relation

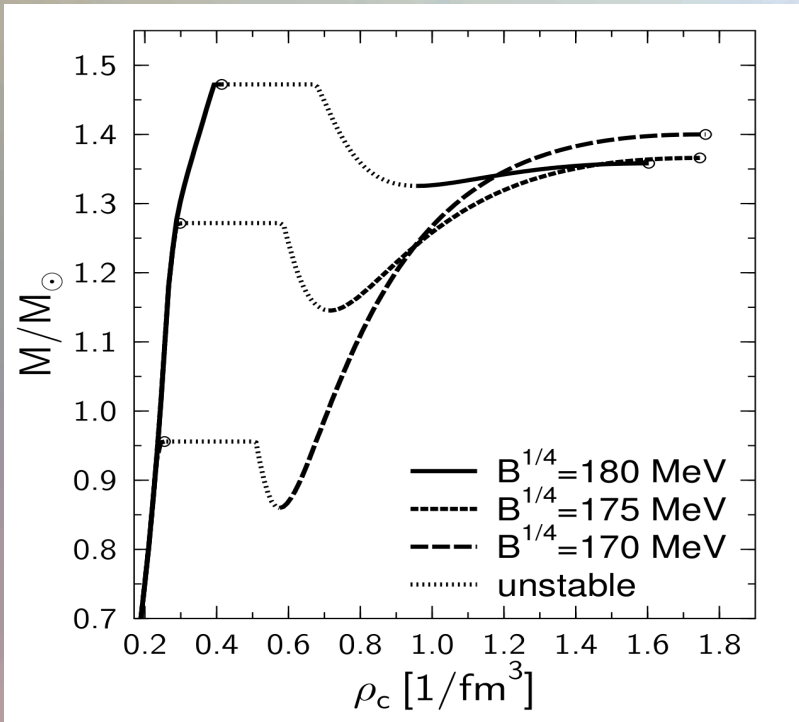

Energy-density profiles

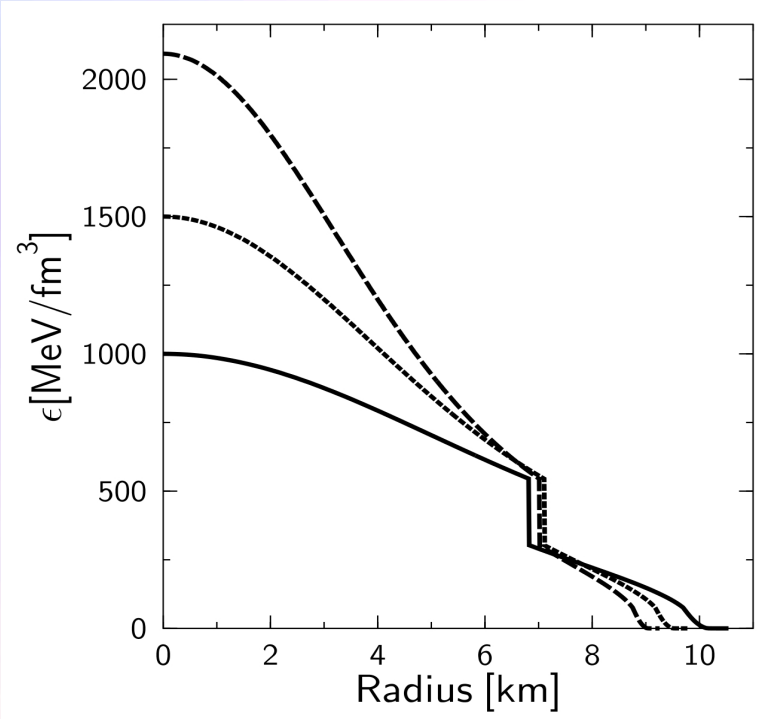

Matthias Hanauske: "How to detect the QGP with telescopes", GSI Annual Report 2003, p.96

Observed Masses of Compact Star Binaries

PSR J1906+0746 Van Leeuwen et al, arXiv:1411.1518

144-ms pulsar, discovered in in 2004
Orbital period: 3.98 hours, Eccentricity: 0.085
Pulsar mass: 1.291(11), Companion mass 1.322(11)
Observed between 1998-2009,
then it disappeared due to spin precession

Double Pulsar PSR J0737-3039

Orbital period: 147 min, Eccentricity: 0.088
pulsar A: P=23 ms, M=1.3381(7)
pulsar B: P=2.7 s, M=1.2489(7)
Pulsar A is eclipsed once per orbit by B (for 30 s)
Kramer, Wex, Class. Quantum Grav. 2009

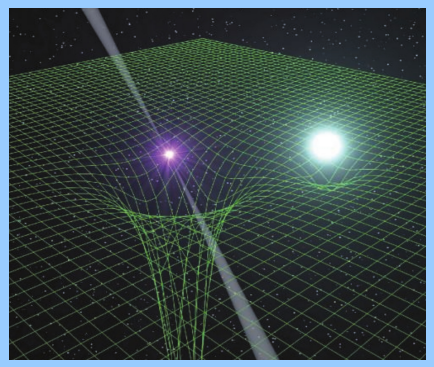

PSR J0348+0432

Orbital Period:
2.46 hours

Pulsar mass:
2.01+-0.04

white dwarf mass:
0.172+-0.003

Picture from J. Antoniadis et.al. Science 2013

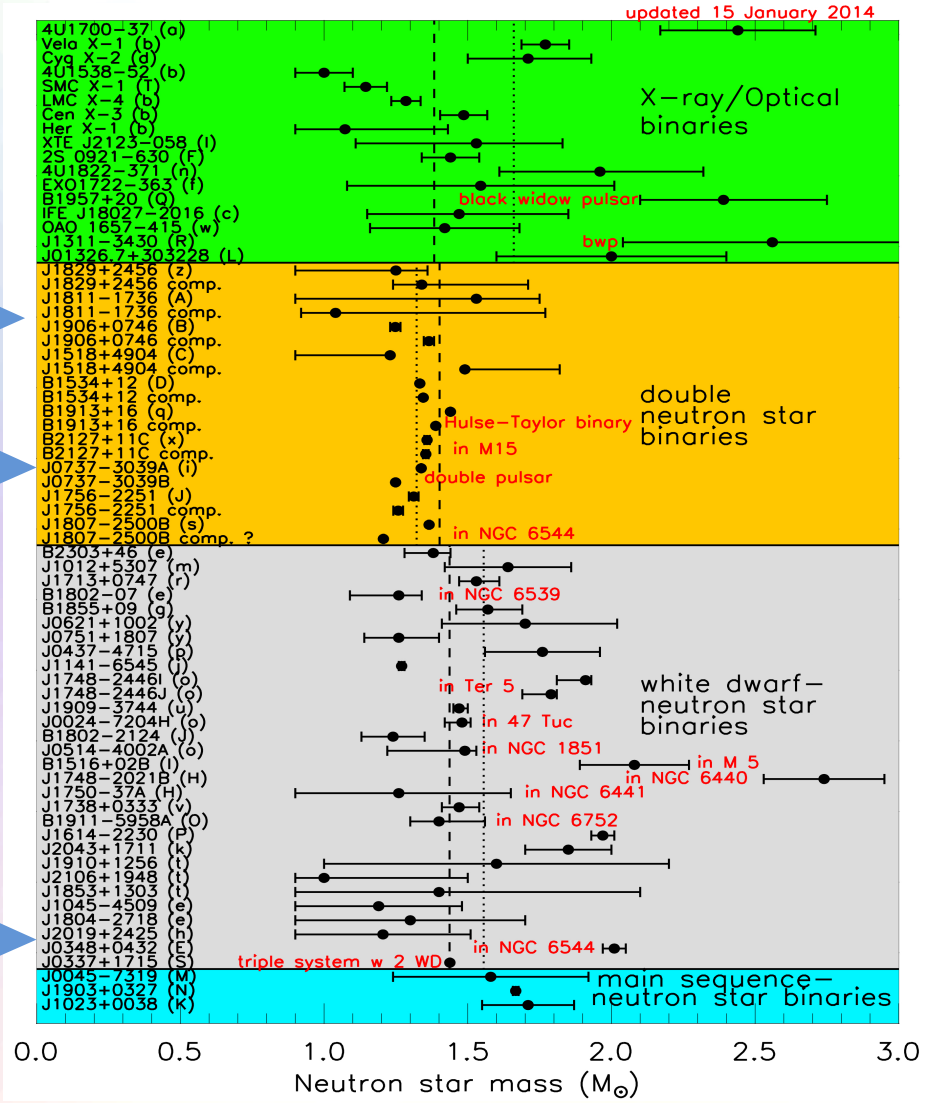

Summary: Neutron Stars

Schematic Structure of a Neutron Star

Outer Envelopes

The outer envelopes of a neutron star constist of a thin plasma atmosphere where the thermal radiation is formed and a outer and inner crust which consist of electrons and nuclei. The whole outer envelope is about one kilometer thick and it occupies the density range $\epsilon \leq 0.5\,\epsilon_0$.

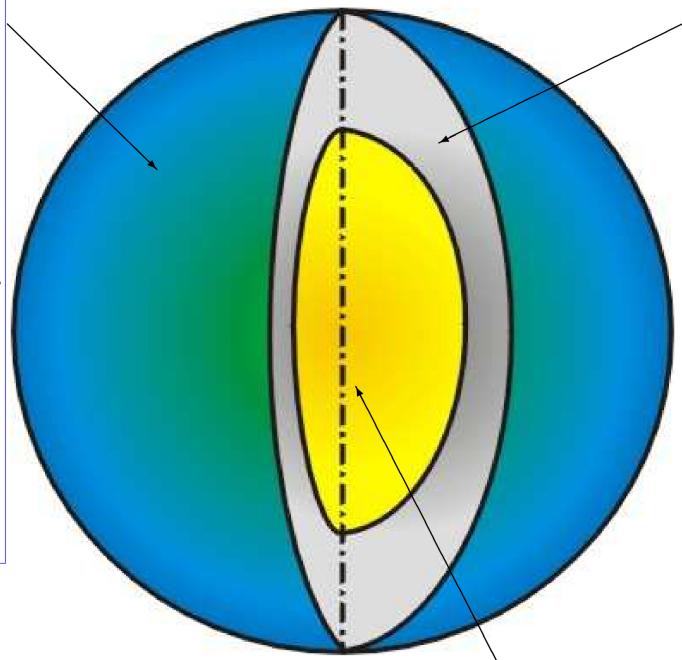

Outer Core

The outer core consists mainly of neutrons with several per cent admixture of protons, electrons and myons. It is several kilometers thick and occupies the density range $0.5\,\epsilon_0 < \epsilon \leq 2\,\epsilon_0$.

Nuclear matter density:
$\epsilon_0 = 2.8 \cdot 10^{14}\ \mathrm{g/cm^3}$

Inner Core

In the inner core of a neutron star hyperonic particles (Σ^-, Λ, Ξ...) are present. The inner core extends to the center of the star where its central density can be as high as $\epsilon \approx 15\,\epsilon_0$.

Neutron Star Matter

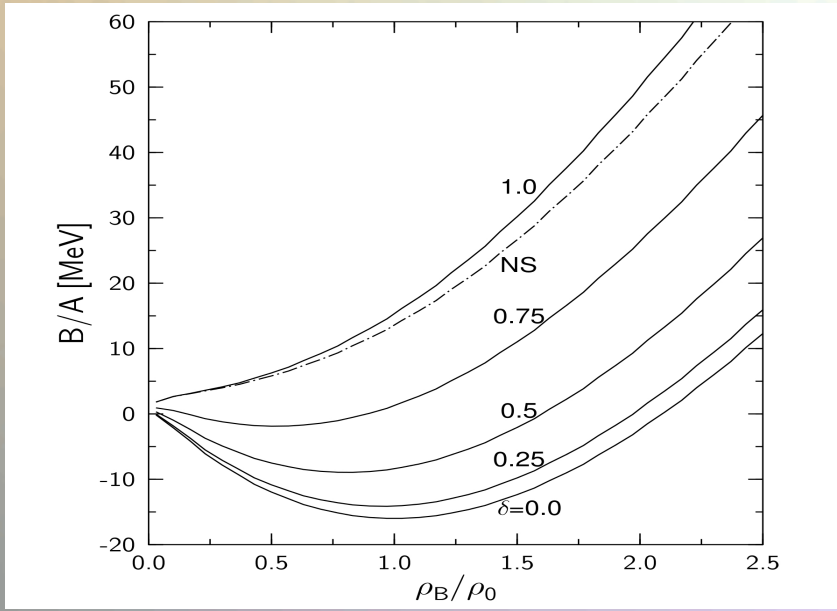

Binding energy per nucleon as a function of the baryonic density for different values of the neutron-proton asymmetry δ. 'NS' describes charge-neutral neutron star matter in β-equilibrium.

1) The equation of state (pressure P of the hadronic matter vs. the baryonic density). The solid curve (npe) describes charge-neutral matter in β-equilibrium consisting of neutrons, protons and electrons, whereas the dotted curve (npeμY) includes muons and hyperons.

In contrast to normal nuclear matter, neutron star matter needs to fulfil three additional conditions:

1) Charge Neutrality
2) β-equilibrium $\quad n \Leftrightarrow p + e + \tilde{\nu}_e$
3) Strangeness production

$$N + N \Rightarrow N + H + M \ ,$$

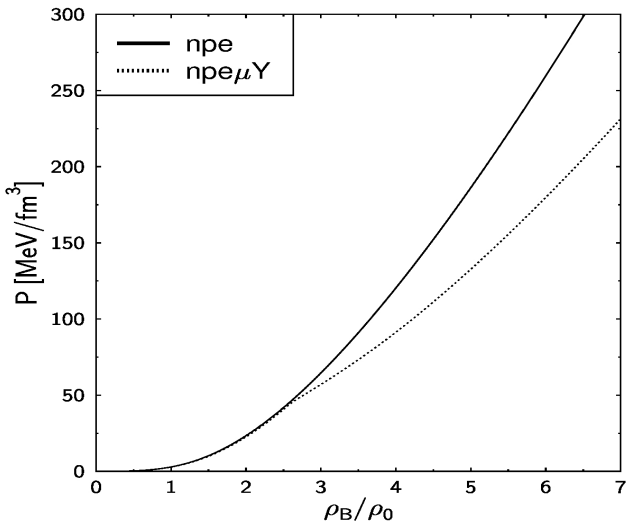

Hybrid Stars

To describe the properties of the Hadron-Quark phase transition happening in Hybrid stars an effective model for the quark phase is needed:

$$\lambda_j \equiv \lambda_{ja}{}^{b}$$

$$\begin{aligned}
\mathcal{L} \;=\; & \underbrace{\overline{\psi}\,(i\,\partial\!\!\!/ - \hat{m}_0)\,\psi}_{\text{Kinetische und Massenbeiträge}} + \underbrace{G_S \sum_{j=0}^{8} \left[\left(\overline{\psi}\,\frac{\lambda_j}{2}\,\psi \right)^2 + \left(\overline{\psi}\,\frac{i\gamma_5\lambda_j}{2}\,\psi \right)^2 \right]}_{\text{Skalare Wechselwirkung}} \\
& \underbrace{- G_V \sum_{j=0}^{8} \left[\left(\overline{\psi}\,\gamma_\mu\,\frac{\lambda_j}{2}\,\psi \right)^2 + \left(\overline{\psi}\,\gamma_\mu\frac{\gamma_5\lambda_j}{2}\,\psi \right)^2 \right]}_{\text{Vektorielle Wechselwirkung}} \qquad \psi \;\equiv\; \psi^{f}_{Aa}{}^{)} \\
& \underbrace{- K \left[\det{}_f \left(\overline{\psi}\,(1-\gamma_5)\,\psi \right) + \det{}_f \left(\overline{\psi}\,(1+\gamma_5)\,\psi \right) \right]}_{\text{Flavour Mischterme}} + \qquad \partial\!\!\!/ \equiv \partial\!\!\!/_A{}^B := \partial_\mu \gamma^\mu{}_A{}^B \\
& \qquad\qquad\qquad\qquad\qquad\qquad\qquad\qquad\qquad\qquad \underbrace{\mathcal{L}_L}_{\text{Leptonische Beiträge}}
\end{aligned}$$

Eg. the Nambu-Jona-Lasinio (NJL) Model or the MIT-Bag model

$$\begin{aligned}
\epsilon^Q &= \sum_{f=u,d,s} \frac{\nu_f}{2\pi^2} \int_0^{k_F^f} k^2 \sqrt{m_f^2 + k^2}\, dk \; + B \\
P^Q &= \sum_{f=u,d,s} \frac{\nu_f}{6\pi^2} \int_0^{k_F^f} \frac{k^4}{\sqrt{m_f^2 + k^2}}\, dk \; - B\,,
\end{aligned}$$

A hybrid model of a compact star is realized by a construction of a phase transition between a hadronic model and a quark model. In contrast to the Maxwell construction of a phase transition, in a Gibbs construction a mixed phase is present in the stars interior, where both phases co-exist. In the mixed phase transition region each phase has a charge; only the overall electrical charge density vanishes. In the mixed phase, the pressure of the hadronic matter has to be equal to the pressure of the quark phase, whereas the particle and energy densities differ.

M. Hanauske, L.M. Satarov, I.N. Mishustin, H. Stöcker, and W. Greiner, Phys. Rev. D 64, 043005 (2001)

The Gibbs Construction

Since the charge neutrality condition is only globally realized, the pressure depends on two independently chemical potentials, the baryonic and charge chemical potential:

$$\begin{aligned} P^H(\mu_B,\mu_e) &= P^Q(\mu_B,\mu_e)\,, \\ \mu_B = \mu_B^H &= \mu_B^Q\,, \\ \mu_e = \mu_e^H &= \mu_e^Q \end{aligned}$$

Charge density neutrality condition:

$$\rho_e := (1-\chi)\rho_e^H(\mu_B,\mu_e) + \chi\rho_e^Q(\mu_B,\mu_e) = 0\,.$$

Overall baryonic density:

$$\rho_B = (1-\chi)\rho_B^H(\mu_B,\mu_e) + \chi\rho_B^Q(\mu_B,\mu_e)\,,$$

$$\mu_i = B_i\,\mu_B + Q_i\,\mu_e$$

$$\begin{aligned} \mu_u &= \frac{1}{3}(\mu_B - 2\,\mu_e) \\ \mu_d = \mu_s &= \frac{1}{3}(\mu_B + \mu_e) \quad . \end{aligned}$$

The Gibbs Construction

$B^{1/4} = 180$ MeV

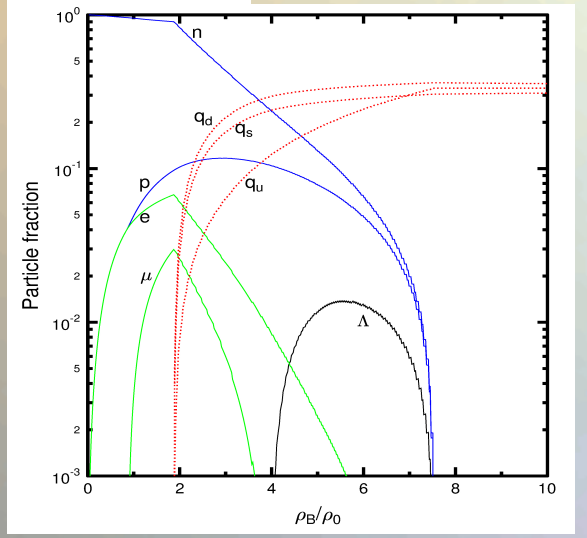

$B^{1/4} = 200$ MeV

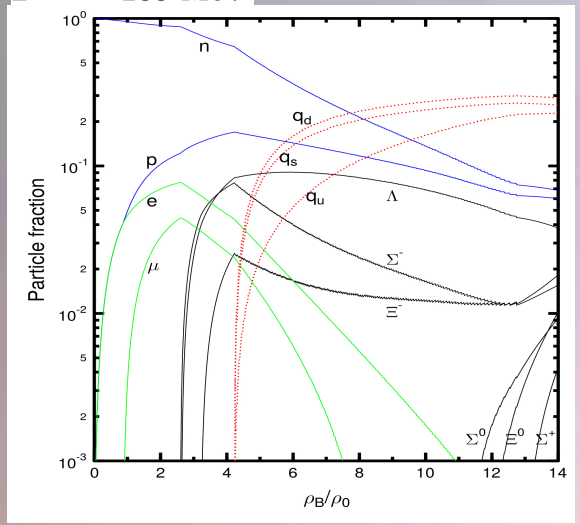

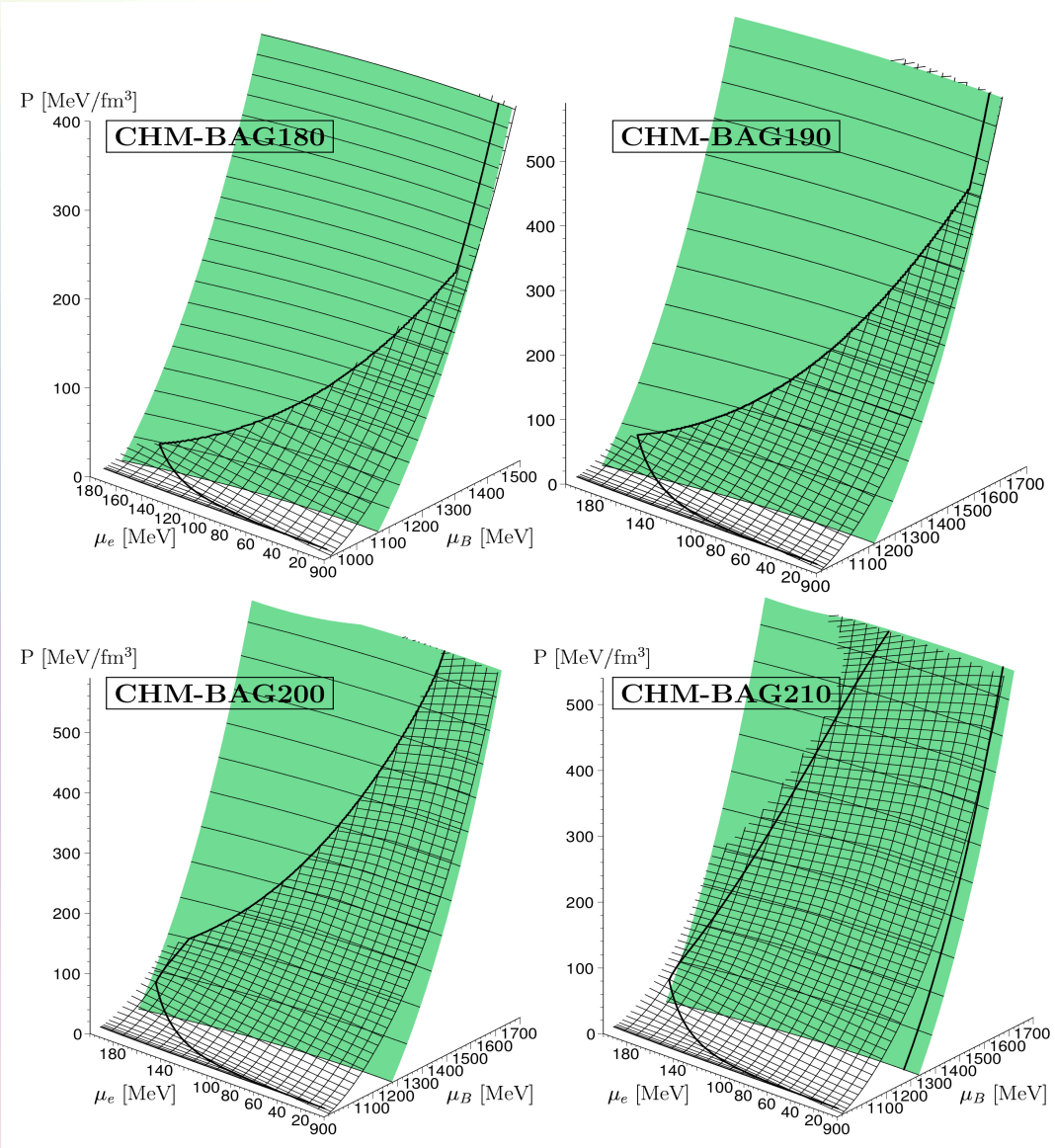

Hybrid Star Properties

Mass-Radius relations within a hybrid star model. The MIT-Bag model, for different values of the Bag parameter, was used for the quark phase, whereas for the hadronic phase the NLZY-model was used.

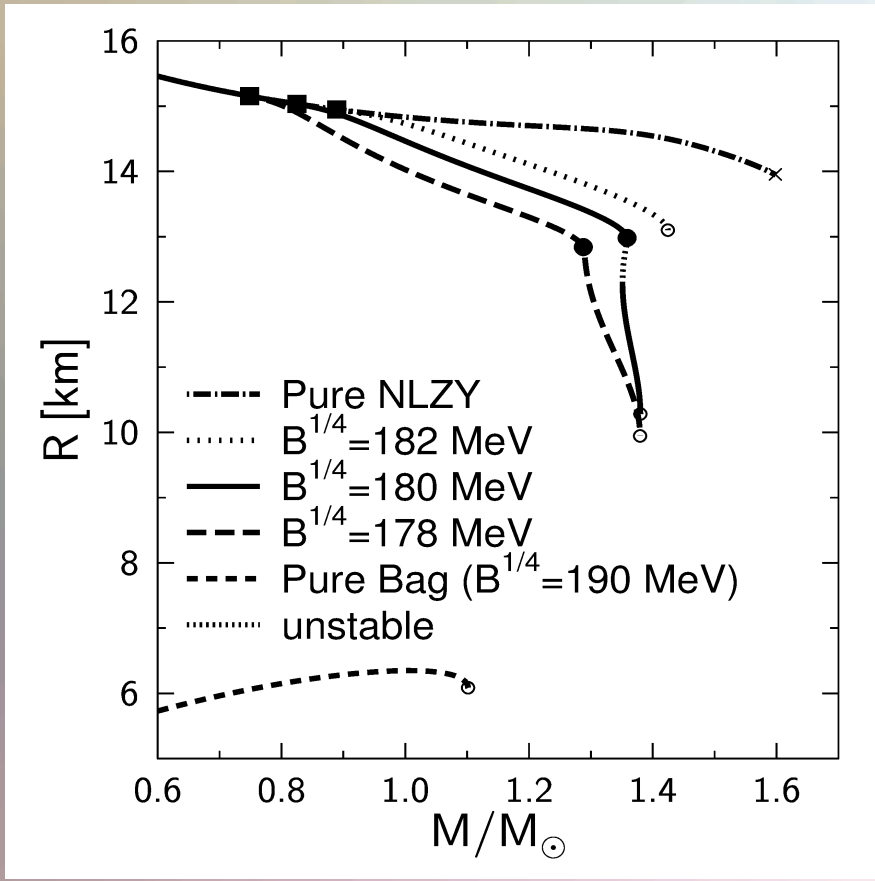

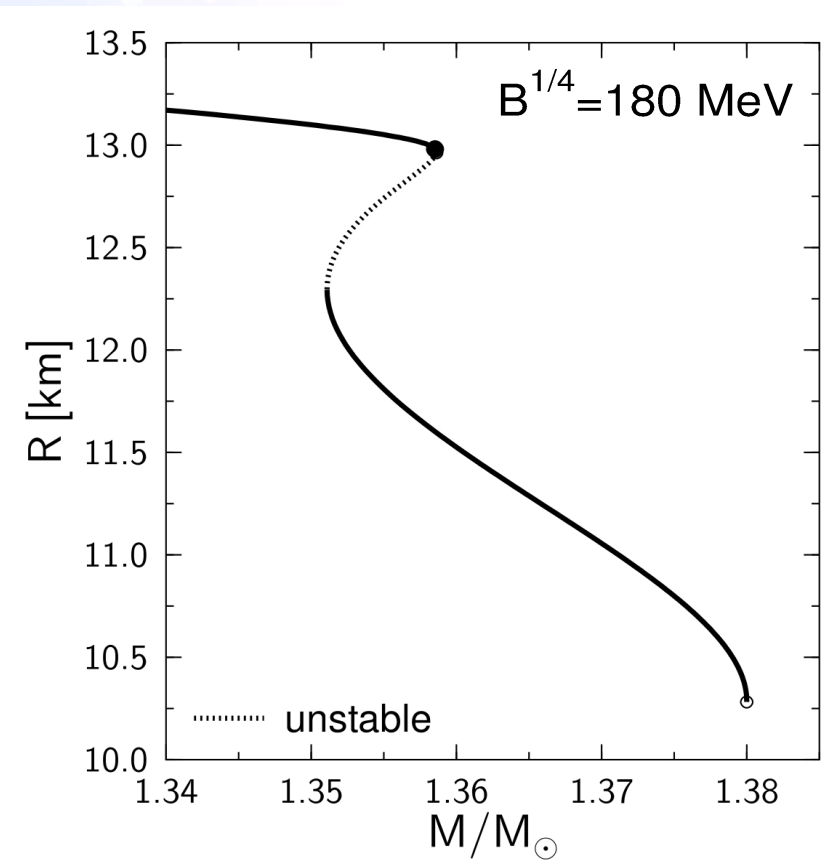

M. Hanauske, Dissertation, "Properties of Compact Stars within QCD-motivated Models"

Hybrid Star Properties

In contrast to the Gibbs construction, the star's density profile within the Maxwell construction (see middle figure) will have a huge density jump at the phase transition boundary. Twin star properties can be found more easily when using a Maxwell construction (see left and right figure).

Mass-Density relation

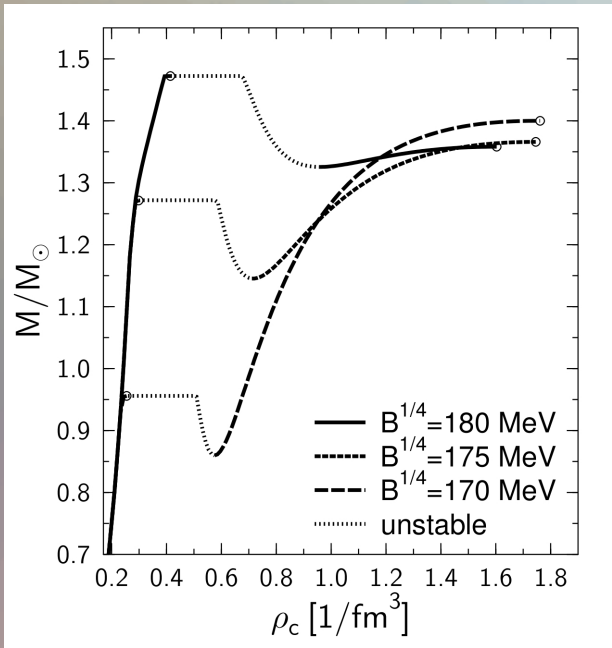

Energy-density profiles

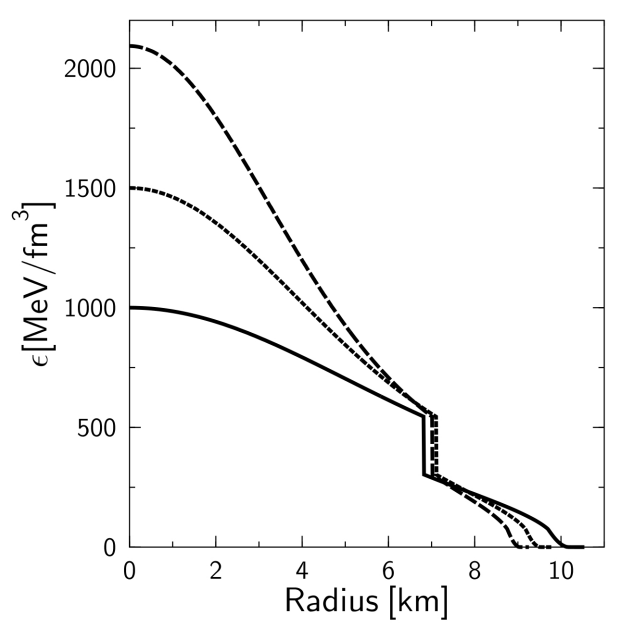

Radius-Mass relation

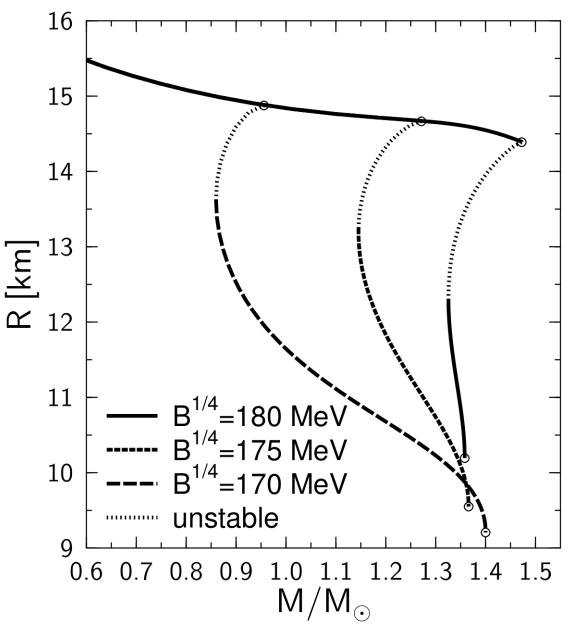

Matthias Hanauske: "How to detect the QGP with telescopes", GSI Annual Report 2003, p.96

Exotic Stars

But, unfortunately, twin stars can not be created solely by a Hadron-Quark phase transition. Extremely bound hyperon mater, or kaon condensation could also form a twin star behaviour.

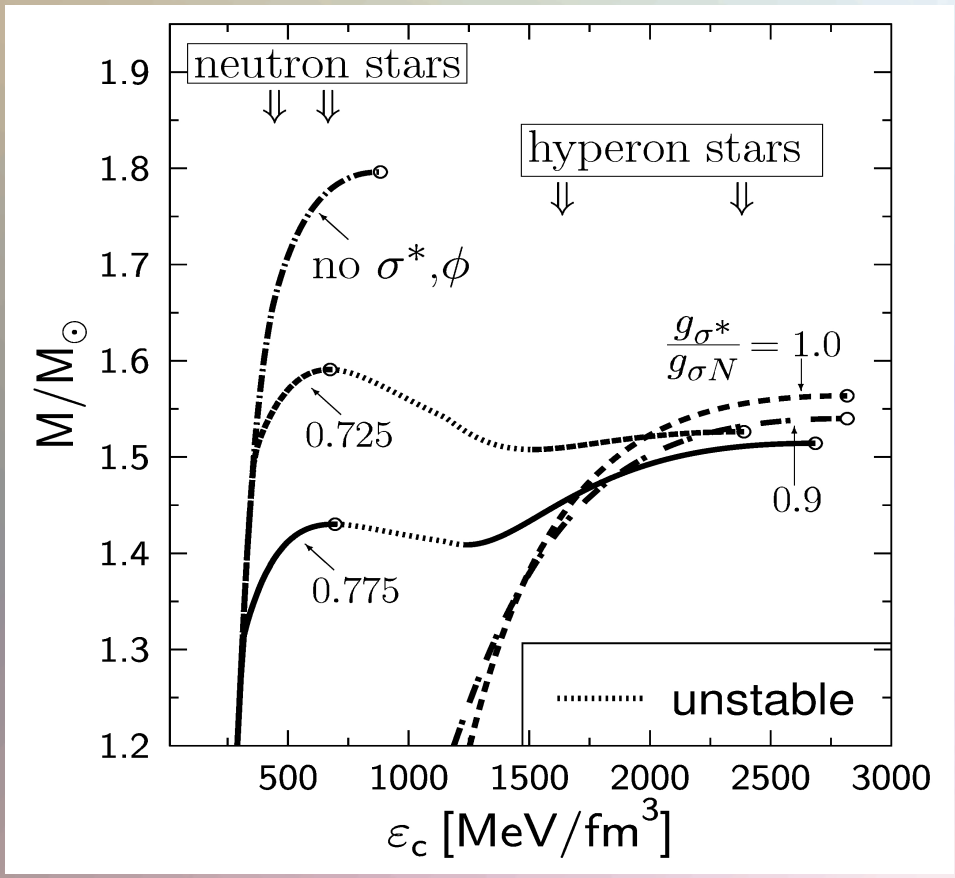

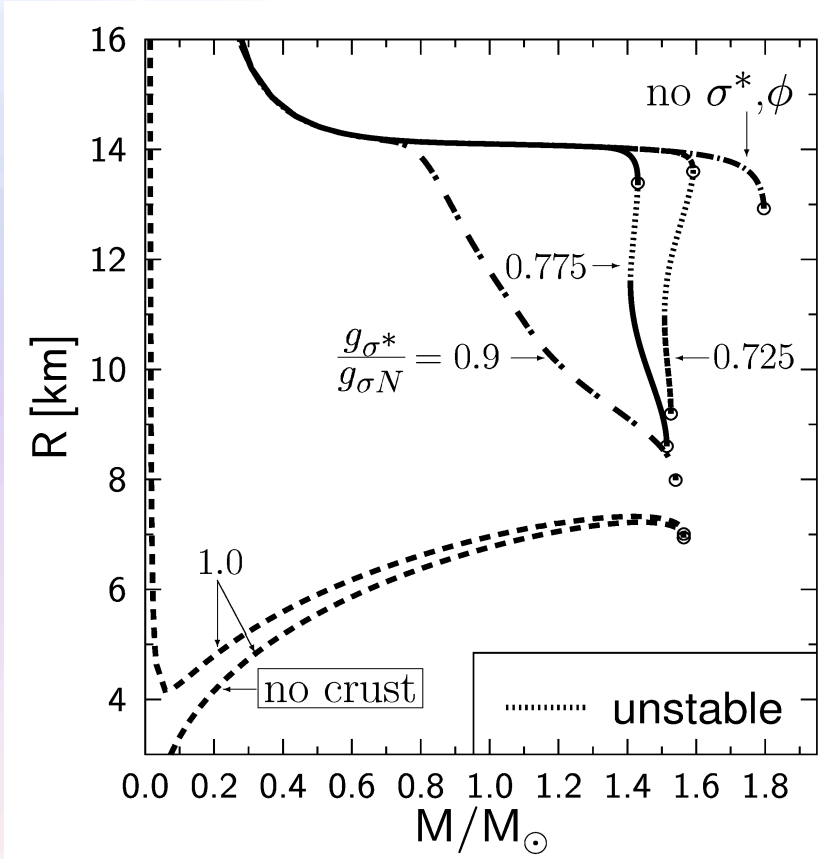

J. Schaffner-Bielich, M. Hanauske, H. Stöcker, and W. Greiner, Phys. Rev. Lett. 89, 171101 (2002)

The Spin Up Effect

A rotating neutron star slowly loses its energy and angular momentum through electromagnetic and gravitational radiation with time. However, it conserves the total baryon number during this evolution. The Figures below show results of uniformly rotating compact stars including a Bose-Einstein condensates of antikaons. The Figure on the right shows the behavior of angular velocity with angular momentum. The mass shedding limit sequence is shown by a light solid line. The stable parts of the normal and supramassive sequences are displayed by dark solid lines and the unstable parts by dotted lines. Curve II indicates a collapse of a neutron star to an exotic star belonging to the third family of compact stars.

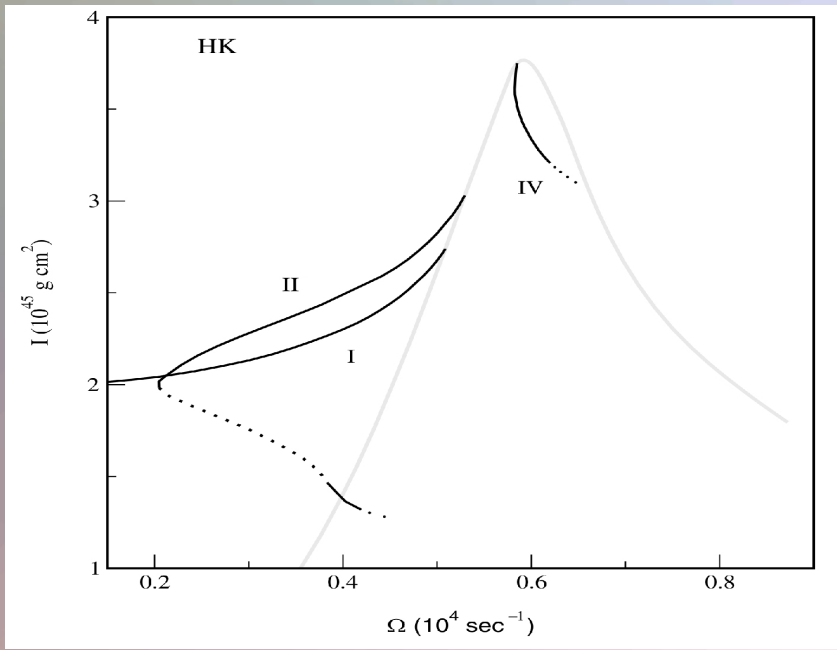

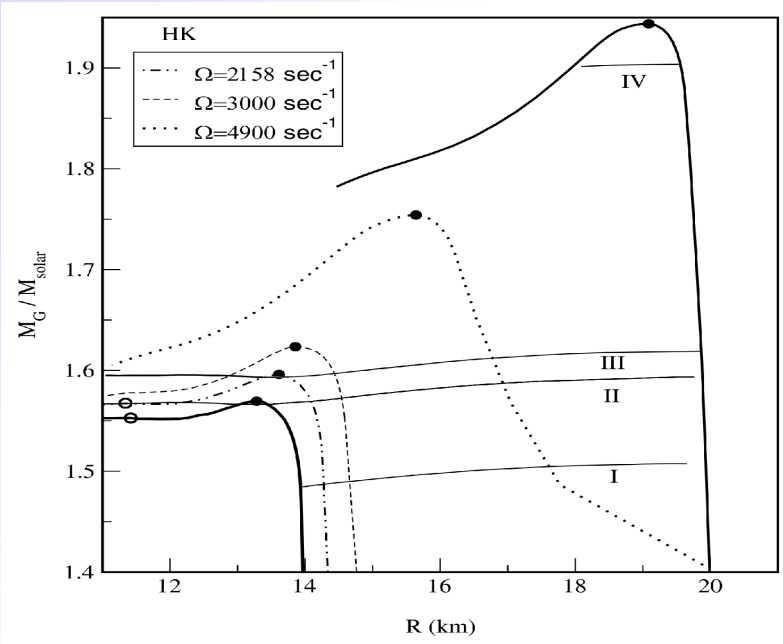

S. Banik, M. Hanauske, D. Bandyopadhyay, and W. Greiner, Phys. Rev. D 70, 123004 (2004)

Focus of the Talk

• How to detect the QCD-phase transition with gravitational wave detectors?
Based on a large number of numerical-relativity simulations of merging neutron star binaries, the differential rotation profiles of the hypermassive neutron stars (HMNS) in the post-merger phase have been analysed.
As already pointed out in (Kastaun/Galeazzi 2014) the differential rotation laws of HMNS show different structure than the profiles commonly used for differentially rotation neutron stars (following the j-constant law).
We want to confirm the results of (Kastaun/Galeazzi 2014)
How the rotation profiles correlate with other properties (e.g. compactness, density profile, GW frequency, …)
What makes the HMNS to stabilize against gravitational collapse to a black hole?

Research Questions:
• How to detect the QCD-phase transition with gravitational wave detectors?
• What happens when two neutron stars merge?
• How does the interior of a neutron star merger product look like?
• How does the space-time structure of a neutron star merger product look like?

"On the Properties of HMNS Formed in Mergers of Spinning Binaries", Wolfgang Kastaun and Filippo Galeazzi, arXiv:1411.7975

From ADM to BSSNOK

Unfortunately the ADM equations are only weakly hyperbolic (mixed derivatives in the three dimensional Ricci tensor) and therefore not "well posed". It can be shown that by using a conformal traceless transformation, the ADM equations can be written in a hyperbolic form. This reformulation of the ADM equations is known as the BSSNOK (Baumgarte, Shapiro, Shibata, Nakamuro, Oohara, Kojima) formulation of the Einstein equation. Most of the numerical codes use this (or the CCZ4) formulation.

The 3+1 Valencia Formulation of the Relativistic Hydrodynamic Equations

$$\nabla_\mu(\rho u^\mu) = 0\,,$$
$$\nabla_\nu T^{\mu\nu} = 0\,.$$

To guarantee that the numerical solution of the hydrodynamical equations (the conservation of rest mass and energy-momentum) converge to the right solution, they need to be reformulated into a conservative formulation. Most of the numerical “hydro codes” use here the 3+1 Valencia formulation.

The ADM equations

The ADM (Arnowitt, Deser, Misner) equations come from a reformulation of the Einstein equation using the (3+1) decomposition of spacetime.

$$\partial_t \gamma_{ij} = -2\alpha K_{ij} + \mathscr{L}_{\boldsymbol{\beta}} \gamma_{ij} = -2\alpha K_{ij} + D_i \beta_j + D_j \beta_i$$

$$\partial_t K_{ij} = - D_i D_j \alpha + \beta^k \partial_k K_{ij} + K_{ik} \partial_j \beta^k + K_{kj} \partial_i \beta^k + \alpha \left({}^{(3)}R_{ij} + K K_{ij} - 2 K_{ik} K^k{}_j \right) + 4\pi\alpha \left[\gamma_{ij} (S - E) - 2 S_{ij} \right]$$

Time evolving part of ADM

$$D_j (K^{ij} - \gamma^{ij} K) = 8\pi S^i$$

$${}^{(3)}R + K^2 - K_{ij} K^{ij} = 16\pi E$$

Constraints on each hypersurface

Three dimensional covariant derivative

$$D_\nu := \gamma^\mu{}_\nu \nabla_\mu = (\delta^\mu_\nu + n_\nu n^\mu) \nabla_\mu$$

Three dimensional Riemann tensor

$${}^{(3)}R^\mu{}_{\nu\kappa\sigma} = \partial_\kappa {}^{(3)}\Gamma^\mu_{\nu\sigma} - \partial_\sigma {}^{(3)}\Gamma^\mu_{\nu\kappa} + {}^{(3)}\Gamma^\mu_{\lambda\kappa} {}^{(3)}\Gamma^\lambda_{\nu\sigma} - {}^{(3)}\Gamma^\mu_{\lambda\sigma} {}^{(3)}\Gamma^\lambda_{\nu\kappa}$$

$${}^{(3)}\Gamma^\alpha_{\beta\gamma} = \frac{1}{2} \gamma^{\alpha\delta} \left(\partial_\beta \gamma_{\gamma\delta} + \partial_\gamma \gamma_{\delta\beta} - \partial_\delta \gamma_{\beta\gamma} \right)$$

Spatial and normal projections of the energy-momentum tensor:

$$S_{\mu\nu} := \gamma^\alpha{}_\mu \gamma^\beta{}_\nu T_{\alpha\beta} ,$$
$$S_\mu := -\gamma^\alpha{}_\mu n^\beta T_{\alpha\beta} ,$$
$$S := S^\mu{}_\mu ,$$
$$E := n^\alpha n^\beta T_{\alpha\beta} ,$$

Extrinsic Curvature:

$$K_{\mu\nu} := -\gamma^\lambda{}_\mu \nabla_\lambda n_\nu$$

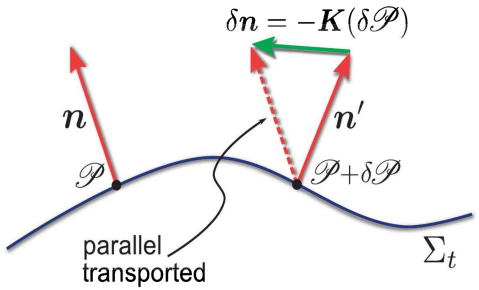

All figures and equations from: Luciano Rezzolla, Olindo Zanotti: Relativistic Hydrodynamics, Oxford Univ. Press, Oxford (2013)

From ADM to BSSNOK

Unfortunately the ADM equations are only weakly hyperbolic (mixed derivatives in the three dimensional Ricci tensor) and therefore not "well posed". It can be shown that by using a conformal traceless transformation, the ADM equations can be written in a hyperbolic form. This reformulation of the ADM equations is known as the BSSNOK (Baumgarte, Shapiro, Shibata, Nakamuro, Oohara, Kojima) formulation of the Einstein equation. Most of the numerical codes use this (or the CCZ4) formulation.

The 3+1 Valencia Formulation of the Relativistic Hydrodynamic Equations

$$\nabla_\mu(\rho u^\mu) = 0\,,$$
$$\nabla_\nu T^{\mu\nu} = 0\,.$$

To guarantee that the numerical solution of the hydrodynamical equations (the conservation of rest mass and energy-momentum) converge to the right solution, they need to be reformulated into a conservative formulation. Most of the numerical “hydro codes” use here the 3+1 Valencia formulation.

Finite difference methods

Discretisation of a hyperbolic initial value boundary problem.

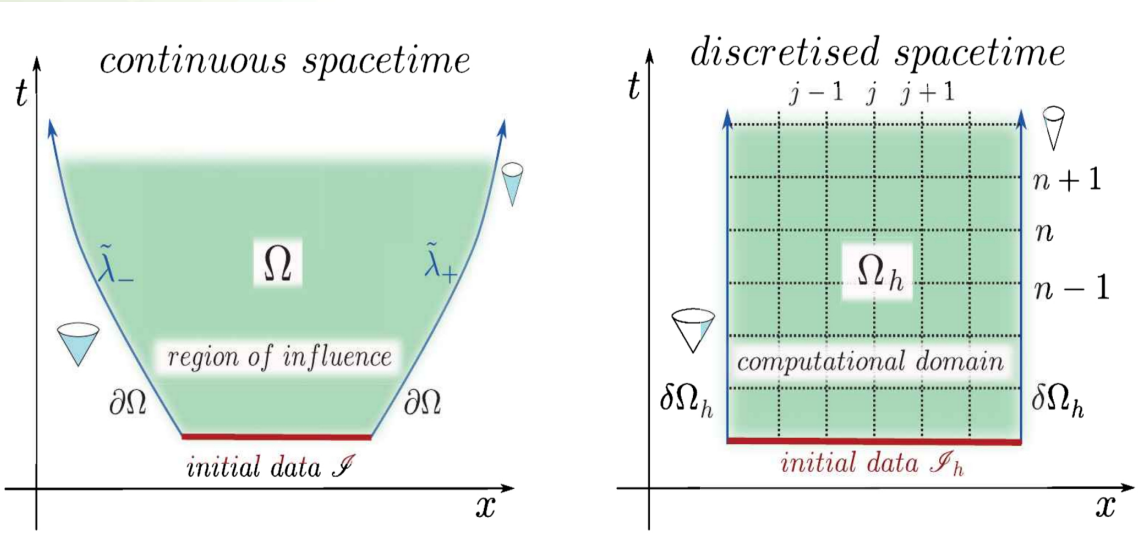

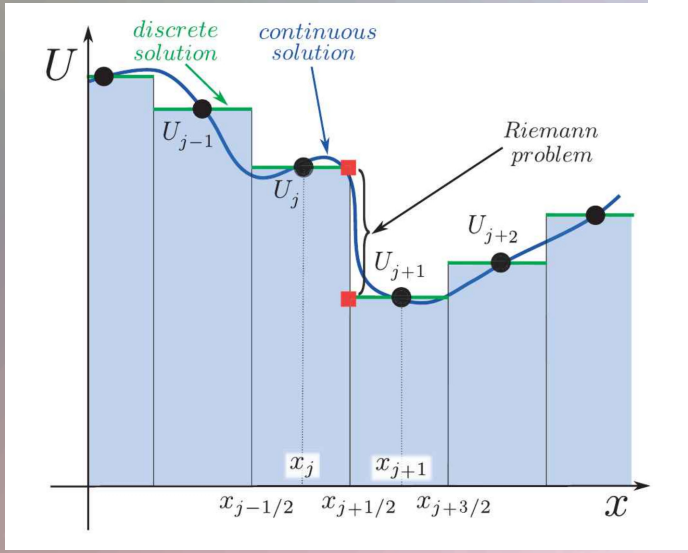

High resolution shock capturing methods (HRSC methods) are needed, when Riemann problems of discontinuous properties and shocks needs to be evolved accurately

All figures from: Luciano Rezzolla, Olindo Zanotti: Relativistic Hydrodynamics, Oxford Univ. Press, Oxford (2013)